On the relation between oscillatory EEG activity and the BOLD signal

René Scheeringa

DONDERS series

50

On the relation between oscillatory EEG activity and the BOLD signal

René Scheeringa

On the relation between oscillatory EEG activity and the BOLD signal
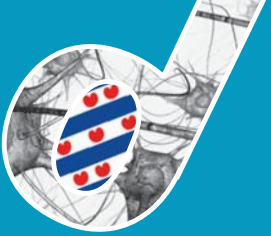
Een wetenschappelijke proeve op het gebied van de Sociale Wetenschappen

Proefschrift

ter verkrijging van de graad van doctor aan de Radboud Universiteit Nijmegen op gezag van de rector magnificus prof. mr. S.C.J.J. Kortmann, volgens besluit van het college van decanen in het openbaar te verdedigen op donderdag 10 februari 2011 om 13.30 uur precies

door

René Scheeringa

geboren op 13 januari 1980 te Leeuwarden

Promotores
Prof. dr. P. Hagoort
Prof. dr. D.G. Norris

Copromotor
Dr. M.C.M. Bastiaansen

Manuscriptcommissie
Prof. dr. M. Ullsperger
Prof. dr. S. Debener (Universität Oldenburg, Duitsland)
Dr. J.C. de Munck (Vrije Universiteit Amsterdam)

TABLE OF CONTENTS

Chapter 1

GENERAL INTRODUCTION AND OUTLINE

Electroencephalography (EEG) and functional magnetic resonance imaging (fMRI) are the two most widely used imaging tools in cognitive neuroscience involving human subjects. Both techniques provide a non-invasive way to study brain activity related to mental functions. EEG is ideally suited to study brain activity with millisecond precision, but the spatial resolution at channel level is limited to roughly a cerebral lobe. FMRI on the other hand is an ideal method to investigate which regions are related to specific mental functions, but its temporal resolution is limited to seconds rather then milliseconds. Each method on its own therefore provides an incomplete picture of what happens in the brain. The promise of integrating EEG with fMRI has therefore always been to obtain excellent knowledge about both when (with EEG) and where (with fMRI) processes in the brain take place.

Integrated analysis of both techniques assumes that the neural components of the two signals are related directly or indirectly. A potential direct link can be found in the notion that both signals are directly linked to perisynaptic activity. The EEG is thought to be generated through the summation of synchronous post-synaptic potentials on the apical dendrites of pyramidal neurons that are oriented perpendicular to the scalp. EEG therefore reflects incoming activity to these pyramidal neurons. Recent insights into the origins of the BOLD signal suggest that it is also closely related to the input that is received by a neuron, in that it is related to the pre-synaptic release of neurotransmitters, particularly glutamate (Friston, 2008).

Although there is evidence for a direct link between EEG and BOLD activity, not all neural activity expressed in the BOLD signals will also be expressed in the EEG and vice versa. EEG as mentioned above is only sensitive for synchronous input to pyramidal neurons of a certain orientation that are close to the scalp. These restrictions do not affect the BOLD signal, and other types of neural activity might very well be expressed in the BOLD signal, without having a direct effect in the EEG. Also the other way around is conceivable. If the BOLD signal is indeed differentially related to different neurotransmitters, as has been suggested, it is possible that certain neural activity is not expressed in the BOLD signal. It has in fact been shown that not all activity observed with EEG also results in BOLD responses and vice versa (Im et al., 2005; Liu et al., 1998; Schulz et al., 2004), which has led to the notion of fMRI blind MEG/EEG sources and MEG/EEG blind fMRI sources (Ritter and Villringer, 2006). An indirect relation between EEG and BOLD activity however is still possible, which can be investigated with an integrated analysis approach. For example activity in subcortical regions like the thalamus and the striatum activity is hard to detect directly

with EEG, but does directly influence activity in cortical regions that do produce measurable features in the EEG. Integrated analysis of fMRI and electrophysiological data can help us understand to which EEG features these subcortical regions are related.

Simultaneously recorded EEG and fMRI is a relatively recently developed technique (see Herrmann and Debener, 2008, for a historical perspective). Before its development integrated analysis of both scalp level electrophysiological measures (EEG and magnetoencephalography; MEG) and hemodynamic measures (e.g. fMRI and positron emission tomography; PET), several studies combined the analysis of separately recorded EEG/MEG and PET/fMRI in the same subjects. Among the first attempts to combine both measures in such a way is the work of Heinze et al. (1994), who investigated the timing and localization of the earliest effects of spatial attention. The event related potential (ERP) revealed the attentional effect with a millisecond resolution, while dipole modelling of this effect yielded the same location as was revealed in the subtraction of both conditions in a PET session. Since then several studies used a similar approach using fMRI and EEG (Linden et al., 1999; Opitz et al., 1999; Wibral et al., 2008) or MEG (Dale et al., 2000; Fujimaki et al., 2002; George et al., 1995; Liu et al., 1998; Moradi et al., 2003; Phillips et al., 2002; Woldorff et al., 1999). The different measurement environments however can influence the nature of the responses. The noise from echo planar imaging has been shown to influence the auditory response in both MEG and EEG (Herrmann et al., 2000; Novitski et al., 2001; Novitski et al., 2003). If effects of mood or brain state are of interest, collecting both measurements simultaneously is also advisable. Sammer and colleagues (Sammer et al., 2005) however reported that well known effects of various cognitive manipulations on EEG features can be replicated inside the scanner.

Although the first report of simultaneously recorded EEG during echo planar imaging already dates back to 1993 (Ives et al., 1993), integrated analysis of simultaneously recorded EEG and fMRI data is of a more recent date. Its development is tightly related to advances in MR compatible hard-ware like EEG amplifiers and electrodes (Lemieux et al., 1997), and specialized software to deal with the artifacts generated in the EEG-unfriendly environment of the MR scanner (Allen et al., 2000; Allen et al., 1998). See Laufs et al. (2008) for a review on these methodological issues. One of the first applications of simultaneously recorded EEG and fMRI was in the field of epilepsy, motivated by the requirement to localize the brain regions related to interictal epileptiform activity (see Laufs and Duncan, 2007, for a review). Simultaneous recording

of EEG and fMRI is essential here, since the occurrence of epileptiform activity is unpredictable, and hard if not impossible to control experimentally.

The advantage of recording epileptiform activity is that this activity is so strong that single events are readily observed at scalp level. It is therefore also not surprising that most of the early research using concurrently recorded EEG and fMRI in a non-clinical setting focused on how changes in the blood oxygenation level dependent (BOLD) signal correlates to the posterior alpha rhythm. This rhythm is also readily detectable at scalp level, and is particularly pronounced at the back of the scalp when people are at rest with their eyes closed. Several studies have correlated fluctuations in power in this resting state alpha rhythm with the blood oxygenation level dependent (BOLD) signal and have all unequivocally found negative correlations between alpha and the BOLD signal in the cerebral cortex (Feige et al., 2005; Goldman et al., 2002; Laufs et al., 2003a; Moosmann et al., 2003). However, in different studies different sets of regions were found to correlate negatively with alpha power. Later research suggested that this relation is more complicated than it first seemed, and that it also depends on the relative contribution of other frequency bands to the total EEG spectrum (Goncalves et al., 2006; Laufs et al., 2008).

As mentioned in the beginning of this chapter, one reason for simultaneous recording of EEG and fMRI could be the requirement of having exactly the same conditions for both measurement modalities. If this is not vital, simultaneous recordings should only be undertaken if this yields valuable information that cannot be obtained from separate measurements. Besides investigating the BOLD correlates of EEG-defined spontaneous neural events like epilepsy, sleep spindles and alpha amplitude fluctuations, the usefulness of simultaneous recordings may lay in the ability to relate trial-by-trial fluctuations in EEG responses to trial-by-trial fluctuations in the fMRI BOLD signal. A first prerequisite for this is that variability over trials in the neural response is expressed in both the fMRI signal and an EEG feature (e.g. an event related potential or power change). Whether this is actually the case cannot be solved a-priori and is best addressed empirically by checking whether there is a trial-by-trial coupling of BOLD and EEG responses that can be related to what is known about the effects in both modalities separately. On a more theoretical ground, however, a plausible case can be made for the presence of meaningful trial-by-trial variation in brain processes. The brain is not a static 'noise' free system. A more realistic view is that the brain is a dynamic system in which the internal state changes continuously, both due to internal interactions, and interactions with the outside world. This continuous change of brain states will

therefore most likely also influence its response to the same external input on a trial-by-trial basis. If these fluctuations are reflected both in the EEG as well as in the fMRI signal, the trial-by-trial coupling between EEG and the fMRI might provide us with information on which brain regions are actually directly related to the task induced effects observed in the EEG. Since both brain regions and EEG features have been linked to specific cognitive operations these results can potentially change the interpretation of the EEG feature in question as well as the fMRI response in a particular region. Additionally, this technique could also help us to better understand the relation between the hemodynamic measures like the fMRI BOLD signal and electrophysiological signals in general, which is still poorly understood.

A problem relating single trial EEG responses to the BOLD response lies in the observation that effects of experimental manipulations on EEG features like, the ERP or frequency specific power changes, are weak compared to the artifacts, noise and other background activity present in the EEG. Therefore, the signal is usually averaged over many repetitions of the same trial type in order to increase the signal to noise ratio. When we want to combine EEG with fMRI at single trial level averaging over trials can not be done. However increasing the strength of the signal of interest relative to artifacts, noise and non-interesting EEG signals by other means is very important. Two articles published almost simultaneously by Eichele et al. (2005) and Debener et al. (2005) demonstrated that it is possible to increase the relative strength of ERPs to obtain single trial estimates that yield interpretable correlations with the BOLD response. Eichele et al (2005) used a combination of independent component analysis (ICA) and wavelet denoising to get reliable single trial estimates of the P2, N2 and P3 components in the ERP. They were able to show that trial-by-trial fluctuations of these three different ERP components correlated with the BOLD response in three different networks of brain regions. This illustrates the ability to differentiate the BOLD response in different regions based on their relation to different EEG features.

While Eichele et al. (2005) only used the EEG sampled in between the acquired fMRI volumes, Debener et al. (2005) measured both modalities fully simultaneously, correcting for the EEG artifacts related to fMRI volume acquisition afterwards. Using ICA to denoise the EEG data, they were able to show that also under these conditions single trial ERPs can be reliably measured. They convincingly showed that the trial-by-trial fluctuations in the amplitude of the Error Related Negativity (ERN), an ERP component that emerges after an error, correlates with the BOLD response in a region that also shows a BOLD activation after an error. Moreover, they showed that a dipole

seeded in this location is able to explain the observed scalp topography of the ERN very well, suggesting a close relation between the ERN and a task induced regional specific BOLD response.

Besides EEG research that focuses on ERPs, the analysis of event related increases and decreases in frequency band specific power using EEG or MEG has become increasingly popular. In the context of simultaneous EEG-fMRI, research mainly focused on the relation between power fluctuations and the fMRI signal in resting state (Goldman et al., 2002; Goncalves et al., 2006; Laufs et al., 2006; Laufs et al., 2003a; Laufs et al., 2003b; Mantini et al., 2007; Moosmann et al., 2003; Scheeringa et al., 2008). Few studies however have addressed the relation between the fMRI signal and frequency specific power effects (Mizuhara et al., 2004; Sammer et al., 2007) in the EEG in experimental contexts.

In this thesis I specifically investigate the relation between oscillatory EEG activity and regional specific changes in the BOLD signal, using simultaneously recorded EEG and fMRI. An important feature of event related power changes is that they can last for several seconds, while ERPs in general are short lived. Since BOLD signal changes can also last for many seconds, changes in oscillatory EEG activity might very well be closely related to the BOLD signal. Animal work has indeed suggested that power in electrophysiological measures are more closely related to the BOLD signal than changes in spiking rate (Logothetis et al., 2001; Niessing et al., 2005) , which are also more transient. In addition, recent studies suggest that the longer lasting ERPs are closely related to changes in EEG or MEG power (Mazaheri et al., 2009; van Dijk et al., 2010).

Outline of the thesis

In this thesis, I present data obtained during a resting state measurement (**chapters 3 and 6**) as well as in experimental contexts (**chapters 4 and 5**). Together with a methodological chapter (**chapter 2**) and a general discussion (**chapter 7**) this thesis demonstrates how simultaneously recorded EEG and fMRI can successfully be applied in cognitive neuroscience to study the relation between frequency specific EEG power fluctuations and changes in the hemodynamic signal as measured with BOLD fMRI.

Chapter 2 elaborates on the general issues regarding methods, design and interpretation that feature throughout the work in the other chapters. It provides further background to the methodological choices and interpretation of the data in the subsequent chapters.

Chapter 3 describes the BOLD correlates related to resting state fluctuations in frontal theta (3-7 Hz) power. Frontal theta oscillations are a prominent feature in the EEG that can be manipulated by cognitive tasks contexts, but can also be observed during resting conditions. Here we find that a well-known network from fMRI literature, the so called default mode network, is negatively correlated to resting state fluctuations in frontal theta power.

Chapter 4 investigates how increases in frontal theta and in right posterior alpha (8-12 Hz) EEG power during working memory maintenance are related to regionally specific changes in the fMRI signal. Trial-by-trial EEG/fMRI correlation reveals two separate networks that are closely related to these working memory induced power increases.

Chapter 5 focuses on how effects in different frequency bands relate to the fMRI signal. Based on work in animals and earlier EEG/fMRI studies, power fluctuations in low frequencies are thought to correlate negatively with the fMRI signal, while fluctuations in higher frequencies, more specifically in the gamma band (roughly from 30-100 Hz), are tightly positively coupled to the BOLD response. Here we use a visual task that is known to modulate power reliably in high as well as low frequencies. MEG source analysis revealed that these effects largely come from the same region in the visual cortex. This gives us the opportunity to study the relation of the fMRI signal across the entire frequency spectrum of the EEG, by correlating each the power for frequency with the BOLD signal from this region.

In the chapters 3-5 we investigated whether and where the fMRI BOLD signal correlates with EEG power fluctuations. This strategy is suited for investigating whether frequency specific changes in EEG power are related to *activations* found in fMRI. In **chapter 6** we adopted a novel approach by investigating whether the *connectivity* within an fMRI-defined resting state network, the visual network, and with regions outside the network is modulated as a function of EEG alpha power. In this chapter, we report a decreased connectivity within the visual system, and a less strong negative relation of the visual cortex with regions of the default mode network when alpha power is high.

Chapter 7 summarizes the results from the previous chapters, and discusses more general issues that are raised by the collection of work presented in the previous chapters. In this chapter I also discuss some potential new lines of research that could benefit from using simultaneously recorded EEG and fMRI.

Chapter 2

METHODS, DESIGN AND INFERENCE

This chapter elaborates on the methods, design and the interpretation of the data that are presented throughout this thesis. The chapter is not intended to give an exhaustive overview on the technical and methodological issues related to simultaneously recorded EEG and fMRI. A historical perspective on this subject can be found in Hermann and Debener (2008); a review on recent advances can be found in Laufs et al. (2008). The first part of this chapter presents a brief introduction to the different types of EEG/fMRI integration that can be distinguished. This will put the work presented in this thesis in a context. In the second part the considerations that formed the basis for the statistical designs are discussed. The third section discusses what inferences can be made from simultaneous recorded EEG/fMRI. The last part discusses independent component analysis (ICA) with a focus on its application in this thesis as a preprocessing tool for EEG data.

Types of EEG-fMRI integration

Several different strategies have been employed to analyze simultaneously recorded EEG and fMRI. In an article proposing a joint forward model for EEG and fMRI, Kilner et al. (2005) distinguish three approaches to fMRI integration: (I) integration through fusion of forward models prediction; (II) integration through constraints; and (III) integration through prediction.

Integration through fusion attempts to model both the EEG features measured at the scalp level as well as the BOLD signal from the region generating that feature through a common (generative) forward model. Kilner et al. (2005) argue that activation as is expressed in the increased BOLD signal, is related to increased energy dissipation, decreased membrane constants, increased effective coupling among neural assemblies, and as a result a shift in the EEG spectral profile to higher frequencies. A more recent and more extensive approach using a Bayesian framework was presented by Daunizeau et al. (2007).

Integration through constraints refers to the procedure in which information in one modality constrains the analysis in the other modality. In integrated EEG-fMRI analysis this usually refers to using the fMRI activation pattern as constraint or prior knowledge in the source estimate of the EEG (or MEG) data (Dale and Halgren, 2001; Phillips et al., 2002). In principle, this procedure does therefore not require simultaneously recorded EEG.

When EEG and fMRI are integrated through prediction, one modality (typically EEG) is used to predict the other (typically fMRI). Most studies using simultaneous EEG and fMRI have employed this strategy. Several of the studies employing this strategy have focused on finding the regions where BOLD correlates with fluctuations in ongoing EEG power (Goldman et al., 2002; Goncalves et al., 2006; Laufs et al., 2006; Laufs et al., 2003a; Mantini et al., 2007; Moosmann et al., 2003). The coupling of variations in single trial estimates of EEG features like ERPs to regional specific BOLD fluctuations also falls under integration through prediction.

The work presented in this thesis largely qualifies as integration through prediction. The only exception is in chapter 3 where we show that one of the regions where the BOLD signal correlates with frontal theta power is also the likely source of frontal theta. This is an example of integration through constraints. In chapter 6 we use integration through prediction in a slightly different manner. Here we use EEG power to predict whether the interaction between regions measured with BOLD differs between periods with relatively high and low EEG power.

Statistical design

As mentioned above, most of the work presented in this thesis qualifies as integration through prediction. The most commonly used tool for achieving this is the general linear model framework (GLM). Since there is no task, and therefore no task regressors, the construction of the design matrix for the linear model in resting state studies is straightforward. Usually HRF-convolved normalized EEG power (or another EEG feature like epileptic activity) forms a regressor in the design matrix that further consists of nuisance regressors (e.g., movement parameters). At the group level the estimated beta-parameters for these regressors are then tested with for example a one-sample t-test. In chapters 3 and 6 we used this approach.

In a task context constructing the design matrix is more complex. Here the goal usually is to investigate which brain regions are related to a particular task related EEG feature (for example ERP amplitude or power increase or decrease). By using single trial estimates of this EEG feature in a regressor, researchers aim at detecting regions where the BOLD signal covaries with the strength of this feature, which can therefore be functionally related to the task evoked effect in this aspect of the EEG signal. However, in a task context the mere presence of an experimental task already poses a problem for the construction of the design matrix. Since both fMRI and EEG are dependent

variables any correlation between the two signals can be caused by the same task manipulation, and does not necessarily imply a more direct relation between the two measures. In the context of correlating trial-by-trial estimates of BOLD and EEG features, the mean task effect on both measures is therefore to be viewed as a potential confound (see figure 2.1 for an illustration). By simply inserting both task and EEG based regressors in the same design matrix the experimental paradigm introduces colinearity between the two types of regressors reflecting their mutual dependence on the task. This reduces the statistical power for detecting effects related to each individual regressor. This colinearity problem can be solved by constructing the EEG based regressors in such a way that they model only uniquely attributable variance in the BOLD signal (e.g. variance that cannot be explained by the regressors modelling the experimental paradigm). In this approach, the benefit of using the EEG features in the analysis of the fMRI data is explicitly accounted for by the EEG based regressors.

 In figure 2.1 a scheme is depicted that shows how these EEG based regressors can be obtained for event related effects in EEG power. The basic idea is that for every single trial the EEG power response can be modelled by three uncorrelated components. The first component consists of the average response across all trials and the entire time interval of the trial (or trial segment). This is the overall mean effect of the task across the entire trial. It is the part that is typically modelled in fMRI studies by box-car regressors, and is therefore the part that causes the colinearity between EEG and task regressors if both are included in the design matrix of the linear model. The second component is the deviation in the average EEG power response from this idealized box car response at the different time points in the trial. This component can be obtained by subtracting the mean power during the trial from the average power time course. Note that this regressor strictly speaking does not necessitate the concurrent registration of EEG and fMRI, if the assumption that the average EEG response is the same across recording sessions and measuring environments holds. The third regressor can be obtained by subtracting the mean power response from each single trial power time-course. This component captures the trial-by-trial variation in the EEG power response. Subsequently three uncorrelated types of regressors can be built from these three subcomponents, each modelling uniquely identifiable parts of variance in the BOLD response. The first types of regressors, consisting of standard box-car regressors, model the average effect, just like in conventional fMRI experiments. The second set of regressors inform about where the EEG power response actually deviates from this
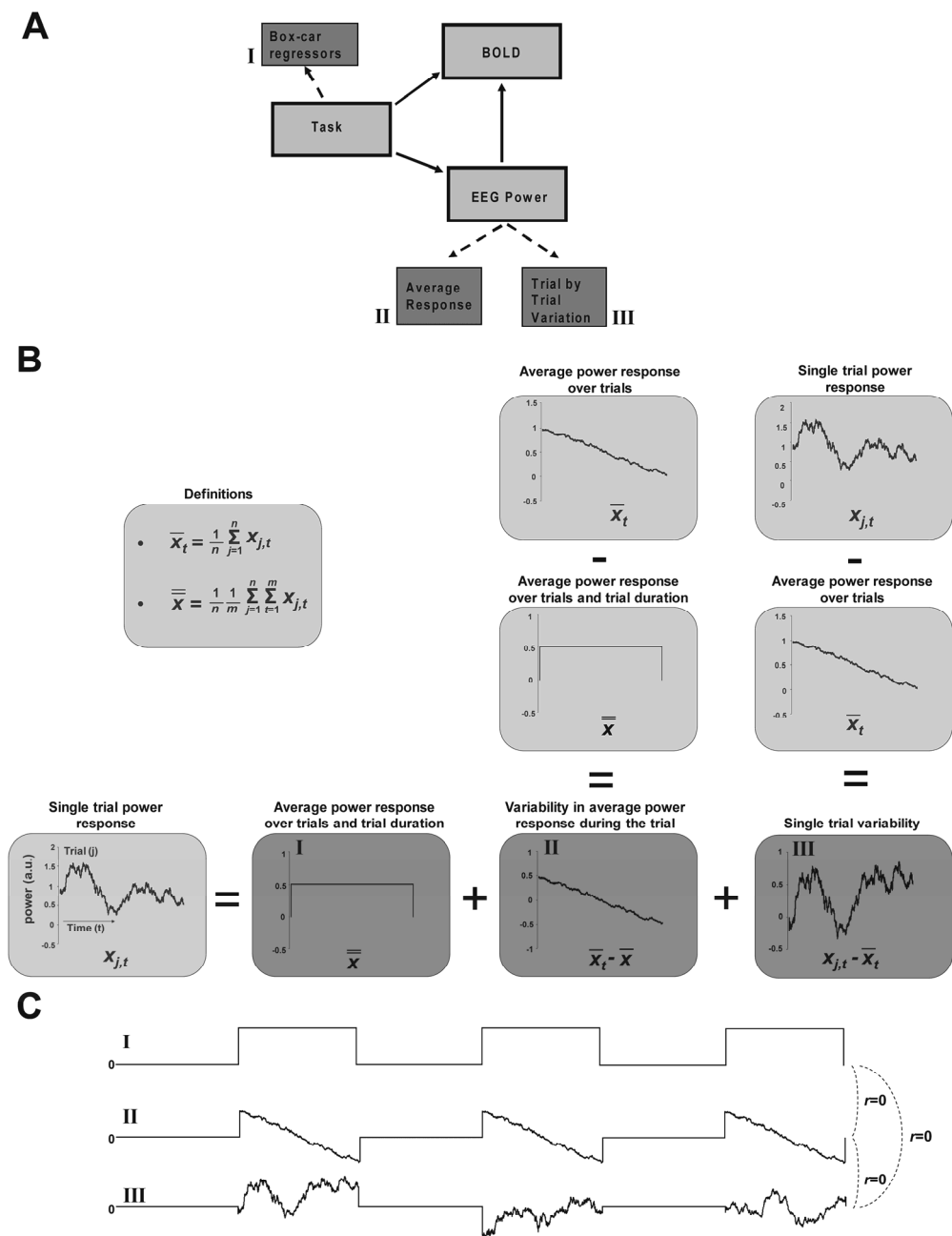
Figure 2.1. Construction of regressors based on EEG power in a task context. Panel A schematically illustrates the colinearity problem when EEG power is used as a regressor in a task

context. Since EEG power and fMRI are modulated by the same experimental paradigm they will be correlated as a consequence. Regions that correlate with EEG power are therefore not necessarily related to the task related EEG power effect, since it can also be related to the experimental manipulation through a different route. To account for this task effect, task regressors can be included in the design. These task regressors are usually based on the assumption that the neural response is stable over the entire time period it models. They model the average neural response over the modeled time period within a trial and over trials (see also Panel B). Since we have the time course of the average EEG power response over trials, we actually have knowledge about the real time course of the EEG power related neural activity. By building a regressor from the average power response we can therefore model the average EEG power related neural response over trials. We therefore can include three types of regressors: (I) the conventional box-car regressors modeling the task; (II) regressors modeling the average power response over trials; and (III) regressors build from the single trial power responses. These regressors are however strongly interdependent, and therefore correlated. This will affect the beta estimates of all the regressors if they were entered in a GLM simultaneously. Therefore we uncorrelated the regressors in a hierarchical way, as is depicted in Panel B. By subtracting the overall mean power, depicted as a box-car, from the average power response, and the average power response from every single trial power estimate we can construct a set of uncorrelated regressors, as is depicted in panel C. This procedure as depicted here implements a Schmidt-Gram orthogonalization on regressors that were not convolved with a hemodynamic response function for illustration purposes. In this thesis, we applied this procedure after convolution. The three orthogonalized types of regressors now model unique parts of the variance in the BOLD signal. The task regressors model the task as is done in conventional fMRI experiments. The orthogonalized average response models the additional information about the shape of the EEG power related activity, and the orthogonalized single trial response models the trial-by-trial deviation from the average power response. This last type therefore explicitly models the information that can be gained from recording EEG and fMRI simultaneously. Regions where the activity underlying the BOLD response is related to the EEG power response of interest should be related to all three types of regressors.

idealized box-car response. The third type of regressor models the trial-by-trial deviation from this average power response, and therefore accounts for the part of the variance in the BOLD signal that can only be explained if EEG and BOLD are acquired by measuring both modalities simultaneously. The construction of these regressors can be achieved before convolution with the HRF by the subtraction scheme presented in figure 2.1, but can also be achieved after convolution by orthogonalizing the regressors hierarchically as is done in chapter 4 (Gram-Schmidt orthogonalization).

In some circumstances it is preferable not to construct the second and third type of regressors separately. When ERPs and not EEG power are at the focus of interest it is usually not possible to construct the second type of regressors, since only one measurement for each trial (usually its amplitude) is available, with the possible exception of very slow evolving potentials that last up to several seconds. In addition,
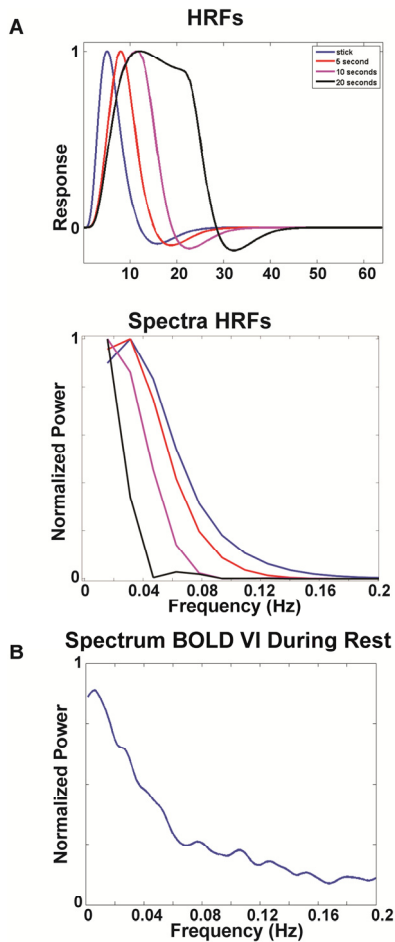
Figure 2.2. The hemodynamic response acts as low pass function on underlying neural activity. Panel A shows the normalized modeled hemodynamic responses and its power spectra to different lengths underlying bursts of neural stimulation. The underlying neural stimulation is modeled as a stick function or box-car responses of different lengths. The power spectra indicate that for all stimulation lengths most power is found below 0.08 Hz, the same range as the so called resting state fluctuations which are depicted in figure B. This panel shows the average normalized power spectrum of over subject from right VI during an eyes open resting state section. This also demonstrates that all neural activity that is reflected in the BOLD signal is necessarily modulated at low frequencies.

when the average EEG power response resembles a box-car regressor or when the trials are short it might not be worthwhile to make separate regressors. If the average response resembles the box–car model (high colinearity), the average regressor has little statistical power.

In the case of short trial lengths the same problem arises. The BOLD response is a temporally smoothed and indirect measure of the underlying neural activity. Due to the filter characteristics of the hemodynamic response, the HRF convolved average power time-course will always resemble the HRF convolved box-car response. The total length of the BOLD response including the undershoot, is estimated to be in the order of tens of seconds, although the greatest dynamic variability (strongest response) occurs during the first 10-12 seconds. These characteristics imply that the BOLD-response acts as a temporal low-pass filter for all the underlying neural activity that is reflected in it (see Fgure 2.2). Therefore also the box-car model, the regressors modelling deviations in the average response and the trial-by-trial regressors must be 'filtered' (and temporally displaced, another characteristic of the BOLD response) by a hemodynamic response function. Since the short trials, because of their short length, can only contain high frequency deviations from the overall average response, these deviations will be largely filtered out after convolution with the HRF.

For these two reasons we did not construct regressors for the average power response in chapter 5. In this chapter the trials were relatively short (maximal 2.1 seconds), while the average power responses in the different frequency bands resembled a box-car model to a great extent.

Inference

Integration of EEG and fMRI as applied in this thesis has been restricted to correlational methods. As a consequence a causal relation between EEG and fMRI can not be directly inferred. Under some circumstances the case for a close and sometimes even causal relation between EEG power effects and the BOLD signal can be made. In the previous section of this chapter we showed how task related EEG power effects can be decomposed into several uncorrelated regressors that explain unique parts of variance in the BOLD signal. Regions where the task related EEG effect is related to the neural processes that give rise to the BOLD signal are expected to show a task effect in the BOLD signal that is similar to the effect present in the EEG (regressor I in figure 2.1). In addition these regions are also expected to show a relation to the regressor modelling the deviation in the average response (regressor II) as well as trial-by-trial variation (regressor III). The signs of the effects also should match: a positive average BOLD response in a region should co-occur with a positive relation of the BOLD signal in that brain region with regressors II and III. If all these effects are observed for

a certain brain region there is strong evidence that there is neural activity in this region that is closely related to the task induced effect in the EEG.

In chapter 4 this reasoning is applied to working memory related EEG power effects observed in the alpha and theta bands. We were able to find regions that showed this pattern, and that were therefore classified as being related to the working memory related EEG power effect. For both rhythms investigated, regions were observed that did not show the full expected pattern, but only a part of it. The reasoning explained above does not imply that there is no neural activity in these regions related to the EEG effect of interest. The previous section of this chapter explained that regressor II can lack statistical power if the average response resembles the box-car response to a great extent. In chapter 4 we therefore qualified regions that showed only a relation with regressors of types I and III as being related to the task related EEG power effects. Other deviations from the expected pattern implicate that there is less evidence for a strong link between the BOLD response in a certain region and task related EEG power effects. If only a relation of BOLD with trial-by-trial variations is observed for a region, this could be caused by the presence of two (or more) effects on the mean BOLD signal in opposite directions, but it could also be related to confounds in the trial-by-trial variation (e.g., other not fully unmixed EEG rhythms). Distinguishing between these two possibilities is in the context of the GLM as is it is used here is not possible.

Resting state is inherently an uncontrolled state, since there is no good knowledge on the mental activities of the subject. Consequently, the inferences that can be made from observed resting state EEG-BOLD correlations cannot be as strong as in a task context. This however does not imply that the results are of little value. In the last few years the number of resting state studies using fMRI alone has grown dramatically. These studies have identified several correlated networks each of which has been related to specific mental activities (Damoiseaux et al., 2006; Smith et al., 2009). Also resting state EEG shows certain typical features like posterior alpha and medial frontal theta rhythms. Resting state coregistration of EEG and fMRI provides a relatively easy means to explore whether and where the observed fMRI resting state networks are related to fluctuations in EEG power (Mantini et al., 2007), and which brain regions are related to pre-specified brain rhythms. In this thesis we followed only the last strategy, since we had a good idea in which brain rhythms we were interested. In chapter 3 we investigated the BOLD correlates of resting state frontal theta power, while in chapter 6 we investigated the central posterior alpha rhythm. A recent study not included in this

thesis (Sadaghiani, 2010) followed the first approach since we were interested in the EEG correlates of two fMRI-defined brain networks. We were able to show that the so called 'salience network' and the 'dorsal attention system' show differential correlational patterns with alpha and beta power. The results of this study and the two studies in this thesis show that these exploratory studies can yield interpretable results that can be further investigated in a more hypothesis driven way in a task context. It is however not a certainty that regions where the BOLD signal is found to be related to a resting state fluctuation in EEG power are also related to task manipulation of the very same rhythm. FMRI research has shown that only parts of a network observed in resting state might show effects of task manipulations (Fox et al., 2006).

A question that naturally arises from correlating EEG features with the BOLD signal, is whether the region(s) where BOLD is found to correlate with an EEG feature is also the source location of that feature. Since the results here are all based on correlations, a definitive answer cannot be given. Based on other converging evidence a good case can often be made whether one or more of the observed regions are also the likely source locations. A first idea can be obtained by comparing the scalp distribution of the EEG feature with the location of the effects observed with fMRI. Frontal regions are for instance very unlikely sources for posterior alpha rhythms, and can already be excluded on this basis. Further evidence can come from source analysis on the EEG features of interest, either on the same data, from other measurements, or from previously published work. If there is good concordance between regions obtained with source analysis and regions found through correlating EEG with the BOLD signal, this suggests that there is a direct relation between the EEG feature of interest and the BOLD signal. We most directly addressed this issue in chapter 5, in which we had good prior evidence from earlier MEG and fMRI research that the source location for the alpha, beta and gamma task effects was the same as for the activation observed with separately measured fMRI. This was also reaffirmed in our study by comparing the MEG source analysis of an experiment using an almost identical task with our observed fMRI effect. Moreover, we showed that there was significant correlation with trial-by-trial variation and EEG and fMRI for all three frequency bands. This makes it very likely that processes that give rise to the observed EEG task effects in alpha, beta and gamma power are indeed also expressed in the BOLD signal recorded form the source location. In addition, in all other chapters regions were observed that are good candidates for being the source location of the EEG rhythms of interest. On the other hand, also regions that are very unlikely source locations were found to be related to

certain EEG power changes. The evidence provided in this thesis, however, suggests that the neural processes that give rise to scalp recorded EEG power fluctuations are also closely related to the BOLD signal.

Independent Component Analysis

Independent component analysis (ICA) is a technique that falls in the category blind source separation techniques, which implies that it can separate data into source signals even if little is known about the exact nature of the underlying sources. It is therefore a general tool that also has applications outside neuroscience. In neuroscience it has been applied both to fMRI (Beckmann and Smith, 2005; Calhoun et al., 2001; Damoiseaux et al., 2006) and electrophysiological data (Makeig et al., 2004; Makeig et al., 2002; Onton et al., 2005) separately, but also as a way to directly integrate both modalities (Moosmann et al., 2008). In this thesis ICA is used as a preprocessing tool to obtain better estimates of single trial EEG power effects. The procedure we followed is similar to the one proposed by Debener et al. (Debener et al., 2006; Debener et al., 2005) for denoising single trial ERPs. In this section we shortly discuss the basic principles of ICA (for an introduction into ICA, see Stone, 2004).

The goal of independent component analysis is to uncover the underlying sources from a linear mixture of those sources represented in the recorded signals. In matrix notation this can be described as:

$$\mathbf{X} = \mathbf{AS} \qquad (1)$$

In which $\mathbf{X}$ is the *m* by *n* data matrix of rank *n*, $\mathbf{S}$ contains the *m* by *n* estimate of the maximally statistically independent sources and $\mathbf{A}$ is the *n* by *n* square matrix that mixes the underlying sources in the recorded data in $\mathbf{X}$.

What is actually solved by the various ICA algorithms is the inverse unmixing problem:

$$\mathbf{S} = \mathbf{WX} \qquad (2)$$

, where

$$\mathbf{W} = \mathbf{A}^{-1} \qquad (3)$$

24

The underlying assumptions of ICA are that the underlying sources are statistically independent, non-Gaussian, and mix linearly and, in the case of time series data like EEG also instantaneously, in the recorded signals. Two variables are statistically independent if one variable does not contain any information of the other variable. This is a stronger criterion than requiring that the sources are uncorrelated, since it also implies that all higher order correlations are zero. The formal mathematical definition is that two variables are statistically independent if and only if its joint power density function can exactly be reconstructed from the product of the two power density functions of the two variables separately:

$$p_{xy}(x,y) = p_x(x)p_y(y) \qquad\qquad (4)$$

The problem is that it is impossible to test whether the sources underlying the recorded data are truly independent. The different algorithms therefore use different measures which under certain assumptions are good approximations for independence. Under ideal (e.g., noise free) circumstances, most algorithms will usually yield very similar results.

One often used strategy is for instance to optimize non-Gaussianity of the underlying signal. This strategy is based on the central limit theorem that states that any mixture of random variables is more Gaussian than each of these variables themselves. All Gaussian variables are fully specified by their mean and variance and thus have the same value for all higher moments. The deviation of these moments from the value for a Gaussian variable can therefore be used as a parameter that can be optimized in the pursuit of the underlying sources. A good example is kurtosis, which basically is an index of the 'peakiness' of a variable's distribution. It turns out that many real world signals tend to have a peaky distribution, meaning that most observations are close to a certain value, while relatively few observations have values that are further removed from this value. In this thesis we use another implementation of ICA (extended infomax), which in stead of optimizing higher order moments like kurtosis works by maximizing the entropy of the source signals (Bell and Sejnowski, 1995; Lee et al., 1999). This algorithm has been shown to work well for EEG data (Makeig et al., 2004a). ICA has shown to be a suitable technique for analyzing EEG data since it can be regarded as a linear mixture of brain activity coming from several distinct regions and artifacts. Due to the blending of the electrophysiological signals from different brain regions and artifactual sources at channel level, interesting signals can be 'swamped' by
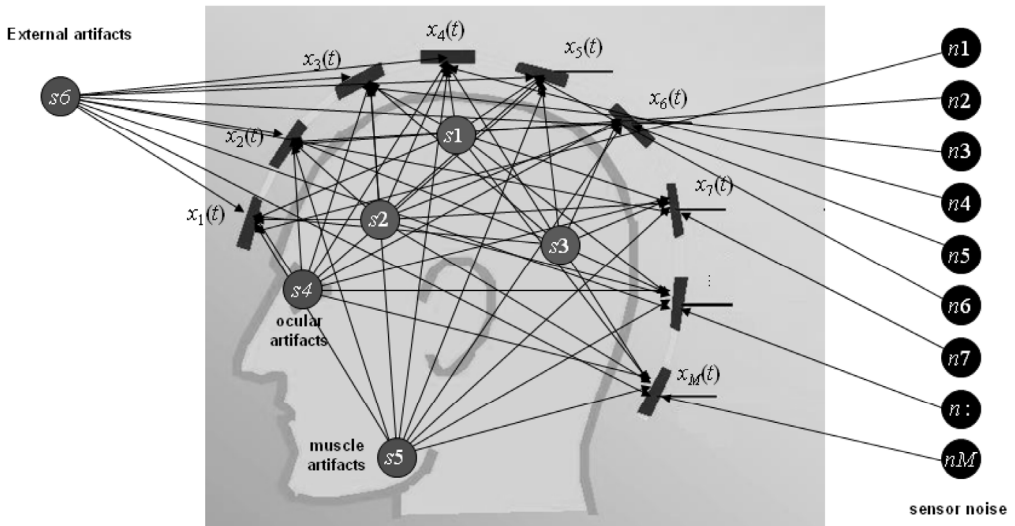
Figure 2.3 Propagation of electrophysiological signals and artifacts to scalp recorded EEG (or MEG). Electrical brain activity (green) and artifacts (red) are assumed to mix linearly to the electrodes at scalp level. The signal recorded at each electrode therefore is a mixture of different brain signals and artifacts. In this thesis we are interested in correlating only activity from one specific brain source (e.g. the source generating medial frontal theta power) on trial-by-trial level. On channel level uninteresting brain sources or artifact will however heavily affect single trial estimates of the signal of interest. If the assumption holds that the source signal of interest is statistically independent from the other brain activity and artifacts, independent component analysis can be used to get an estimate of the source activity of interest that is largely free of other brain activity and artifacts. The figure is kindly provided by Christian Hesse.

other more prominent brain activity or artifacts (see figure 2.3). By capturing the different brain rhythms and artifacts in different components ICA can uncover some of these interesting signals. This is of interest for simultaneously recorded EEG and FMRI since time point by time point or trial-by-trial estimates of features are heavily influenced by spurious electrophysiological activity and artifacts. Debener et al. (2005) demonstrated that ICA is able to remove or reduce the presence of these signals of no interest to a large extent by capturing the ERP of interest (the Error Related Negativity or ERN in this case) in one component, while ignoring the other components modelling non-interesting brain signals and artifacts. By using trial-by-trial variation in the amplitude of the ERN that was observed in one of the components, they were able to detect a region where the BOLD signal was related to the ERN.

In this thesis we used ICA in a similar way to obtain 'clean' estimates of EEG power. While applying ICA we observed that not all non-interesting features present in the

EEG recorded inside the MR scanner are easily captured in single components. Both residual MR gradient artifacts as well as residual cardio-ballistic artifacts are usually distributed over several components. This is due to the fact that both processes do not have a stable topographical distribution over time. These artifacts are therefore not one-dimensional and cannot be modelled as a single component. For the cardio-ballistic artifact this is related to the pulsating blood in the arteries that reaches the scalp under different electrodes at different moments. The residual MR gradient artifact is related to local disturbances (e.g. electrode movement) that affect electrodes differentially over time. However, despite these problems, we were still able to reliably separate the alpha and theta effects of interest from non-interesting signals and artifacts.

In chapter 4 we were able to select a component that captured the alpha effect from ICA in broad band filtered data. In chapters 3 and 4 we applied a band-pass filter around the theta band before running ICA. This strategy proved to be more successful in separating the frontal theta rhythm from other (noise) signals present in the same frequency band than applying ICA on broad band filtered data. This is likely related to the fact that theta is not as dominant in the EEG as alpha power. Since the dimensionality of all the underlying sources in the EEG recorded inside the scanner most likely exceeds the number of channels, the less prominent features in the EEG are not adequately unmixed from other features. By band-pass filtering the data around the frequency band of interest we reduce the dimensionality of the data and thereby increase the salience of in this case frontal theta oscillations before applying ICA. This positive experience prompted us to use the same strategy in chapters 5 and 6.

In chapter 5 band-pass filtering in combination with ICA dramatically increased the relative prominence of the gamma effect. However, we were not able to obtain a single component that modelled the posterior gamma increase here. The gamma increase was usually spread over a few components. Given the very strong presence of the gamma effects in these components, this is most likely not related to incomplete unmixing. The gamma effect seems to be present in multiple brain networks (e.g. the left and right visual cortices) and is strongly coherent between the different regions (see figure 2.4). As long as the phase difference between the gamma oscillations in the differed networks is not exactly 0 or 180 degrees the coherent activity cannot be captured in a one component, because of its multidimensional nature. In this situation ICA does not identify one component that captures the effect of interest, but a set of components that together span a subspace that captures the gamma effect. Since the axes of this subspace are not necessarily rotated such that they separate the different gamma rhythms coming
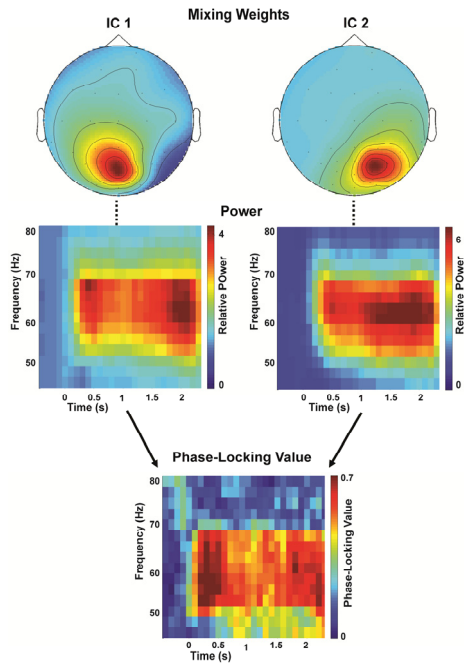
Figure 2.4. ICA source estimates of different unmixed components can be strongly coherent. The full captions can be found on page 29.
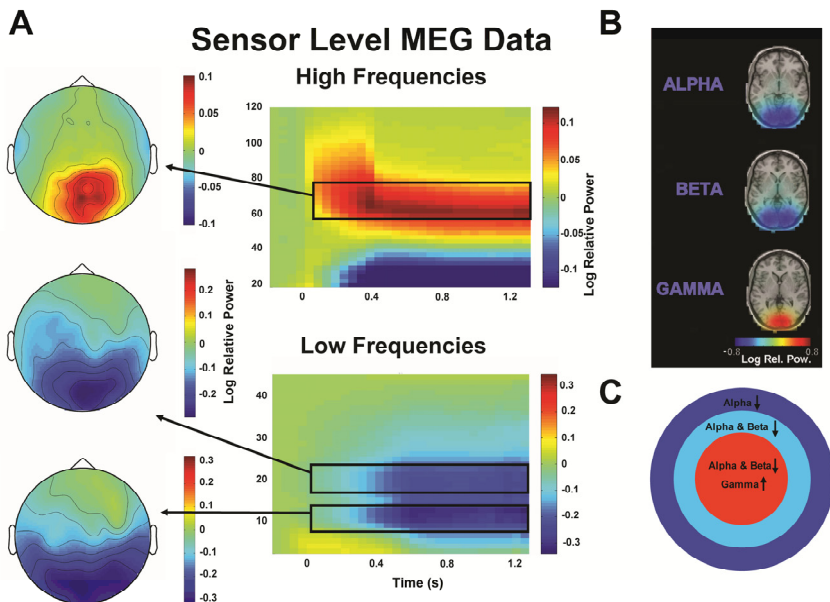

Figure 2.5. MEG data showing alpha, beta and gamma effects in chapter 5 largely overlap. The full captions can be found on page 29.

Figure 2.4 (page 28, top). ICA source estimates of different unmixed components can be strongly coherent. Unmixing the source signal of interest in a single component is not always possible. The task used in chapter 5 induces a strong gamma power response. This response however is usually not captured in one single component but shows up in multiple components (usually 2 or 3, maximally 5 in this chapter). This is related to the fact that this gamma band activity is present in multiple regions (e.g. left and right hemisphere). The gamma band activity generated in these regions is however very coherent. However, if the amplitude variation is not perfectly correlated and the phase lag not 0 or 180 degrees, the activity will be observed in multiple components. The data shown in this figure comes from a pilot subject performing the task described in chapter 5. Presented are the topographies and the time-frequency representations of power of two independent components that show a strong gamma increase. The bottom row shows the time-frequency representation of the phase-locking value between the two components. This shows a very large increase in phase-locking in the same time-frequency range as the power increase. A clear separation in left and right hemisphere components as in this figure was however not observed for all subjects. In these cases a subspace of multiple components can be identified that accounts for the signal of interest.

Figure 2.5 (page 28, bottom). MEG data showing alpha, beta and gamma effects in chapter 5 largely overlap. The topographies in panel A and the source reconstructions in panel B suggest that the gamma is generated in a sub-part of the cortex spanned by the decrease in beta and alpha power. Beta power decrease on its turn seems to be generated-in a sub-part of the cortex that also shows an alpha power decrease. This pattern is schematically depicted in panel C. This pattern illustrates why the ICA unmixing weights estimated on gamma band filtered data will also capture the alpha and beta decrease but unmixing weights obtained from data filtered in the alpha and beta weights do not adequately capture the gamma effect.

from the different regions, we back-projected the activity to channel level, and constructed our regressors from an average of the channels with the largest gamma effect.

In chapter 5 we re-used the unmixing weights obtained from data that was band-pass filtered around the gamma frequency, by applying them to the unfiltered data. In this case the unmixing weights function as spatial filters that enhance activity in other frequency bands that project in the same way onto the electrodes as the underlying gamma sources. There are two main reasons why we did this. The first reason is that the gamma band is spared from the ballisto-cardiac artefact. This is of high dimensionality and would therefore influence the unmixing negatively. By first band-pass filtering we could fully remove this artifact before applying ICA. The second and most important reason is that prior MEG measures suggest that the gamma power increase is nested within a larger region showing alpha and beta power decreases (see figure 2.5). Since low frequency EEG rhythms and artifacts are several orders of magnitude larger in amplitude than the gamma band response, the gamma band effect is almost never

unmixed into its own component(s) when ICA is applied on unfiltered data. Therefore, applying unmixing weights estimated on low-pass filtered or unfiltered data results in more gamma band noise that is mixed into the signal from channels where the gamma band effect is weak or virtually absent.

In this thesis we selected only the independent components that showed the power effects we were interested in. In conventional EEG research there would be a real danger in picking only the effects that suit the hypothesis best. The chance is great that the effect you observe then is largely based on a biased sampling of noise. There are two reasons why this is not a problem in this thesis. The first reason is that we do not select our components on the feature that we test for. What we finally test for is always the relation between EEG and BOLD, while we select our EEG components on EEG features only. Therefore, the selection of EEG components capturing a certain feature is independent from the relation this EEG feature has with the BOLD signal. Finding a significant relation between an EEG feature and the BOLD signal at group level implies that there is a systematic feature present in the selected components for the different subjects. The second reason is that in all cases we had very good prior knowledge about which features to select our components on. In chapters 3, 5 and 6 we used published data as prior knowledge to select our component of interest. In chapter 4 the prior knowledge consisted of effects observed in a separate recording session of the same subjects performing the same task outside the scanner, while we used MEG recordings using the same stimuli as prior knowledge in chapter 5. In all these chapters, we were able to show that the effects we observed in the components we picked were very similar to the effect we used as prior knowledge.

Chapter 3

FRONTAL THETA EEG ACTIVITY CORRELATES NEGATIVELY WITH THE DEFAULT MODE NETWORK DURING RESTING STATE

ABSTRACT

We used simultaneously recorded EEG and fMRI to investigate in which areas the BOLD-signal correlates with frontal theta power changes, while subjects were quietly lying resting in the scanner with their eyes open. To obtain a reliable estimate of frontal theta power we applied ICA on band-pass filtered (2-9 Hz) EEG data. For each subject we selected the component that best matched the mid-frontal scalp topography associated with the frontal theta rhythm. We applied a time-frequency analysis on this component and used the time course of the frequency bin with the highest overall power to form a regressor that modelled spontaneous fluctuations in frontal theta power. No significant positive BOLD correlations with this regressor were observed. Extensive negative correlations were observed in the areas that together form the default mode network. We conclude that frontal theta activity can be seen as an EEG index of default mode network activity.

INTRODUCTION

The simultaneous recording of EEG and fMRI signals has sharply increased in popularity over the last few years. While the initial efforts in this multimodal enterprise were aimed at solving technical problems stemming mainly from artifacts in the EEG generated in the MR environment (Allen et al., 2000; Allen et al., 1998; Bonmassar et al., 1999; Bonmassar et al., 2002), subsequent research has explored the relationship between EEG and BOLD from various vantage points. For instance, quite some effort has been devoted to identifying BOLD correlates of epileptiform EEG activity (Aghakhani et al., 2004; Al-Asmi et al., 2003; Benar et al., 2006; Lemieux et al., 2001; Salek-Haddadi et al., 2006; Salek-Haddadi et al., 2002). More recently, simultaneous EEG/fMRI has been successfully applied to investigate cognitive phenomena such as performance monitoring (Debener et al., 2005) and sustained attention (Eichele et al., 2005). Apart from epilepsy research most studies have focused on the BOLD correlates of ongoing oscillatory activity during resting state (i.e., recorded while the subject was quietly lying in the scanner, with no explicit task), focusing on the posterior alpha rhythm and, to a lesser extent, the beta rhythm (Feige et al., 2005; Goldman et al., 2002; Goncalves et al., 2006; Laufs et al., 2006; Laufs et al., 2003a; Laufs et al., 2003b; Moosmann et al., 2003). In these studies, the general idea has been that spontaneous fluctuations in the amplitude of a given oscillatory signal can be correlated with

spontaneous fluctuations in the BOLD signal. It has been suggested that such BOLD correlates are indicative of functionally connected brain structures that are related to the rhythmic neuronal activity observed in the EEG.

Studies investigating the BOLD correlates of spontaneous fluctuations in alpha activity (Feige et al., 2005; Goldman et al., 2002; Goncalves et al., 2006; Laufs et al., 2006; Laufs et al., 2003a; Moosmann et al., 2003) have shown that the expected posterior visual regions and also other regions across the cortex are negatively correlated with posterior alpha fluctuations. Recent findings suggest that there is considerable individual variation in areas that are observed to correlate with the alpha fluctuations and that these can be linked to differences in the total power spectrum of an individual (Goncalves et al., 2006; Laufs et al., 2006). Laufs et al. (2006) observed that negative alpha-BOLD correlations in posterior visual areas go together with relatively high theta power during alpha desynchronization, while relative high beta power during an entire session is related to negative alpha-BOLD correlations in regions thought to be related to attention in the parietal and frontal lobes. A few studies (Laufs et al., 2006; Laufs et al., 2003b; Moosmann et al., 2003) have also reported BOLD correlates of beta activity. Where Moosmann et al. (2003) observed mainly negative beta-BOLD correlations, Laufs et al. (Laufs et al., 2003b) reported positive correlations in regions that show an overlap with the default mode network (Fox et al., 2005; Raichle et al., 2001).

An interesting new avenue in the analysis of resting state data is to investigate which brain regions correlate with the oscillatory components associated with more specific cognitive operations. An example of such a component is the frontal theta rhythm, which is well known from both EEG and MEG literature. This component has a frequency range of roughly 3-8 Hz, and is most prominent over (midline) fronto-central electrodes. Frontal theta has been observed during various cognitive activities that require attention or short term memory (Burgess and Gruzelier, 1997; Inanaga, 1998; Laukka et al., 1995; Lazarev, 1998; Smith et al., 1999), and is often studied during mental arithmetic (Asada et al., 1999; Burgess and Gruzelier, 1997; Inanaga, 1998; Inouye et al., 1994; Iramina et al., 1996; Ishihara and Yoshii, 1972; Ishii et al., 1999; Lazarev, 1998; Mizuki et al., 1980; Sasaki et al., 1996; Smith et al., 1999). More recently, frontal theta power has been found to increase with working memory load (Gevins et al., 1997; Jensen and Tesche, 2002; Krause et al., 2000; Onton et al., 2005), indicating a possible role of theta oscillations in working memory maintenance. Source modelling attempts have localized the frontal theta rhythm to the anterior cingulate or the medial frontal cortex (Asada et al., 1999; Gevins et al., 1997; Ishii et al., 1999; Onton et al., 2005).

Interestingly, Mizuhara et al. (2004) as well as Sammer et al. (Sammer et al., 2007; Sammer et al., 2005) demonstrated that frontal theta increases can be observed in the EEG acquired during fMRI. Both Sammer et al. (2007) and Mizuhara et al. (2004) report positive correlations between BOLD and theta in the insula, hippocampus, superior temporal cortex, cingulate cortex and frontal areas while subjects performed a mental arithmetic. Where Sammer et al. (2007) reported only positive correlations, Mizuhara et al. (2004) reported predominantly negative correlations between frontal theta and BOLD in medial frontal, posterior cingulate, temporal and inferior parietal areas.

The present study aims at delineating the BOLD correlates of spontaneous fluctuations in frontal theta power, in a simultaneous EEG/fMRI setting. Srinivasan et al. (2006) report that theta power is highest at frontal midline electrodes in resting state, indicating that the frontal theta rhythm is also detectable outside task conditions. Since most studies investigating the relation between oscillatory activity and the BOLD signal used the resting state paradigm, we decided to follow this line of research. To our knowledge this is also the first time the relationship between frontal theta and the BOLD signal is studied in conditions where subjects did not perform a task. To this end, we first identify the theta rhythm in the EEG during an eyes open, resting state recording session. Subsequently we correlate the theta power with the BOLD signal. Separation of the frontal theta rhythm from artifacts and other rhythms in the theta frequency range with different spatial distributions is accomplished by applying independent component analysis (ICA). Previous studies (Makeig et al., 2002; Onton et al., 2005) have demonstrated that ICA can successfully be applied to EEG data to separate frontal theta activity from other (oscillatory) activity. Debener et al. (2006; 2005) demonstrated that ICA can be applied to EEG data measured in the MRI scanner to obtain single trial measures of evoked potentials that can be successfully correlated with the BOLD signal. Similarly, by correlating power fluctuations of the frontal theta components obtained by ICA with the BOLD signal in resting state, we hope to gain some insight into the neuronal structures that are associated with the frontal theta rhythm in humans.

METHODS

Subjects

Twenty right handed volunteers (17 female, 3 male, age range: 18-28) participated in the study after giving written informed consent. None had a neurological impairment, experienced neurological trauma or had used neuroleptics. The subjects were paid a small fee for their participation.

Design and procedure

Subjects came to the F.C. Donders Centre one hour before the scanning session started. First the electrode cap was applied and an instruction for a working memory task was given. While in the scanner, the subjects first participated in a working memory experiment for approximately one hour, divided in three blocks. After this experiment a resting state measurement was carried out in which subjects were asked to watch a black fixation cross presented on a grey background for 10 minutes. At the end of the scanning sessions a T1 weighted anatomical MRI was acquired. This anatomical scan is not used in the analysis of the fMRI data presented in this paper. Between measurements there were small breaks of a few minutes. Subjects were also allowed to go outside the scanner during these breaks. Only the data from the resting state session is used in the analysis presented here.

Electrophysiological recordings

EEG was recorded at 29 scalp sites (Fp1, Fp2, F3, F4, C3, C4, P3, P4, O1, O2, F7, F8, T7, T8, P7, P8, Fz, Cz, Pz, FC1, FC2, CP1, CP2, FC5, FC6, CP5, CP6, TP9, TP10) with a MR compatible BrainAmp MR amplifier (Brainproducts, Munich, Germany) and an MR-compatible electrode cap equipped with carbon wired sintered Ag/AgCl electrodes (Easycap, Herrsching-Breitbrunn, Germany). The reference electrode was located at FCz. To record the vertical EOG one electrode was placed under the right eye. The ECG was measured by two dedicated electrodes attached to the electrode cap. One electrode was placed on the sternum; the other electrode was placed on the clavicle, near the shoulder. A 250-Hz hardware filter was placed between the electrode cap and the amplifier. The EEG was recorded with a 0.16 s time constant and a 100 Hz low pass-

filter and continuously sampled at 5 kHz. Impedances were kept under 5 kΩ. All recordings were done with Brain Vision Recorder software (Brainproducts).

Image acquisition

MRI measurements were performed using a 1.5 T Sonata whole body scanner (Siemens, Erlangen, Germany). Functional images were acquired using a gradient echo EPI sequence (TR 2.34 s including 50 ms dead time; FOV=224 mm, TE = 30 ms, 33 slices, 3.0 mm slice-thickness with 0.5 mm slice-gap; voxel-size 3.5 x 3.5 x 3.0 mm).

MRI artifact removal

The EEG data were corrected for gradient and pulse artifacts along the lines described by Allen et al. (2000; 1998) using Vision Analyzer (Brainproducts). A 20-volume, baseline corrected sliding average was used for the correction of the gradient artifacts. In order to achieve this, 10 extra volumes were recorded before and after the 10 minutes of data used for analysis. After gradient correction the data were low-pass filtered at 100 Hz and down sampled to 500 Hz. The average pulse artifact was calculated based on a sliding average, time locked to the R-peak present in the bipolar derivation of the two ECG electrodes. This sliding average was scaled to an optimum least squares fit for each heart beat using the scaling option in Vision Analyzer before it was subtracted from the data. The data were subsequently rereferenced to a common average reference. The original reference channel was recomputed as FCz.

Regressor construction

Since we were specifically interested in frontal theta activity, and the recorded EEG is a mixture of artifacts and different theta sources, we applied infomax independent component analysis (ICA) (Bell and Sejnowski, 1995) on the entire 10 minutes of resting state data to obtain a 'clean' frontal theta estimate.
For this analysis a weight change of 10-7 was used as a stop criterion with the maximum number of iterations being 512. This proved to be sufficient to obtain a stable solution for the data from all subjects. To remove the residual gradient artifacts and low frequency noise as much as possible before applying ICA, a 2-9 Hz band-pass filter was

applied to the data. ICA was carried out in the Fieldtrip toolbox for EEG/MEG-analysis (FC Donders Centre for Cognitive Neuroimaging, Nijmegen, The Netherlands; see http://www.ru.nl/fcdonders/fieldtrip), using the runica algorithm (Makeig et al., 1997) implemented in EEGLAB version 5.03 (Delorme and Makeig, 2004). Both Fieldtrip and EEGLAB run under matlab (MathWorks, Natick, MA).

For each subject, the component with a topography that showed a dipolar pattern that best matched the fronto-central scalp distribution of the clusters of theta components reported by Makeig et al. (2002) and Onton et al. (2005) was selected for further analysis. If more than one component with a fronto-central distribution was observed, the component accounting for the most variance was selected (4 subjects in total). A time-frequency analysis of power was applied on the time series of the selected component. For this we used a multi-taper approach (Mitra & Pesaran, 1999). Power was analyzed from 1.25 - 10 Hz in 1.25 Hz steps for every 100 ms. Multitapering was performed with 800 ms time smoothing and 2.5 Hz frequency smoothing.

For each selected IC the time course of one frequency bin was used to form a regressor. This was done by selecting from the frequency bins centred on 3.75, 5 and 6.25 Hz the one with the maximal power. The maximum was based on the average power in these frequency bins over the 10 minute recording session. The entire time series for the selected frequency bin was extracted to form the basis for the regressor. First this time series was z-transformed. In order to remove artifacts, time points with a higher absolute z-score than 5 were set at zero. The high z-score of 5 was chosen because of the skewed distribution of values. The resulting time-series was again z-transformed before it was convolved with the canonical hemodynamic response function (HRF) implemented in SPM5 (Wellcome Department of Imaging Neuroscience, London, UK see: http://www.fil.ion.ucl.ac.uk/spm), resulting in an EEG-based regressor that models spontaneous fluctuations in frontal theta power (for a schematic representation of the regressor construction see figure 3.1).

FMRI analysis

Processing and analysis of the fMRI data were carried out in SPM5. The fMRI data was corrected for movements, corrected for differences in slice acquisition time, anatomically normalized to the canonical EPI template provided by SPM5 and smoothed with an isotropic Gaussian kernel (FWHM=10mm).
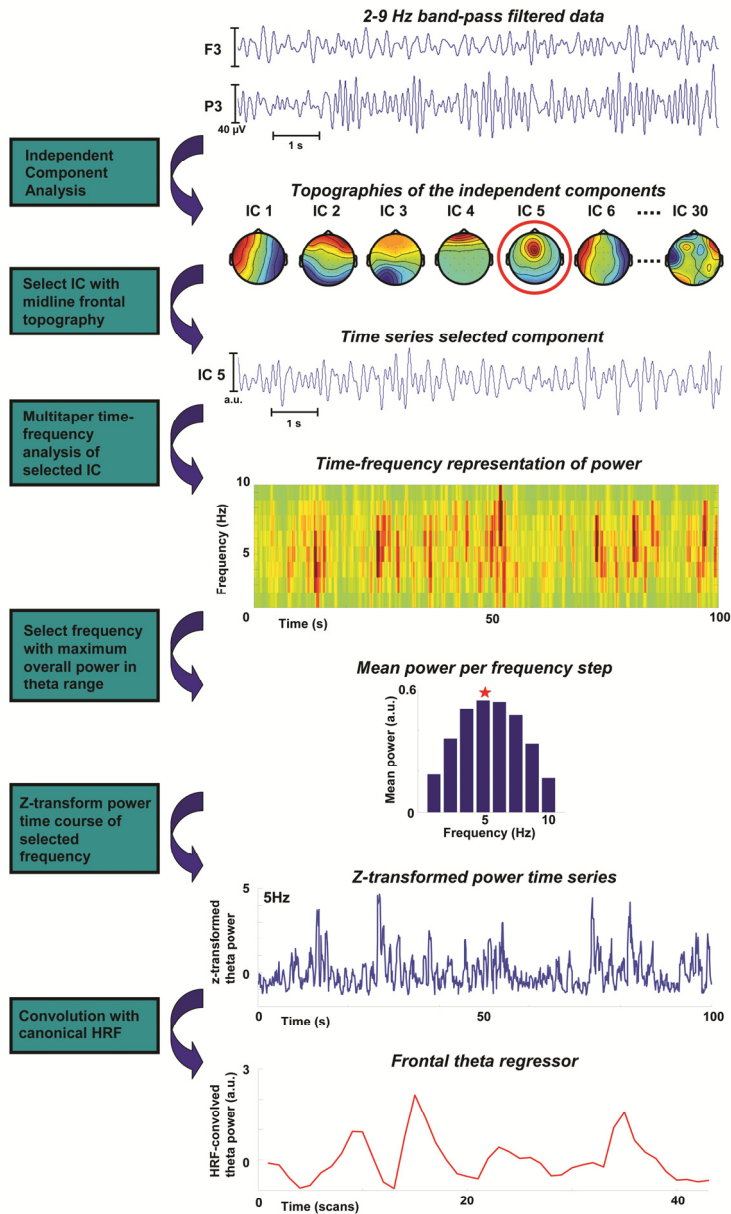
Figure 3.1. Schematic representation of the different steps in the construction of the regressor modelling fluctuations in frontal theta activity starting at the 2–9 Hz band-pass filtered data. This procedure is in more detail described in the Methods section.

A linear model was formed by the theta based regressor and the six movement regressors consisting of the realignment parameters provided by the realignment preprocessing step. At the group level, in a random effects analysis, the beta values associated with the theta regressor were tested against zero in a one sample t-test. We used a voxel-wise false discovery rate to correct for multiple non-independent comparisons (Benjamini and Hochberg, 1995; Genovese et al., 2002) at the 0.05 level. For the purpose of interpretation we only report clusters that contain >50 significant voxels.

Dipole fitting

We compared the brain regions that showed a theta-BOLD correlation with a source location associated with frontal theta based on the following dipole fitting approach. A single dipole was fitted to a grand average scalp topography using the Fieldtrip software. This grand average scalp topography was obtained by computing the average over the individual root-mean-square normalized topographies of the selected ICs mixing weights (see figure 3). As a head model, we used a standard realistic 3-compartment (brain/CSF, skull and skin) boundary element model (BEM) based on the MNI template brain (Oostenveld et al., 2001). In a first approximation the optimal location was found by fitting the dipole at each point of a grid with a resolution of 20 mm. Subsequently, the optimal grid coordinate was used as starting point for a more precise fit using a nonlinear search algorithm.

With this unconstrained fit we obtained an optimal dipole location that is located outside the clusters that show a significant BOLD-theta correlation (see results). To compare this location with possible locations inside the nearest BOLD-theta cluster, two constrained dipole fits were done. For the first constrained fit, the nearest significant voxel was determined. The amplitude and orientation was fitted for a dipole that was fixed at this position. In the second constrained fit, the amplitude and orientation were first fitted separately for each local maximum in the nearest BOLD-theta cluster. Subsequently, the optimal dipole localization that coincides with a local maximum in this BOLD-theta cluster was determined based on the residual variance.

RESULTS

Independent Component Analysis

The grand-average topography in figure 3.2a of the normalized mixing weights shows a clear frontal distribution that resembles the frontal theta component described by others (Makeig et al., 2002; Onton et al., 2005). In figure 2b the topographies of the selected component for each subject are depicted. Figure 2c shows the individual and grand-average spectra of the selected components with a clear peak in the theta frequency range at 6.5 Hz. This spectrum is based on the Fourier analysis of 2 s long Hanning tapered segments, resulting in frequency bins of 0.5 Hz. Note that the time-frequency analysis used in the construction of the regressor is not based on this frequency analysis.

FMRI analysis

No significant positive correlations with fluctuations in theta power were observed. However, a considerable number of brain regions across the cortex and the cerebellum were negatively correlated with frontal theta oscillations (see figure 3.3). A list of negatively correlating regions can be found in table 3.1. This list of regions indicates that in addition to a medial frontal region there is a network of brain regions across the cortex and the cerebellum that correlates with the spontaneous frontal theta power fluctuations observed in resting state.

Dipole fitting

The dipole fitting procedure yielded an optimal dipole location in the anterior cingulate cortex, (residual variance: 2,34%; MNI coordinates: -3, 29, 18; see figures 3.4 and 3.5). This location is just outside the region where the BOLD signal correlates significantly with the theta regressor. The dipole location is approximately 12 mm from the nearest significant voxel in the medial prefrontal BOLD-theta cluster (MNI coordinates: -4, 40, 24). A dipole restricted to this location results in a residual variance of 3.57%. The local maximum in the BOLD-theta cluster that explains the most variance of the EEG scalp topography was found at MNI coordinates -2, 56, 6 (residual variance 4.51%), which is 29 mm from the overall optimal fit.
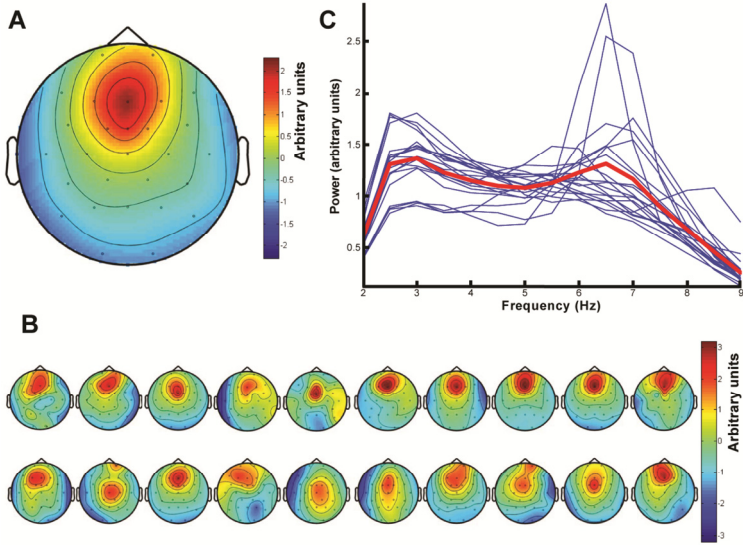
Figure 3.2. Grand-average scalp topography of root-mean-square normalized mixing weights of the selected independent components. B: Individual root-mean-square normalized scalp topographies of the selected independent component. C: Average (red) and individual power spectra of the time courses of the selected component. Individual spectra are normalized to the average power in the 2–9 Hz range.

Figure 3.3. Significant negative correlations with frontal theta power rendered on a standard MNI brain (A) and in saggital, transversal and coronal slices (B).

Table 3.1. Brain regions showing significant negative correlations with frontal theta power. Only clusters larger than 50 voxels are listed.

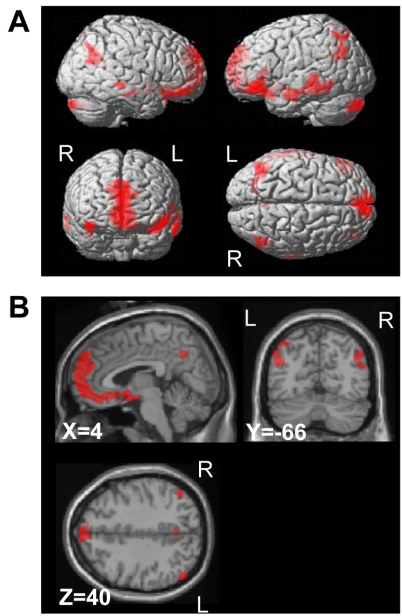| Brodmann area	Anatomical structure	Size (voxels)	MNI coordinates			t-value
			x	y	z	
9/10/32/12	Medial prefrontal cortex	4274	-6	20	-14	6.95
47/11	Left inferior frontal gyrus	879	-48	30	-14	6.28
21	Left middle temporal gyrus	874	-62	-2	-24	5.83
	Left cerebellum	601	-28	-88	-34	5.87
39	Left inferior parietal lobule/angular gyrus	489	-42	-68	28	4.42
47/11	Right inferior frontal gyrus	414	38	44	-18	7.41
39	Right inferior parietal lobule/angular gyrus	363	46	-64	36	4.20
	Right cerebellum	347	26	-90	-32	5.76
21	Right middle temporal gyrus	96	70	-32	-8	4.08
21	Right middle temporal gyrus	61	64	-16	-18	3.66
31	Right precuneus/anterior cingulate cortex	52	2	-60	38	3.67

DISCUSSION

In the present study, we used simultaneously recorded EEG and fMRI to investigate the BOLD correlates of spontaneous frontal theta power changes, while subjects were quietly lying in the scanner without performing any task. No significant positive correlations between frontal theta power changes and the BOLD signal were observed. Instead, we observed significant negative correlations in medial frontal regions, precuneus/posterior cingulate cortex and bilaterally in the inferior frontal, inferior parietal and middle temporal cortices as well as the cerebellum.

Together, these brain regions constitute the default mode network (DMN) as identified with PET and fMRI (Damoiseaux et al., 2006; Fox et al., 2005; Raichle et al., 2001; Shulman et al., 1997). This is an intrinsically correlated network of brain regions that is regularly observed to deactivate during attention-demanding cognitive tasks. Activation of this network has recently been linked to stimulus-independent thought, or in other words, mind-wandering (Mason et al., 2007). The presently observed negative correlation of frontal theta power with the DMN therefore suggests that frontal theta activity can be used as an index of DMN activity, at least in the resting state condition.
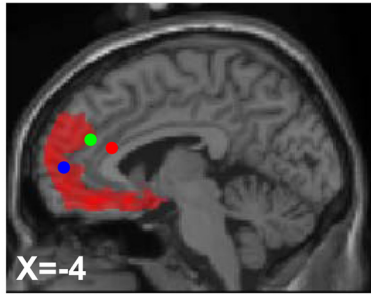
Figure 3.4. Dipole locations shown as dots on a saggital slice depicting the mid-frontal cluster of BOLD-theta correlations, for the optimal location (red), the nearest voxel showing a significant correlation with theta power (green), and the local maximum in the medial cluster with the lowest amount of unexplained variance (blue).
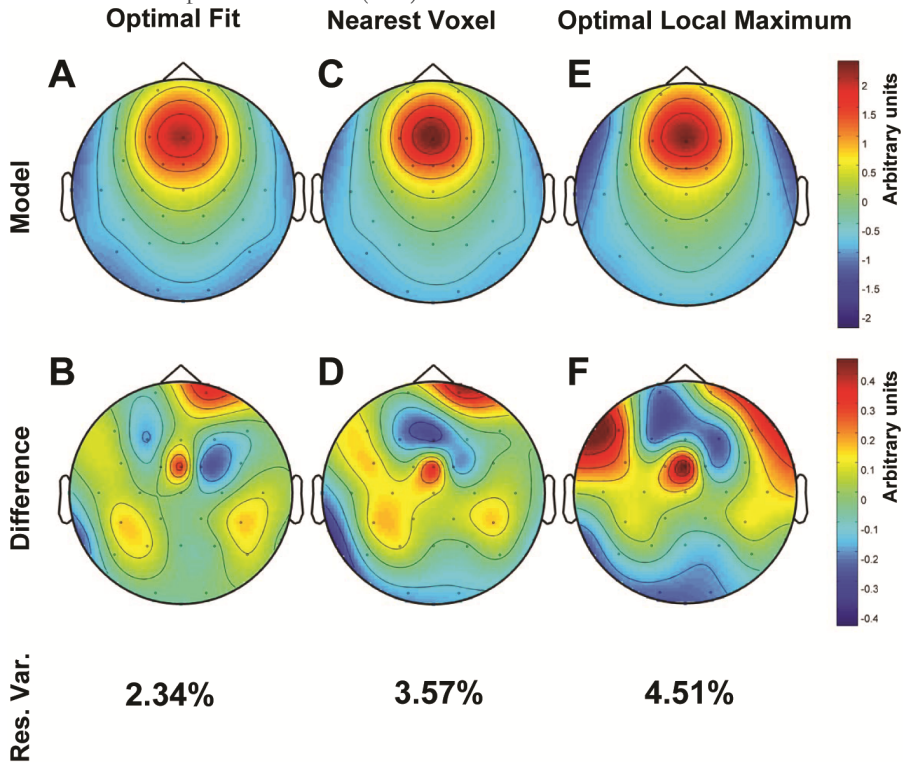
Fig. 3.5. Scalp topographies of the modelled part of the grand-average scalp topography of the normalized mixing weights (A, C and E) and the corresponding difference between the model and the grand average (B, D and F). A and B: Dipole explaining maximal amount of variance; C and D: dipole located at the significant voxel closest to the dipole location explaining the most variance; E and F: dipole located at the local maximum in the medial frontal cluster that explains the most variance. For the scalp topography to which the dipoles were fitted we refer to figure 3.2A

We envisage three possible accounts for the negative correlation between fluctuations in frontal theta and the BOLD signal in the DMN. The first possibility is that mid-frontal theta is not generated in any of the DMN regions. The negative correlations are observed in brain regions that respond with a BOLD-signal decrease to an increase in frontal theta originating from a region where no (significant) BOLD correlation was observed. In this case, the theta-generating process is different from activity in the DMN, although there is a systematic covariation between theta power fluctuations and the DMN. The second possibility is that one (or more) of the observed clusters, most likely the medial frontal region, is the source of mid-frontal theta. Because of the intrinsic correlations within the DMN, the other areas pertaining to this network also show a correlation with theta, although they do not by themselves generate theta-band activity. The third possibility is that the fluctuations in theta amplitude observed on the mid-frontal electrodes is a reflection of the fluctuations in theta present in all the clusters observed in this study. If this is the case, then theta-band activity is present throughout DMN, but the frontal theta source is the only part of the network that is readily detectable with scalp-recorded EEG.

There is some evidence supporting the second and third possibilities rather than the first. The first line of evidence is that it has been shown that the medial frontal cortex (our major cluster) is a likely source of frontal theta activity. Source modelling attempts have located the source of frontal theta effects in medial frontal areas (Asada et al., 1999; Gevins et al., 1997; Ishii et al., 1999; Onton et al., 2005). However, most of these attempts used equivalent dipole models and located the frontal theta in or near the anterior cingulate region, somewhat posterior and deeper than the observed medial frontal theta-BOLD cluster (Asada et al., 1999; Gevins et al., 1997; Onton et al., 2005). Also in our dipole modelling attempt the best fit was found for a dipole location in the anterior cingulate. However, for a dipole that is placed either at the nearest supra-threshold voxel or at the local maximum in the medial frontal cluster that explains the most variance, the dipole fit was qualitatively similar to the unconstrained fit. Interestingly, Ishii et al. (1999) used a beamformer approach on MEG data to estimate the location of the theta source, and located it in a region that largely overlaps with the medial frontal fMRI cluster observed in this experiment. If the cluster is the source location of the frontal theta activity, the substantial size of this cluster suggests a distributed source for frontal theta. The discrepancy observed here between the unconstrained fit and the medial frontal BOLD-theta cluster may be explained by the

fact that equivalent dipole models tend to estimate the source location too deep when there is in reality a more superficial distributed source (De Munck et al., 1988).

Another line of evidence suggests that amplitude increases in low frequency oscillations (e.g. delta, theta and alpha) are related to a decreased BOLD signal. Based on theoretical considerations, Kilner et al. (2005) suggest that higher energy dissipation, and therefore a higher BOLD-signal, is related to a relative shift in neuronal activity from lower to higher frequencies. This would result in, for instance, reduced delta and theta and increased beta and gamma amplitudes. A relative increase in theta oscillations could therefore lead to a decrease in the BOLD signal. Simultaneous recording of hemodynamic responses and intracortical electrophysiological responses in the visual cortex of cat (Niessing et al., 2005) and monkey (Logothetis et al., 2001; Shmuel et al., 2006) corroborate this notion. In the cat, Niessing et al. (2005) reported negative correlations in between lower frequencies (delta and theta) and the hemodynamic responses, and strong positive correlations with gamma band activity during visual stimulation. Shmuel et al. (2006) found that the negative BOLD response in the monkey primary visual cortex during partial visual field stimulation is accompanied with decreased neural activity in the gamma range (30-130Hz). Logothetis et al. (2001) showed that increased gamma band activity during visual stimulation is tightly coupled to the positive BOLD response. In addition, Mizuhara et al. (2004) found predominantly negative relationships between BOLD and frontal theta activity during mental arithmetic. Although, they did not identify these areas as part of the DMN, the pattern is quite similar to that of the present study. In contrast to the latter results, as well as the present results, Sammer et al. (2007) report only positive correlations with theta power. Evidence that an increase in high frequency oscillatory activity results in a BOLD increase in the DMN is provided by Laufs et al. (2003b), who report a positive correlation between beta (17-23 Hz) amplitude and the BOLD signal in the DMN. The relationship between activity in cortical networks, oscillatory activity and hemodynamic measures in these cases can however be more complex than explained above and more comprehensive spectral EEG information may need to be correlated with hemodynamic measures (Laufs et al., 2006).

More supporting evidence for a direct link between decreased DMN activity and increased frontal theta amplitude lies in the fact that both phenomena are observed in attention-demanding task conditions (for the DMN see Gusnard and Raichle, 2001; Raichle et al., 2001 for frontal theta activity see Burgess and Gruzelier, 1997; Inanaga,

1998; Ishihara and Yoshii, 1972; Laukka et al., 1995; Lazarev, 1998; Smith et al., 1999). It is, therefore, plausible that the inverse relationship also holds in these task conditions. Above we have presented evidence that suggests a direct link between decreased DMN activity and increased frontal theta amplitude. If this is indeed the case, a common functional interpretation is needed for both phenomena. Currently, the DMN is interpreted as a network of brain regions that is more active when one is not engaged in a cognitively demanding task, while the reverse holds when one is engaged in such tasks. A speculative hypothesis then is that the DMN operates in theta mode (which is reflected in the scalp EEG by an increase in frontal theta) when it becomes less active (i.e., during engagement in a task). This would not only explain the observed BOLD decreases during engagement in a task (Gusnard and Raichle, 2001; Raichle et al., 2001), but it would also explain why frontal theta power has been shown to increase in a wide range of cognitive tasks, such as mental arithmetic (Asada et al., 1999; Burgess and Gruzelier, 1997; Inanaga, 1998; Inouye et al., 1994; Iramina et al., 1996; Ishihara and Yoshii, 1972; Ishii et al., 1999; Lazarev, 1998; Mizuki et al., 1980; Sasaki et al., 1996; Smith et al., 1999), error detection tasks (Luu et al., 2003; Luu et al., 2004), language comprehension tasks (Bastiaansen et al., 2002; Hald et al., 2006) and working memory tasks (Gevins et al., 1997; Jensen and Tesche, 2002; Krause et al., 2000; Onton et al., 2005). However, although this suggestion would account for the observed pattern of theta power increases, it appears to contradict several previous functional interpretations that increased frontal theta oscillations reflect synchronous activity in brain regions that are involved in cognitively demanding tasks (Inanaga, 1998; Ishihara and Yoshii, 1972; Jensen and Tesche, 2002; Laukka et al., 1995; Onton et al., 2005; Smith et al., 1999). We feel that more experimental work is needed in order to differentiate between these two opposing possibilities.

The present study has focused on fluctuations in frontal theta power during resting state. There are also many other brain regions that display oscillatory dynamics in the theta frequency range (for a review see Kahana et al., 2001). It is possible that theta-band activity in different brain regions is associated with different types of neural and cognitive processes. In addition, the sign of the correlation between theta power and BOLD might differ between brain regions. For instance, in intracranial recordings in humans, Canolty et al. (2006) found a strong modulation of theta activity on gamma oscillations, but also reported a positive amplitude correlation between the two rhythms. Since gamma is demonstrated to correlate positively with BOLD (Logothetis et al., 2001; Niessing et al., 2005), and theta seems to correlate negatively with BOLD

(Mizuhara et al., 2004; Niessing et al., 2005; present study), it is difficult to predict the sign of the correlation between BOLD and theta or gamma. This illustrates that more insight is needed in how different oscillatory signals from different brain regions relate to the hemodynamic measures obtained by fMRI and PET. This will be crucial for linking the knowledge about cognitive processes obtained with electrophysiological and hemodynamic research methods.

Chapter 4

TRIAL-BY-TRIAL COUPLING BETWEEN EEG AND BOLD IDENTIFIES NETWORKS RELATED TO ALPHA AND THETA EEG POWER INCREASES DURING WORKING MEMORY MAINTENANCE

ABSTRACT

PET and fMRI experiments have previously shown that several brain regions in the frontal and parietal lobe are involved in working memory maintenance. MEG and EEG experiments have shown parametric increases with load for oscillatory activity in posterior alpha and frontal theta power. In the current study we investigated whether the areas found with fMRI can be associated with these alpha and theta effects by measuring simultaneous EEG and fMRI during a modified Sternberg task This allowed us to correlate EEG at the single trial level with the fMRI BOLD signal by forming a regressor based on single trial alpha and theta power estimates. We observed a right posterior, parametric alpha power increase, which was functionally related to decreases in BOLD in the primary visual cortex and in the posterior part of the right middle temporal gyrus. We relate this finding to the inhibition of neuronal activity that may interfere with WM maintenance. An observed parametric increase in frontal theta power was correlated to a decrease in BOLD in regions that together form the default mode network. We did not observe correlations between oscillatory EEG phenomena and BOLD in the traditional WM areas. In conclusion, the study shows that simultaneous EEG-fMRI recordings can be successfully used to identify the emergence of functional networks in the brain during the execution of a cognitive task.

INTRODUCTION

Working memory (WM) has been one of the central themes in cognitive neuroscience research for the past decades. A considerable number of studies have either used hemodynamic (e.g. PET and FMRI) or electrophysiological recordings (e.g. MEG, EEG, intracranial recordings). PET and fMRI have been successful in linking different brain regions to task and modality specific WM processes (Cabeza and Nyberg, 2000; D'Esposito et al., 2000; Fletcher and Henson, 2001). Across modalities and tasks, dorso- and ventrolateral prefrontal and posterior parietal regions have been often linked to WM processes (Cabeza and Nyberg, 2000). In recent years, regions in the medial temporal lobe have also been implicated in WM, suggesting WM and long term memory share in part the same neural substrate (Cabeza et al., 2002; Petersson et al., 2006; Piekema et al., 2006; Ranganath et al., 2005; Ranganath and D'Esposito, 2001).

The high temporal resolution of EEG and MEG makes it possible to study WM-related processes at a millisecond time-scale. WM-related increases in oscillations observed in

the EEG or MEG have been reported in the theta band (Gevins et al., 1997; Krause et al., 2000; Onton et al., 2005), alpha band (Jensen et al., 2002; Jokisch and Jensen, 2007; Klimesch et al., 1999; Schack and Klimesch, 2002; Tuladhar et al., 2007) and gamma band (Jokisch and Jensen, 2007; Kaiser et al., 2003; Lutzenberger et al., 2002; Tallon-Baudry et al., 1998). More specifically, parametric increases with WM load in the maintenance interval have been reported for posterior alpha (Jensen et al., 2002) and frontal theta power (Gevins et al., 1997; Jensen et al., 2002; Onton et al., 2005). Different functional roles have been proposed for these different frequency bands. Theta and gamma have been hypothesized to be a direct neural correlate of WM maintenance, possibly in cooperation with medial temporal structures (Jensen, 2006; Jensen and Lisman, 1998). Alpha power increases have been linked to active inhibition of neuronal activity that could otherwise disturb the WM process (Jokisch and Jensen, 2007; Klimesch et al., 2007). Differential alpha power effects can be seen in upper and lower sub-bands (Klimesch, 1999). Decreases in power in the lower alpha band have been linked to higher task demands and attentional processing, whereas decreases in power in the upper alpha band reflects have been related to increased declarative memory performance. Klimesch et al. (1999) observed an increase during WM maintenance of character strings and they suggest that this is related to inhibition of memory activities that could otherwise disturb the WM process.

Based on these previous findings the question arises whether the regions observed with PET and fMRI are also functionally related to the oscillatory phenomena as measured with MEG and EEG. To address this question, we simultaneously measured EEG and fMRI while subjects performed a modified verbal Sternberg WM task. By relating single trial estimates of WM related power increases to changes in the BOLD signal we hope to uncover which brain regions are functionally related to these WM induced power increases. Successful single trial coupling between EEG measures (ERPs) and the BOLD signal has been demonstrated by Eichele et al. (2005) and Debener et al. (2005).

The relation between alpha power on the one hand and the BOLD signal on the other hand has been investigated in previous studies. Posterior alpha is most prominent during eyes closed alert wakefulness, and usually decreases with increased visual processing (Klimesch, 1999). We therefore expected posterior alpha to correlate with the BOLD signal regions involved in visual processing. Posterior alpha has indeed been found to correlate with posterior visual areas in eyes closed resting state conditions (Feige et al., 2005; Goldman et al., 2002; Moosmann et al., 2003). More recently Laufs et al. (2006) and Goncalves et al. (2006) showed that the observed networks that correlate

with alpha power might depend on the relative strengths of other frequency bands in the entire power spectrum. Meltzer et al. (2007) showed in separate EEG and FMRI sessions, that load dependent increases in alpha power during WM maintenance correlate negatively with the midline parietal-occipital cortex across subjects.

Frontal theta is a prominent feature in the EEG that is reported to increase in tasks that require attention or WM. It is often studied during mental arithmetic (Inanaga, 1998; Inouye et al., 1994; Ishihara and Yoshii, 1972; Ishii et al., 1999; Lazarev, 1998; Mizuki et al., 1980; Sasaki et al., 1996; Smith et al., 1999), but more recently it has also been associated with WM maintenance (Gevins et al., 1997; Jensen, 2006; Jensen and Tesche, 2002). Recently, two studies investigated the BOLD correlates of frontal theta activity during mental arithmetic (Mizuhara et al., 2004; Sammer et al., 2007). While Sammer et al. (2007) reported only positive correlations between BOLD and theta in the insula, medial temporal lobe, superior temporal cortex, cingulate cortex and various frontal regions. Mizuhara et al. (2004) reported predominantly negative correlations in medial frontal, posterior cingulate, temporal and inferior parietal regions. In a recent resting state experiment we only observed negative correlations with frontal theta power in a collection of regions that together form the default mode network (DMN; (Scheeringa et al., 2008). This negative correlation between frontal theta and DMN activity was also observed by Meltzer et al. (2007) across subjects in a WM task.

Regions in which correlations between single trial EEG power measures and the BOLD signal are observed cannot be directly interpreted as being functionally related to the WM induced parametric power increases. The reason for this is that the relation between BOLD signal in a region, and single trial estimates of power could also be related only to task independent fluctuations in power. These task independent power fluctuations could be related to EEG activity coming from other sources than the one that shows a WM induced power change, that leak into the single trial estimates of power. Another potential source of task independent variation in power could lie in trial-by-trial coupling of task related regions with task unrelated regions, which has been observed between the motor cortices using fMRI (Fox et al., 2006). This task independent trial-by-trial coupling could possibly also be reflected in the trial-by-trial variation of EEG power components that do show an average effect of WM load. Therefore we argue here that regions functionally related to WM induced alpha and theta EEG power increases should show a BOLD response that is in line with the observed WM effects in these bands and also show a relation with the single trial variation in power.

METHODS

Subjects

Twenty right handed volunteers (16 female, 4 male, age range: 18-28) participated in the study. All subjects reported to be free of neurological or psychiatric impairment, experienced neurological trauma or from using neuroleptics. Subjects gave written informed consent prior to the measurements and all subjects were paid a small fee for their participation.
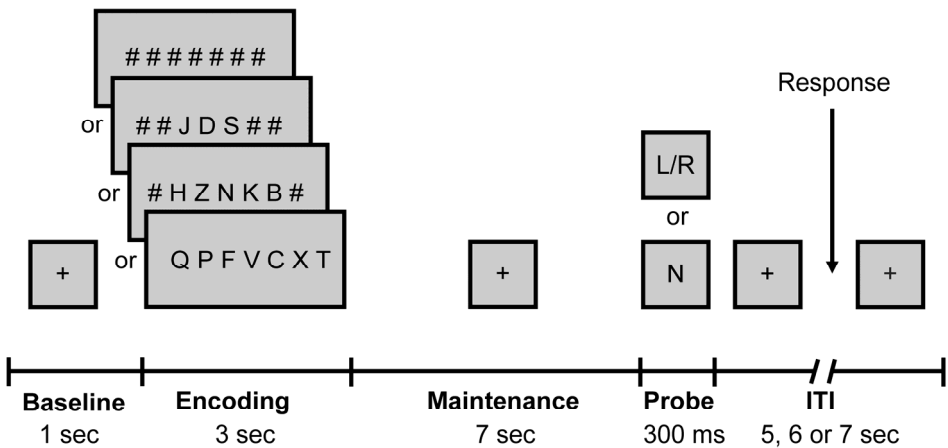
Figure 4.1. Schematic representation of the modified Sternberg paradigm used in this study. The task is described in more details in the Methods section.

Design and procedure

Subjects performed a variant of the Sternberg WM task (see also figure 4.1). They had to remember a string of 0, 3, 5 or 7 consonants that was presented for 3 seconds. When less than 7 consonants were presented, filler symbols (# 's) were added on the left and right side of the string in order to make the sensory input for the four conditions comparable. After a 7 second maintenance interval a probe was presented for 300 milliseconds. All responses were made with the right hand. Subjects had to press a

button with the index finger if the probe matched one of the consonants in the memory set, or with their middle finger if the probe did not match. When no consonants were presented during the encoding phase (i.e., the baseline condition), the probe consisted of either an L or an R, requiring a right handed index or middle finger response respectively. We avoided the use of the letters L and the R in the other WM conditions. Subjects were instructed to make fast and accurate responses. The inter-trial interval varied between 7, 8 and 9 seconds. A fixation cross was presented during the maintenance interval and the ITI. During the trial, the letters and the fixation cross were presented in black on a gray background. After the button press the fixation cross turned green, indicating the subject was allowed to make eye blinks. One second before the start of the next trial the fixation cross turned black again. Subjects were instructed not to blink from this moment until they had pressed a button.

All subjects participated in two experimental sessions. For both sessions, subjects read a written instruction before and after the application of the EEG electrodes. The first session took place in the EEG laboratory, the second session a few weeks later in the MR scanner where simultaneously EEG and fMRI were acquired. Each session consisted of three blocks with 72 trials each. Within each block, 18 trials of each WM condition were presented. Half of the trials in each condition required an index finger response (Match trials in Load 3, Load 5 and Load 7). For each WM load condition there were 18 trials in each block. One block took approximately 22 minutes. In the session inside the MR scanner, a 10 minute resting state measurement with simultaneous EEG and fMRI and a 10 minute anatomical MR scan were recorded after the three WM blocks. Prior to the start of each session subjects did a short practice block of eight trials, two for each WM condition. When necessary, subjects were allowed to do a second block of eight practice trials. The recording session in the EEG laboratory took approximately 1 hour and 10 minutes and the recording session in the MR scanner measurements took approximately 1 hour and 30 minutes.

Behavioural data

Repeated measures ANOVA's were carried out on the reaction times and on the numbers of errors. Factors were WM load (four levels: Load 0, Load 3, Load 5, Load 7) and response (two levels, index finger/match and middle finger/mismatch). The main and interaction effects were tested. Where appropriate, the Greenhouse-Geisser correction for non-sphericity was applied.

Electrophysiological recordings

EEG was recorded at 29 scalp sites (Fp1, Fp2, F3, F4, C3, C4, P3, P4, O1, O2, F7, F8, T7, T8, P7, P8, Fz, Cz, Pz, FC1, FC2, CP1, CP2, FC5, FC6, CP5, CP6, TP9, TP10) using an MR-compatible electrode cap equipped with carbon wired Ag/AgCl electrodes (Easycap, Herrsching-Breitbrunn, Germany). One additional electrode was placed under the right eye and vertical EOG was measured by calculating the bipolar derivation between Fp2 and this EOG channel, horizontal EOG was measured by calculating the bipolar derivation between F7 and F8. ECG was measured by two dedicated electrodes. One electrode was placed on the sternum and the other on the clavicle, near the shoulder. The ECG was calculated as the bipolar derivation between these two electrodes. A 250-Hz analogue hardware filter was placed between the electrode cap and the EEG amplifier (Brainproducts, Munich, Germany). The EEG was recorded with a 10 s time constant and a 100Hz low pass-filter and continuously sampled at 5 kHz. Impedances were kept under 5 kΩ. All recordings were done with Brain Vision Recorder software (Brainproducts). EEG recordings outside the scanner were performed in the same way as inside the scanner, except that the sampling rate was 500 Hz.

Image acquisition

MRI measurements were performed using a 1.5 T Sonata whole-body scanner (Siemens, Erlangen, Germany). Functional images were acquired using a gradient echo EPI sequence (TR=2.34 s including 50 ms dead time, TE=30 ms, 33 slices, 3 mm thickness with 0.5 mm gap, FOV=224mm, resulting in an isotropic voxel-size 3.5 by 3.5 by 3.5 mm) A 3D MPRAGE pulse sequence was used for the anatomical scan.

Analysis of EEG data

The EEG data recorded inside the MR scanner were corrected for gradient and pulse artifacts along the lines described by Allen et al. (2000; 1998) using Vision Analyzer (Brainproducts). The major residual scan artifact is determined by how many slices are acquired in one second. Measuring 33 slices in 2.29 s resulted in a main residual artifact

at 14.4 Hz and its higher harmonics, which spared the alpha (8-12 Hz) and theta (4-7 Hz) frequency bands that we were primarily interested in.

The data corrected for MR artifacts was subsequently low-pass filtered at 100Hz, downsampled to 500 Hz and re-referenced to a common average reference. The original reference electrode was recalculated as FCz, yielding a total of 30 EEG channels. In the subsequent step, residual eye blinks during the trial were corrected by applying the Gratton and Coles algorithm (Gratton et al., 1983). Subsequently, the trials were visually inspected for residual eye movements or other artifacts. Contaminated trials were subsequently excluded (9 % of the trials on average).

Time-frequency analysis using a multi-taper approach ((Mitra and Pesaran, 1999) was carried out with the Fieldtrip toolbox for EEG/MEG-analysis (FC Donders Centre for Cognitive Neuroimaging, Nijmegen, The Netherlands; see http://www.ru.nl/fcdonders/fieldtrip) running under Matlab (MathWorks, Natick, MA). The EEG power was analyzed from 1.25 - 20 Hz in 1.25 Hz steps for every 100 ms. Multitapering was performed with a 800 ms time smoothing and 2.5 Hz frequency smoothing. Time-frequency analysis of higher frequency bands (up to 100 Hz) indicated no observable WM modulations of power.

To reduce inter-subject variability and to normalize power changes across different frequency bands, power changes were calculated relative to a 0.5 s pre-trial baseline. The statistical significance of the WM load dependent power increases across the time frequency representations of these loads was evaluated by a cluster-based randomization procedure (Maris and Oostenveld, 2007). This test effectively controls the Type-1 error rate in a situation involving multiple comparisons. This procedure allows for the use of user defined test statistics tailored to the effect of interest within the framework of a cluster based randomization test. In our case we constructed a test statistic that reflected a parametric increase of power over WM loads.

First, for every electrode-time-frequency point the slope of the regression line fitted through the power values of the four loads was calculated. Subsequently, a one tailed single sample t-test was performed on these slopes (giving uncorrected p-values). All data points that do not exceed a pre-set significance level (here 5%) are zeroed. Clusters of adjacent non-zero data points in electrode-time-frequency space are computed, and for each cluster a cluster-level test statistic is calculated by taking the sum of all the individual t-statistics within that cluster. This statistic was entered in the cluster-based randomization procedure.

For comparison with the region of interest analysis of the fMRI data (see below) we also performed pair-wise comparisons for the average alpha and theta power during WM maintenance of the selected independent component (see below). For each subject we first averaged the relative power across all time steps in the maintenance interval for the frequency bin used for the construction of the EEG-based regressors. Subsequently we log transformed the EEG power data to make its distribution more Gaussian.

Since previous work showed the WM related alpha power increase is mainly observed in the upper alpha band, we performed an analysis for the alpha sub-bands for both channel level data, as well as for the selected alpha independent component (see below). For channel level data we chose channel O2, since the WM effect was maximal at this location. The alpha sub-bands were defined along the lines of (Klimesch et al., 1999). The individual alpha frequency (IAF) was determined by calculating the average power over all channels and over the 10 seconds spanning both the encoding and maintenance intervals. This 10 second window was subdivided in 5 segments of 2 seconds, resulting in a frequency resolution of 0.5 Hz. IAF was defined as the frequency with the largest power in the 8-12 Hz range. Subsequently the power was estimated for each load. For this, the middle 6 seconds of the retention interval were divided in 3 segments of 2 seconds, discarding the first and last 0.5 seconds. The alpha sub-bands were defined relative to IAF as follows: the lower-1 alpha band ranged from IAF-4Hz to IAF-2Hz; the lower-2 alpha band ranged from IAF-2Hz to IAF; the upper band ranged from IAF to IAF+2Hz. The power values for each frequency were normalized by dividing the power estimates for each load by the average power over the four loads. For the statistical analysis, a linear trend was fitted through the power values of the four loads for each subject separately. An increase in power with load should result in a significant positive slope, which was tested in a single sample one-tailed t-test. The false discovery rate (Benjamini and Hochberg, 1995) was used as a correction for multiple comparisons (FDR=0.05).

Except for the correction for MR gradient and pulse artifacts, pre-processing and time-frequency analysis for the data outside the scanner was the same as for inside the scanner.

Construction of EEG based alpha and theta regressors

Figure 4.2 presents a flow-chart of the preprocessing steps involved in the construction of the EEG regressor. To get denoised trial-by-trial estimates of the observed increase

in alpha and theta power during the maintenance interval (see results) we applied infomax independent component analysis (ICA) (Bell and Sejnowski, 1995) as implemented in EEGLAB version 5.03 (Delorme and Makeig, 2004). To obtain a component that modelled the WM alpha effect we low pass filtered under 25 Hz before applying ICA. For three subjects a 6-17 Hz band-pass filter was applied because none of the independent components showed clear increased activity in the alpha band during the maintenance interval when the low-pass filter of was applied. Frontal theta activity is in general less pronounced than the alpha activity, and therefore less likely to be separated from other sources and artifacts. For the construction of the theta regressor we therefore applied a 2-9 Hz band-pass filter prior to applying ICA to reduce the presence of other sources and artifacts in the analyzed data.

ICA was performed on the concatenated trials of all WM loads of all the three blocks. The trials started 2.5 seconds before onset of the encoding and ended 3 seconds after probe onset. A weight change of 10^{-7} was used as a stop criterion and the maximum number of iterations set at 512.

The same multitaper technique with the same time and frequency smoothing as applied on the channel-level EEG time series was also applied on the independent component-level time series. Subsequently the average time-frequency representation of power was calculated for each component for each WM load separately. For each subject one component for each frequency band was selected based on (i) the presence of an (parametric) average alpha or theta WM effect during the maintenance interval and (ii) a topography of the mixing weights that resembled the topography of the effects observed both inside and outside the scanner. In the situation where more than one component passed these criteria, we chose the component that explained the most variance in the channel level data (4 times for alpha, 2 times for theta). Significance of the alpha effect in the ICA data was assessed with the same cluster randomization technique as described above, except that only clustering in the time and frequency domains was used, since the selected component activity was a weighted mixture of all channels.

For the alpha effect, the peak frequency in the 7.5-13.75 Hz range of the selected IC was determined by calculating the average power over time and WM loads for each frequency bin during WM maintenance. The frequency with the highest average alpha power was selected to represent the trial-by-trial variation in alpha power, since the multitaper approach already integrated the power over a 5 Hz frequency range for each frequency step. The same procedure was followed for the theta effect in the 3.75-7.5 Hz
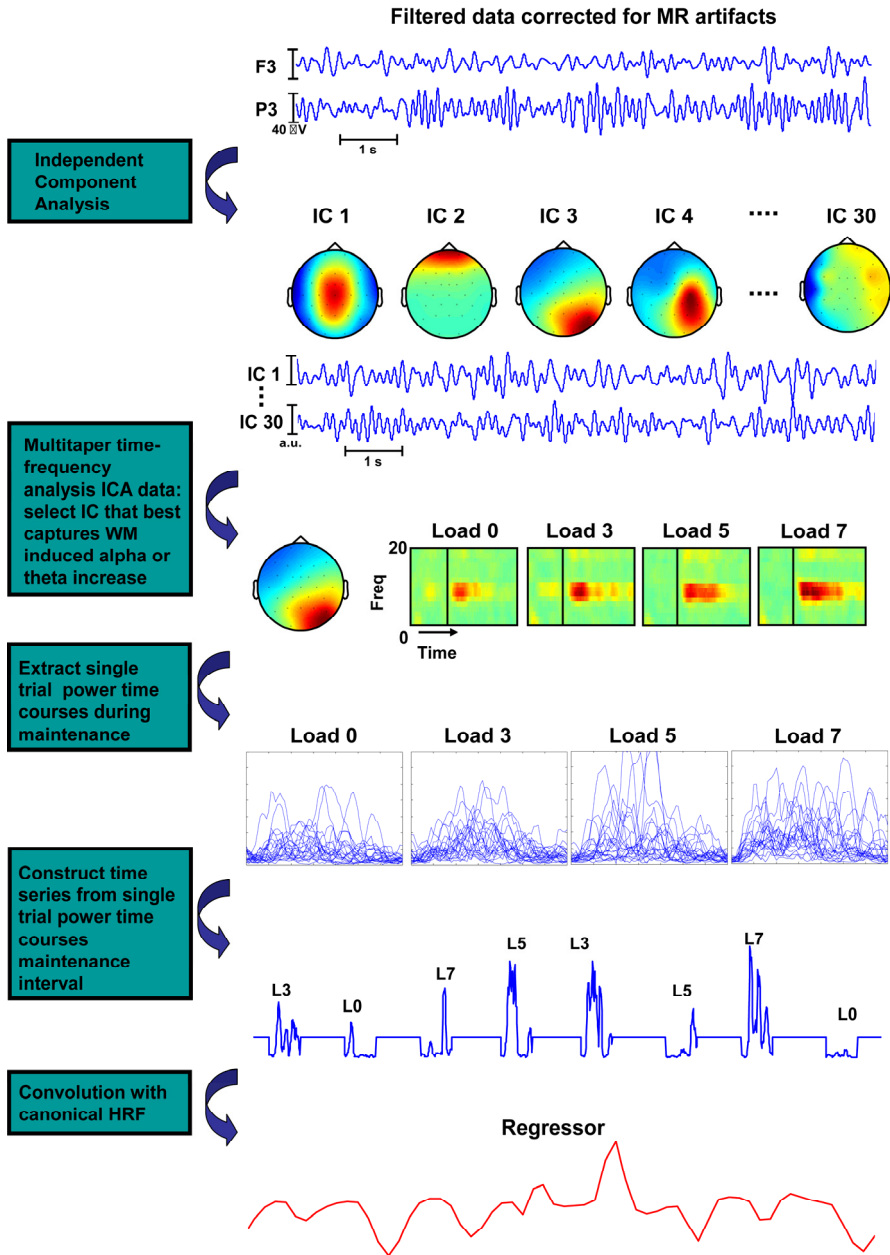
Figure 4.2. Schematic representation of the construction of the regressor modelling trial-by-trial variation in alpha or theta power in the WM maintenance interval. In the example we selected an alpha component, but theta components were selected in the same way. For regressors modelling the average power response, the average power time was inserted in stead of the single trial power time courses. This procedure is described in more detail in the Methods section.

range. For both frequency bands the individual average power time courses and the single trial power time courses during the maintenance interval of the selected component constitute the basis for two regressors.To construct the first regressor, the power values across all trials and WM loads within one block of trials were first z-transformed. For the trials that were excluded at the artifact rejection stage, the average power response of that WM load was used. The z-transformed single-trial power time series were then used to construct a time series that contained zeros outside the maintenance intervals. This time series was convolved with the canonical hemodynamic response function (HRF) from SPM5 (Wellcome Department of Imaging Neuroscience, London, UK; see http://www.fil.ion.ucl.ac.uk/spm) and resampled to obtain a single sample for every fMRI volume. This regressor was constructed for both the alpha and theta effect. Since these regressors reflect the variability of power across trials, they are termed $TRL\alpha$ and $TRL\theta$.

For the second regressor, the individual average power response across trials for each WM load was used instead of the single trial power time-courses. Z-transformation, convolution and re-sampling was carried out in exactly the same way as for the first regressor. This regressor models the individual subjects' average alpha and theta response for each WM load and is therefore termed $AVG\alpha$ and $AVG\theta$ for alpha and theta respectively.

FMRI model construction

Preprocessing and analysis of the fMRI data was carried out in SPM5. The fMRI data was corrected for subject movement, corrected for differences in slice acquisition time, anatomically normalized to the canonical EPI template provided by SPM5 and smoothed with an isotropic Gaussian kernel of 10 mm full-width-at-half-maximum.

For the standard analysis a general linear model was constructed. Box-car functions convolved with the canonical HRF were used to model the encoding, retrieval and inter-trial intervals. Different functions were used for the different WM loads in the encoding and maintenance intervals. The retrieval interval was defined as the time between probe onset and the button press. The realignment parameters were added to control for movement related effects. Erroneous trials were modelled by separate regressors. The Load 3 versus Load 7 contrast was used to assess which regions were activated. An uncorrected voxel level threshold of 0.001 was used with a cluster level threshold of 0.05 corrected for multiple comparisons. This analysis was complemented with a ROI

analysis over all the levels for the significant regions obtained in this contrast. Since the Load 3 versus Load 7 contrast already indicates a WM effect on BOLD, only repeated contrasts were computed (e.g. Load 0 vs. Load 3, Load 3 vs. Load 5 and Load 5 vs. Load 7) between the average regression coefficients (so called beta weights) related to the regressors of the four WM loads.

In the first model that included EEG regressors (Model I) the box-car regressors modelling the maintenance interval were replaced by either TRLα or TRLθ. All the other stages of the trial were still modelled with HRF convolved box-car functions. The realignment parameters were again added to control for movement related effects. Second level single sample t-tests were used to test for regions showing a significant relation to TRLα and TRLθ. Significant clusters were identified as those clusters passing an uncorrected voxel level threshold of 0.001, and a corrected cluster-level threshold of 0.05 (Gaussian random field correction).

The explained variance in the TRLα/θ regressor Model I is a sum of variances that could also be related to (1) box-car regressors modelling the maintenance interval, (2) the average individual power time course for each WM load and (3) the trial-by-trial variation in power. A Gram-Schmidt orthogonalization procedure was followed (for similar use see (Eichele et al., 2005)) to obtain uncorrelated regressors that model these three sources of variance. The regressors included in the design matrix of Model II consists of (1) HRF convolved box-car functions for all the different stages of the trial, (2) the AVGα/θ regressors orthogonalized to these box-car regressors and (3) TRLα/θ regressors orthogonalized to both box car regressors and AVGα/θ regressors. The realignment parameters were also included. The clusters where the BOLD signal was found to be related to single trial alpha and theta estimates in Model I were used as the templates for regions of interest (ROI) analyses on which the analyses in Model II were based. All effects were tested on group level and based on the beta weights associated with the regressors introduced here.

If a region was functionally related to the observed WM-induced theta or alpha increases, it should in theory show an effect when analyzed with all three orthogonalized sets of regressors. That is, the regions should show a parametric BOLD response (as analyzed by the box-car regressors) that is in line with the parametric increase in alpha or theta power. If we assume that the average deviation from the box-car response was reflected in the BOLD signal and there was variation in the strength of the response over trials that was also related to the BOLD signal, these regions should show a significant relation to the orthogonalized AVG and TRL regressors respectively. The

parametric WM effects for the ROIs were tested for a linear trend over loads, followed up with repeated contrasts between the levels to indicate where and how the pattern deviated from a linear increase with load. The significance of the relation between the ROIs and the orthogonalized AVGα/θ and orthogonalized TRLα/θ was then assessed by single sample two sided t-tests. If the BOLD response in a region is related to WM induced power increases, the sign of this relation should be consistent for the regressors modelling the three sources of variance. This means that a positive parametric BOLD effect observed in a region should go together with a positive relation between BOLD and the orthogonalized AVG and TRL regressor.

In practice it was found that the orthogonalized AVG regressor can lack sensitivity and statistical power. Since the WM related alpha effect decreased during the maintenance interval, the AVGα also mostly models decreases, while the average theta response after convolution with the HRF does not deviate much from the HRF convolved box-cars. We therefore consider regions to be functionally related to the WM load-related alpha and theta power increases if they show a significant parametric BOLD modulation with WM load, as well as a significant relation with the orthogonalized TRLα/θ regressors.

RESULTS

Behavioural data

Analysis of variance of the reaction time data reveal significant main effects for the factors Load $(F(3,57)=48.14, p<0.001)$ and Response Finger (Match and Mismatch) $(F(1,19)=18.40, p<0.001)$. A significant Load by Response Finger $(F(3,57)=4.26, p<0.05)$ interaction effect is observed.

The main effect of Load is related to an increase of reaction time with WM load. (linear contrast: $(F1,19)=59.97, P<0.001$) The main effect of Response finger is related to a faster response to match/index finger responses than to mismatch/middle finger responses. The Load by Response Finger interaction effect indicates that the difference is only present in the Load 3, Load 5 and Load 7 conditions. Simple main effects also indicate this (see figure 4.3A). The difference is not significant for Load 0 $(t(19)= 0.78$, not significant) but is significant for Load 3 $(t(19)=4.58, p<0.001)$, Load 5 $(t(19)=4.71, p<0.001)$ and Load 7 $(t(19)=2.511, p<0.05)$. These results are in line with previous behavioural results on Sternberg WM tasks.

Figure 4.3B shows that the number of errors significantly increased with WM load ($F(3,57)=17.36$, $p<0.001$), and significantly more errors were made in the match than mismatch condition ($F(1,19)=6.04$, $p<0.05$). A significant linear trend is observed for the increase in the number of errors with load ($F(1.19)=31.68$, $p<0.001$). Figure 3B suggests the difference in the number of errors between match and mismatch trials might have increased with load. However, the Load by Response interaction effect shows this effect is only marginally significant ($F(3,57)=2.93$, $p=0.07$). Simple main effects however reveal significantly more errors for Match trials in load 7 ($t(19)=2.35$, $p<0.01$), but not in the other load conditions (Load 0: $t(19)=-0.57$, not significant; Load 3: $t(19)=1.57$, not significant; Load 5: $t(19)=1.39$, not significant).
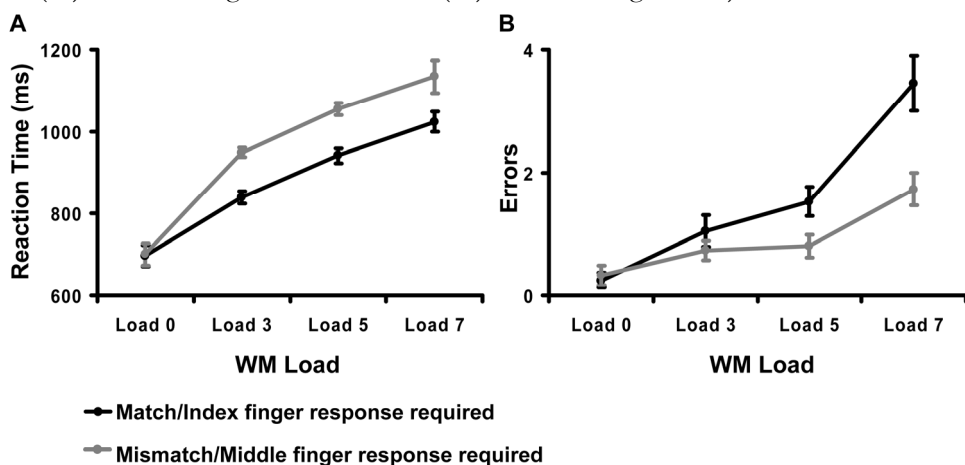

Figure 4.3. Results of the analysis of the behavioural data of the session inside the MR canner. (A) Average reaction time for the different loads and response fingers. (B) Average number of errors for the different loads and response fingers. Error bars indicate the standard error.

EEG data

Figure 4.4 shows a parametric increase of alpha power with WM load during maintenance on right posterior electrodes for the data outside the scanner, for the data recorded inside the scanner and for the selected independent components from the data inside the scanner. The results displayed in first two columns of figure 4.4 indicate that inside and outside the MR scanner qualitatively the same parametric alpha increase was measured. Figures 4.4H and 4.4I illustrate a clear increase in the relative power during WM maintenance after ICA. This indicates that ICA separates the right posterior alpha effect from other components that contributed to this frequency band, and as a
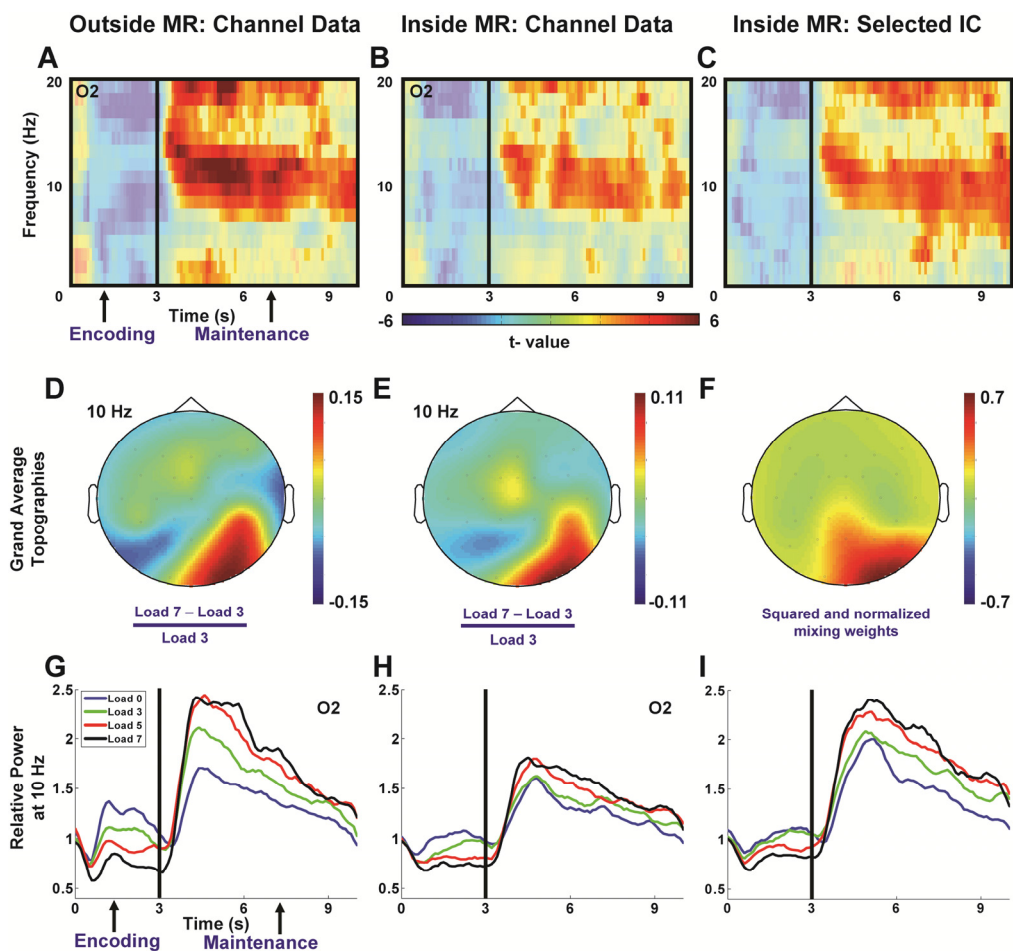
Figure 4.4. Results of the EEG channel data measured inside and outside the scanner and the ICA data inside the scanner for the posterior alpha effect. Panels A–C show in a time frequency representation the t-value of the slope through the WM loads for each time frequency point. Bright colours indicate a significant positive slope and therefore a significant increase of power with WM load. Significant increases of alpha power with WM load were observed for the channel data measured outside (A) and inside the scanner (B) and for the selected IC (C). Panels D–F illustrate the topographical distributions of these effects. Panels D and E were calculated by dividing the power difference in the maintenance interval between Load 7 and 3 by the power in Load 3. Panel F was constructed from the average of the squared individual mixing weight normalized to the maximum. Panels G–I show the power time course at 10 Hz for the channel data outside (G) and inside (H) the scanner and the selected IC inside the scanner (I). The power is relative to a 500 ms pre-trial baseline. The increase in signal to noise gained by ICA is illustrated here by the increased relative power during the maintenance interval at 10 Hz in panel I compared to panel H. For the channel level data in panels A, B. G and H channel O2 is shown.
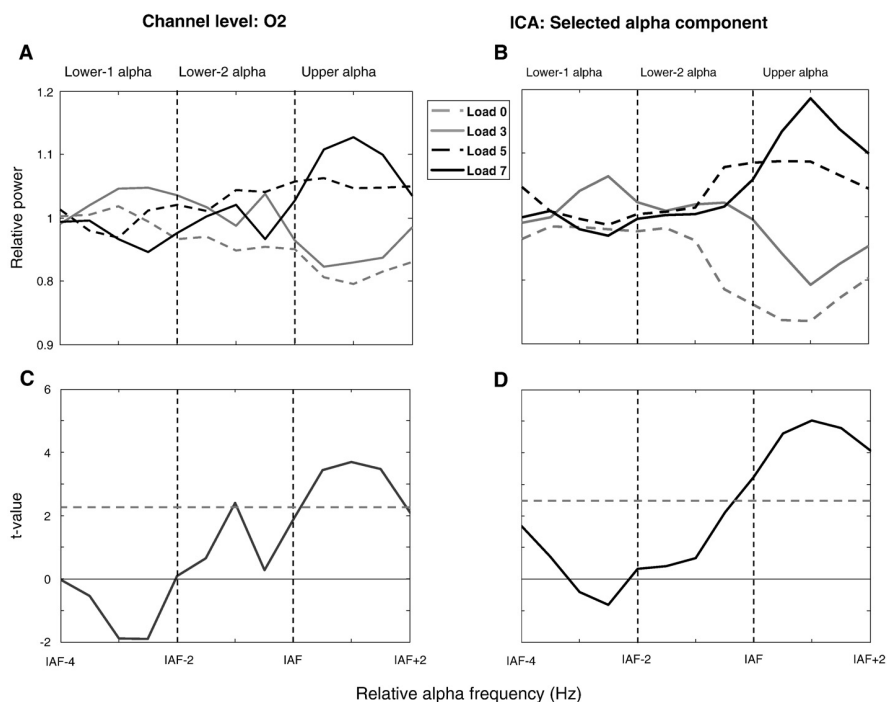
Figure 4.5. The effect of WM load on alpha power in the maintenance interval for the alpha sub-bands. The frequency axis is relative to the individual alpha frequency (IAF). A and B show the relative power values from IAF−4 Hz until IAF+2 Hz for the four WM loads for channel O2 and the selected alpha IC respectively. Similarly, panels C and D show the t-values for the single sample t-test applied on the slope through the four Loads for each frequency bin. Values above the dashed red line are significant after correction for multiple comparisons.

consequence increases the signal to noise ratio. Pair-wise comparisons for the average alpha power during WM maintenance reveal significant differences between Load 3 and Load 0 and between Load 5 and Load 3, but not between Load 7 and Load 5 (see figure 9I). The analysis for the different alpha sub-bands reveals, that both for channel level and the IC data, the increase of alpha power with load can mainly be attributed to the effect in the upper alpha band (see figure 4.5). The average individual alpha frequency is observed at 9.5 Hz (SD= 0.8 Hz).

Figure 4.6 shows the results for the frontal theta effect in a similar way as figure 4 does for right posterior alpha. Also the frontal theta effect can be observed outside as well as inside the scanner. The topographies clearly show the mid-frontal distribution associated with frontal theta (see Makeig et al., 2002; Onton et al., 2005). Applying ICA again
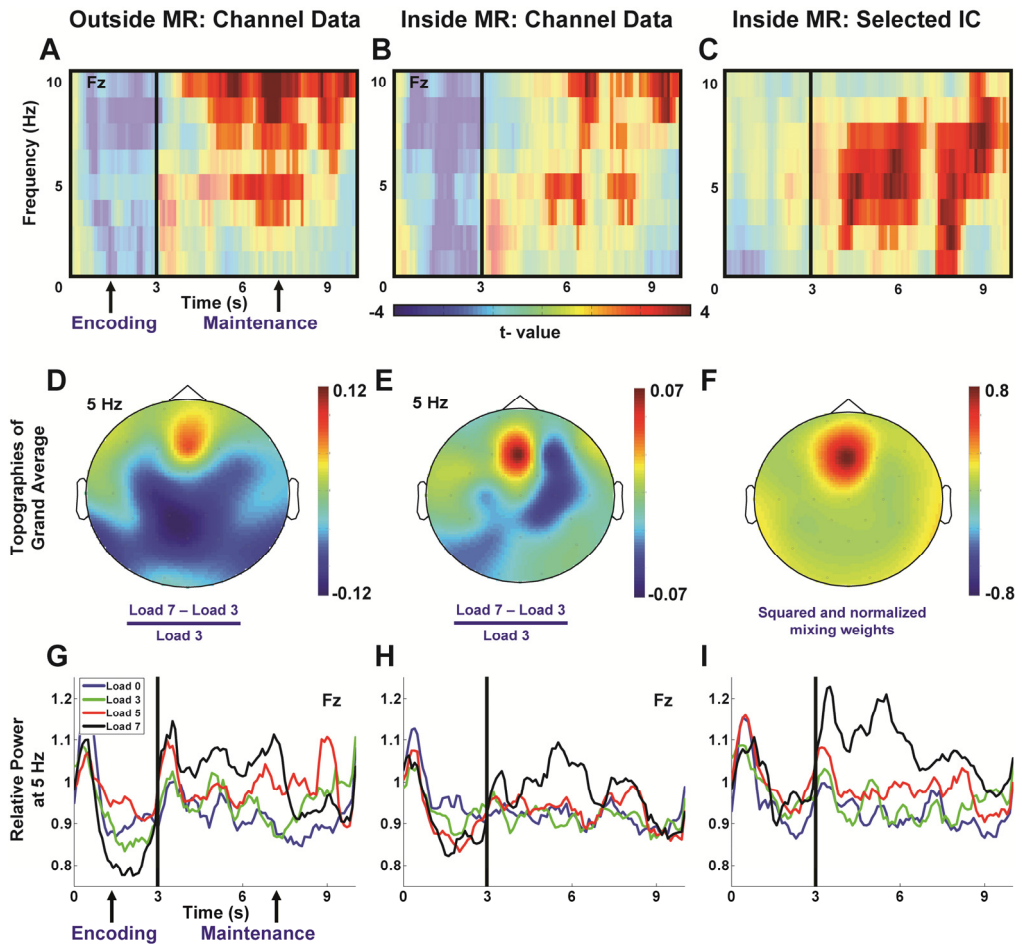
Figure 4.6. Similar as figure. 4.4, but then for the frontal theta effect. Here ICA not only increased the relative power, but also the extent of the significant WM effect in panel C.

increases the signal to noise ratio as expressed in a relative power increase. In this case ICA also leads to a better contrast between the four loads (see figure 4.6I). Pair-wise comparisons for the average theta power during WM maintenance reveal significant differences between Load 5 and Load 3 and between Load 7 and Load 5, but not between Load 3 and Load 0 (see figure 10I).

For the EEG data recorded inside the scanner correlations were computed between reaction time and the average relative alpha and theta power during the maintenance interval for the selected independent component (see figure 4.7). This was done for each WM load separately. Significant (two sided) negative correlations between reaction time

Figure 4.7. Correlations between reaction time and relative power across the maintenance interval for the four WM loads for the selected frequency bin of the selected IC for both right posterior alpha (A–D) and frontal theta (E–H).
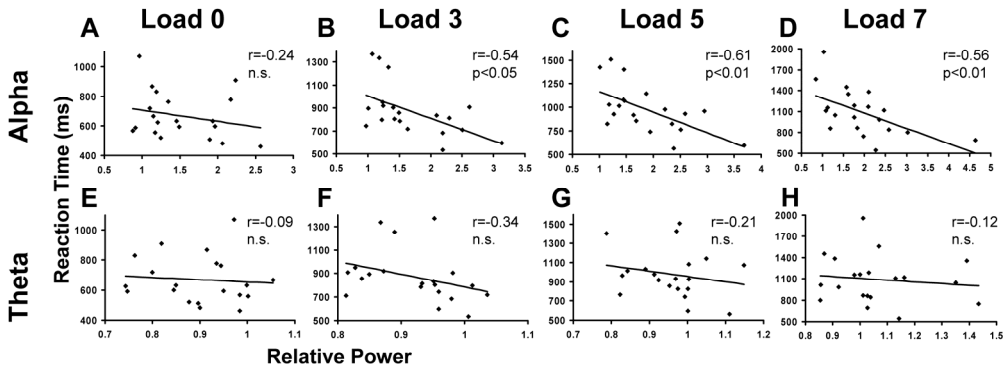
and alpha power in the maintenance interval are observed for Load 3, 5 and 7. For theta power no significant correlations with reaction time were observed.

FMRI data

Conventional fMRI analysis

The Load 7 versus Load 3 contrast shows significant clusters of activity in the right dorsolateral prefrontal cortex (DLPFC), medial frontal cortex, left inferior parietal lobule and a left lateralized cluster spanning the left ventrolateral frontal cortex, a part of Broca's region and the insula (see table 4.1 and figure 4.8). At a higher voxel-level threshold (p=0.0001, uncorrected for multiple comparisons) this cluster splits in two clusters (results not shown) that are significant at cluster level (corrected for multiple comparisons). The first cluster is mainly located in Broca's region (BA 44 and BA 45), but also stretched into to more dorsolateral areas (BA9 and BA 6). The second cluster is inferior to the first, mainly in the left insula. Negative effects are present in various regions in parietal, occipital cortices, left temporal and medial frontal regions. ROI analysis (see figure 4.8B) reveal that for all these regions activity is higher in the Load 0 than in the Load 3 condition. From Load 3 to Load 7 a monotonic increase in activity with WM load is observed in all regions except the superior parietal cortex, although only the differences between Load 5 and 7 are significant.
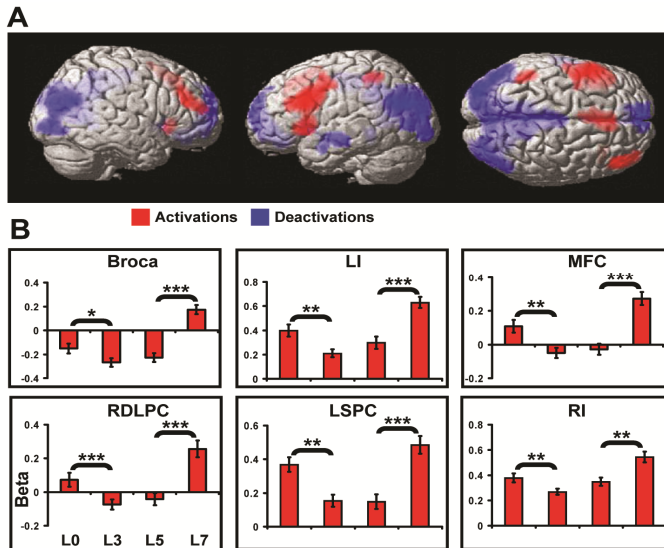
Figure 4.8. Load dependent FMRI activity during working memory maintenance. (A) Rendering on a standard MNI brain of activated and deactivated clusters for the Load 7 versus Load 3 contrast in the conventional fMRI analysis. Regions depicted here passed a 0.001 uncorrected voxel-level and a 0.05 family wise error corrected cluster-level threshold. Activations are in the red, deactivations in blue. (B) Average beta values for the activated regions in panel A for all the four WM loads. Error bars indicate the standard error. Broca: Broca's area; LI: left insula; right insula; MFC: medial frontal cortex; RDLPC: Right dorsolateral prefrontal cortex; LSPC: left superior parietal cortex; RI: right insula. Asterisks indicate a significant difference as tested with the repeated contrasts in the ROI analysis. $*|t(19)|>2.093$, $p<0.05$; $**|t(19)|>2.861$, $p<0.01$; $***|t(19)|>3.883$, $p<0.001$.

Integrated EEG/fMRI analysis

<u>Alpha</u>

Table 4.2 lists the clusters where the BOLD signal show a significant negative relation with TRLα in model I, where the single trial alpha power time courses model the maintenance interval (figure 4.9A). No positive clusters are observed. The linear trend analysis for the ROIs in Model II (figures 4.9C-E) reveal significant decreases in BOLD signal with WM load for the right middle temporal gyrus ($F(1,19)=43.59$, $p<0.001$), primary visual cortex: ($F(1,19)=22.03$, $p<0.001$) left cerebellum ($F(1,19)=33.79$, $p<0.001$) left supramarginal gyrus ($F(1,19)=20.11$, $p<0.001$) right supramarginal gyrus ($F(1,19)=34.92$, $p<0.001$). No significant linear trend is observed for the right middle frontal gyrus: ($F(1,19)=0.01$, not significant). Pair-wise comparisons however reveal that

Table 4.1. Regions showing a significant WM modulation in the Load 7 versus Load 3 contrast.

Brodmann area	Anatomical structure	Size (voxels)	MNI coordinates			t-value
			x	y	z	
Positive effects						
44/45/9/6	Broca's region/left inferior frontal gyrus/Insula	3012	-48	18	28	6.71
8/6	Left superior medial frontal gyrus/pre-SMA	932	-2	20	50	5.78
9/46	Right dorsolateral prefrontal cortex	507	46	42	26	5.53
	Right insula	250	34	24	-4	4.73
7	Left superior parietal cortex	244	-48	-42	54	4.37
Negative effects						
23/31/17/18/19/37/38/39	Various regions in parietal and occipital cortices	15841	8	-48	30	7.02
9/10/32/12	Medial frontal cortex	3029	0	62	-4	5.61
21	Left middle temporal gyrus	397	-60	2	-24	4.05

only the primary visual cortex and the posterior part of the right middle temporal gyrus show a pattern of decreased activity that is in line with the pattern of increase in alpha power (figures 4.9 C and 4.9I). The cerebellum shows the same pattern for the lowest three loads, but shows a non significant increase in Load 7 compared to Load 5. Other regions show no significant load dependent decreases in activity beyond Load 3. ROI analysis for orthogonalized-AVGα regressor reveal significant negative correlations with the right middle temporal gyrus, primary visual cortex, and the left cerebellum (see figure 4.9D) For TRLα-orth the ROI analysis reveals that all regions show a significant negative correlation with this regressor (see figure 4.9F). In summary, the right middle temporal cortex and the primary visual cortex show both a parametric decrease with WM load that is in line with the frontal theta increase and a negative correlation with TRLα-orth. We therefore conclude that load dependent BOLD decreases in these regions are related to the load dependent increases in alpha power (see figure 9B).

Theta

In contrast to the correlation to alpha power, negative as well as positive correlations with TRLθ are observed in model I (see table 4.3 and figure 4.10A). For the regions where BOLD correlates positively with TRLθ in model I, the ROI analyses in Model II reveal that there are no significant linear trend observed for the left $(F(1,19)=0.12$, not
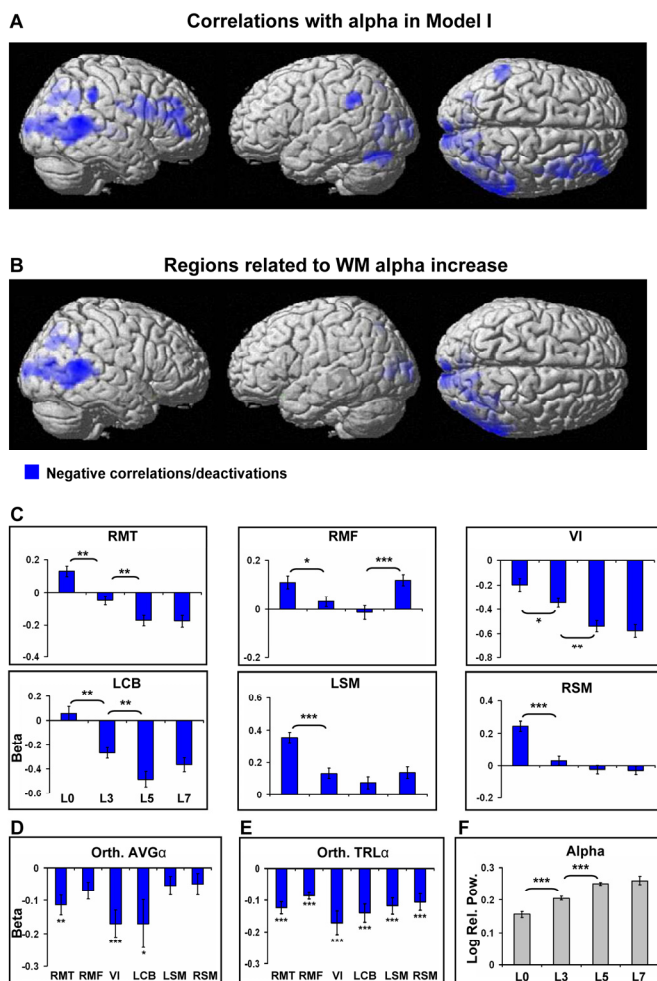
Figure. 4.9. Results of the integrated EEG fMRI analysis for the right posterior alpha effect. Panel A shows the clusters where the BOLD signal significantly correlated with TRLα in model I. Regions depicted here passed a 0.001 uncorrected voxel-level and a 0.05 family wise error corrected cluster-level threshold. Panel B shows which of these regions are functionally related to the WM-induced right posterior alpha increase. These clusters correlated significantly with the orthogonalized TRLα regressor as depicted in panel E and showed a significant WM modulation that is in line with the parametric alpha increase (see panel C). Panel C shows the average beta weights associated with the regressors in Model I modelling different WM loads for ROIs that were based on the regions shown in panel A. Panels D and E show the average beta weights for these ROIs for the orthogonalized AVGα and orthogonalized TRLα regressor in Model II respectively. Panel F shows the average of the log transformed relative alpha power increases for the different WM loads in the maintenance interval. Both TRLα and AVGα regressors are based on individually selected right posterior alpha independent components (see also Fig. 4). Abbreviations of the anatomical structures: RMT: right middle temporal gyrus; RMF: right

69

middle frontal gyrus; VI: primary visual cortex; LCB: left cerebellum; LSM: left supramarginal gyrus; RSM: right supramarginal gyrus. *|t(19)|>2.093, p<0.05; **|t(19)|>2.861, p<0.01; ***|t(19)|>3.883, p<0.001. Errors bars indicate the standard error.

Table 4.2. Relation between the BOLD signal and right posterior alpha activity

Brodmann area	Anatomical structure	Size (voxels)	MNI coordinates			t-value	Par. WM	Orth. AVG α	Orth. TRL α
			x	y	z				
Negative effects									
37/21/19	Right middle temporal gyrus	2002	62	-48	10	8.28	+	+	+
9/46/6	Right Middle frontal gyrus	1621	38	38	20	6.91			+
17	Left and Right primary visual cortex	1100	14	-90	10	5.72	+	+	+
	Left cerebellum/left middle occipital gyrus	654	-30	-70	8	5.14		+	+
40	Left supra marginal gyrus	228	-52	-46	38	5.52			+
40	Right supra marginal gyrus	210	58	-38	38	5.20			+

+ Regions that show a parametric modulation with WM load, a significant correlation to the orthogonalized AVGα regressor or orthogonalized TRLα in Model II.

significant.) and right (F(1,19)=2.61, not significant) inferior frontal gyrus. Both these regions do not show a significant relation (see figure 4.10D) with orthogonalized-AVGθ but do show a significant positive relation with orthogonalized-TRLθ (see figure 4.10E). The regions where BOLD correlates negatively with TRLθ in Model I do show an significant linear decrease with WM load (medial prefrontal cortex: F(1,19)=15.08, p<0.01; posterior cingulate cortex F(1,19)=35.59, p<0.001; left angular gyrus: F(1,19)=34.27, p<0.001; right angular gyrus: F(1,19)= 21.48, p<0.001). Except for the right angular gyrus, these regions show a monotonic decrease with WM load that is strongest for the Load 7 condition (figure 4.10C). This strong decrease in activity in Load 7 is in line with the strong increase observed in frontal theta power (figure 4.10I). ROI analyses for orthogonalized-AVGθ reveal only a significant negative correlation with the medial prefrontal cortex (see figure 4.10D). All selected regions show a significant negative relation with orthogonalized-TRLθ (see figure 4.10E). In summary, the medial prefrontal cortex, posterior cingulate/precuneus and the left angular gyrus

show both a parametric decrease with WM load that is in line with the increase in frontal theta power and a negative correlation with TRLθ-orth. We therefore conclude that load dependent BOLD decreases in these regions are related to the load dependent increases in theta power (see figure 4.10B).

DISCUSSION

In the present study, we used simultaneously recorded EEG and fMRI to investigate if the brain regions related to WM maintenance by previous fMRI studies are also functionally related to WM-induced posterior alpha and frontal theta increases. Analysis of the EEG data inside and outside the MR scanner revealed parametric increases with WM load in right posterior alpha and frontal theta power. Conventional analysis of the fMRI data yielded an increase in activity from Load 3 to Load 7 in a set of regions that have been related to verbal WM tasks (Cabeza et al., 2002). In the Load 0 condition these regions also showed increased activity compared to Load 3, indicating this condition did not function well as a high level baseline. The integrated single trial EEG/fMRI analysis revealed a functional relation between WM induced right posterior alpha increases and BOLD decreases in right middle temporal gyrus and primary visual cortex. The WM induced frontal theta power was found to be related to decreased activity in the default mode network (DMN; Gusnard and Raichle, 2001; Raichle et al., 2001; Shulman et al., 1997). The results of this integrated analysis are discussed in more detail below.

Right posterior alpha-BOLD correlations

The right posterior alpha increase with WM load is in line with earlier results obtained by Jensen et al. (2002) and Tuladhar et al. (2007). Interestingly, Jensen et al. (2002), who also used a verbal WM task, also reported a predominantly right lateralized effect, although their effect seems to have a more anterior scalp distribution than the effect we observed.

We found a variety of regions, predominantly located in the right hemisphere, where the BOLD signal correlated negatively with the right posterior alpha power increase (TRLα). Of those regions, only the right primary visual cortex (BA17) and the right middle temporal gyrus (BA 37) showed a significant relation with the three sources of variance that is in line with this monotonic increase in alpha power. For these two
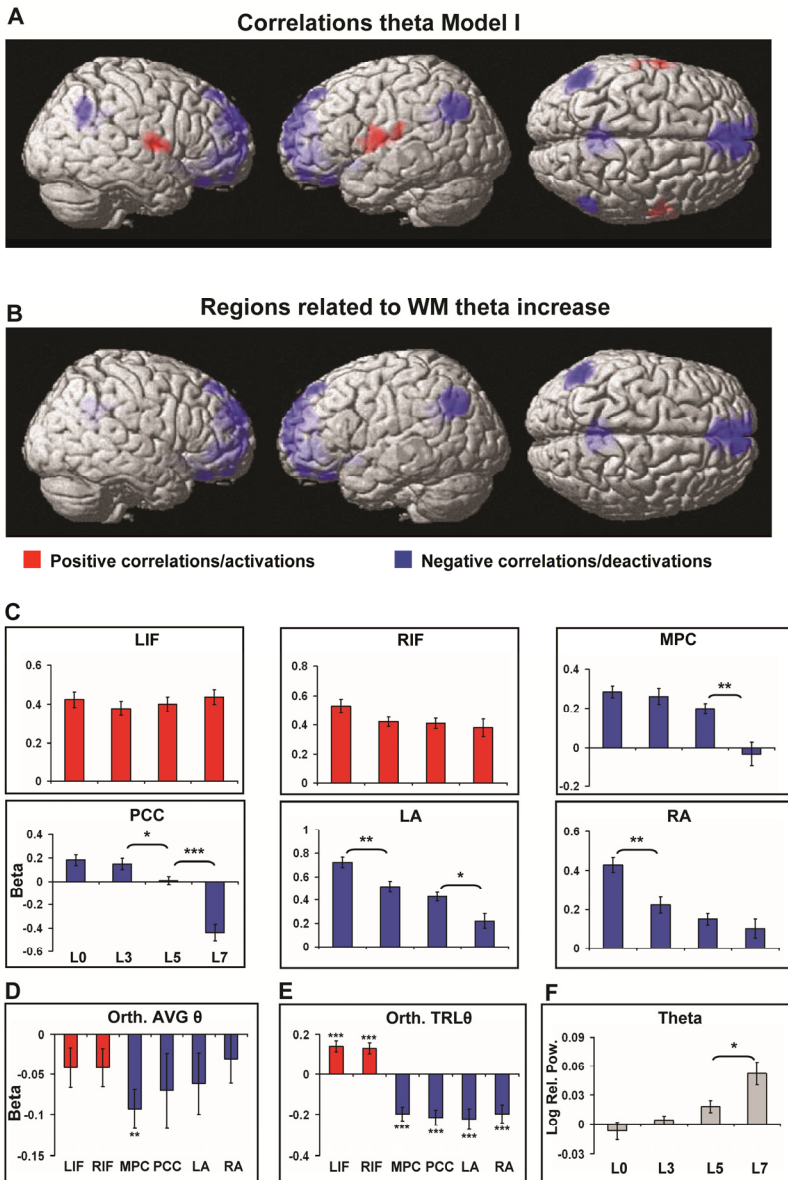
Figure 4.10. Similar as Fig. 4.9, but then for the frontal theta effect. Both TRLθ and AVGθ regressors were based on individually selected frontal midline theta independent components (see also Fig. 6). Similar as in panel A, the colour of the bars in panels C, D and E indicate negative positive (red) and negative (blue) correlations with TRLθ. Abbreviations for the anatomical regions: LIF: Left inferior frontal gyrus; RIF: right inferior frontal gyrus; MPC: medial prefrontal cortex; PCC: posterior cingulate cortex/precuneus; LA: left angular gyrus; RA: right angular gyrus.

Table 4.3. Relation between the BOLD signal and frontal theta activity.

Brodmann area	Anatomical structure	Size (voxels)	MNI coordinates			t-value	Par. WM	Orth. AVG θ	Orth. TRL θ
			x	y	z				
positive effects									
43	Left Inferior frontal gyrus	272	-64	-4	14	6.23			+
43	Right inferior frontal gyrus	250	58	0	8	5.34			+
negative effects									
9/10/32	Medial prefrontal cortex	3772	6	60	32	6.82	+	+	+
23/31	Posterior cingulate cortex/precuneus	970	-2	-52	28	6.60	+		+
39	Left angular gyrus	420	-52	-68	38	5.75	+		+
39	Right angular gyrus	157	54	-60	42	5.51			+

+ Regions that show a significant relation to the three sources of variance in Model II that is in line with the sign of the correlation with TRLθ.

regions, a monotonic decrease in the BOLD signal with WM load as well as negative correlations with orthogonalized AVGα and orthogonalized TRLα regressors were observed. We therefore conclude these regions and possibly also the left cerebellum, where only the Load 7 condition showed a deviation from the expected pattern, were functionally related to the observed WM induced alpha power increase.

For the other regions that correlated with alpha power fluctuations there is less evidence that they were functionally related to the WM alpha increase. All these regions showed a significant negative correlation with orthogonalized TRLα and except the left supramarginal gyrus also with orthogonalized AVGα. Although all these regions showed a significant modulation of BOLD by WM load, the ROI analysis shows that the pattern of activity across the four loads is not in line with the alpha increase. These regions were therefore more likely related to spontaneous non-WM-related fluctuations in alpha power.

The results detailed above are in line with the inhibition hypothesis relating increased alpha power to top-down functional inhibition of regions that can possibly perturb WM maintenance (Jokisch and Jensen, 2007; Klimesch et al., 2007). The negative correlations between alpha power and reaction time suggest a behavioural relevance of the deactivation of primary visual cortex and of the posterior part of the right middle temporal gyrus further supporting this hypothesis. The analysis of the different alpha

sub-bands revealed that the power increases with load mainly in the upper alpha band, which is in line with observations by Klimesch et al. (1999) in a similar WM task. Decreases in power in the upper alpha band have been related to increased performance in declarative memory tasks (Klimesch, 1999).

Frontal theta

Both inside and outside the MR scanner a significant parametric increase in theta power was detected for the Fz electrode. This midline frontal distribution is typical for the frontal theta response (Asada et al., 1999; Gevins et al., 1997; Onton et al., 2005). Applying ICA not only increased the relative power change, but also increased the time-frequency range for which a significant parametric increase with load was observed. The results also show that the theta response is particularly strong in Load 7.

Based on resting state correlations (Scheeringa et al., 2008) and similar findings by Meltzer et al. (2007) who correlated EEG and fMRI measured in separate sessions, we hypothesized that also during task conditions frontal theta activity would correlate negatively with the BOLD signal in the default mode network (Gusnard and Raichle, 2001; Raichle et al., 2001; Shulman et al., 1997). The results obtained here confirm this. We found that the medial prefrontal cortex, anterior cingulate cortex/precuneus and left and right the angular gyrus correlated negatively with single trial estimates of frontal theta power (TRLθ). If we split this regressor in three sources of variance, we saw that these regions also correlate negatively with trial-by-trial fluctuations in frontal theta power (orthogonalized-TRLθ). In addition, for three of the four regions the pattern of decreased activation with increasing WM load is in line with the observed frontal theta increase. The decrease of the BOLD signal in the right angular gyrus for the higher loads was not significant here, but this region typically is also part of the DMN.

The left and right inferior frontal gyrus showed significant positive single trial correlations modelled in Model I by TRLθ. For model II, no significant effect of WM load was however observed for these regions when analyzed in the conventional way, and no significant relation with orthogonalized-AVGθ was observed. There is only a significant positive relation with trial-by-trial variation modelled by orthogonalized-TRLθ. These regions are therefore probably only related to non-task-related fluctuations in frontal theta power.

The question arises whether one or more of the regions in which the BOLD signal correlated with frontal theta is the location where the frontal theta rhythm is generated.

Equivalent dipole models report sources of frontal theta to be predominantly in or near the anterior cingulate (Asada et al., 1999; Gevins et al., 1997; Onton et al., 2005; Scheeringa et al., 2008). This is just outside the largest negatively correlating cluster we observed in the medial prefrontal cortex. This discrepancy may be explained by the fact that equivalent dipole models tend to estimate the source location too deep when there is in reality a more superficial distributed source (De Munck et al., 1988). Interestingly, Ishii et al. (1999), who applied a beamformer approach on MEG data, and Miwakeichi et al. (2004) and Martinez-Montez et al. (2004), who applied distributed source models on EEG data, located frontal theta activity in a region in the medial prefrontal cortex that overlaps considerably with the medial frontal region observed here. We therefore assume that the medial frontal cluster is the likely source location for the frontal theta component.

The data presented above strongly suggests that increased frontal theta EEG power can be regarded as a direct consequence of the decreased default mode network activity as measured by fMRI. This notion unites the large body of literature on both topics. Both decreased DMN activity and increased frontal theta activity have been linked to increased cognitive demands. Increased frontal theta is reported in a wide variety of tasks, such as mental arithmetic (Inanaga, 1998; Inouye et al., 1994; Ishihara and Yoshii, 1972; Ishii et al., 1999; Lazarev, 1998; Mizuki et al., 1980; Sasaki et al., 1996; Smith et al., 1999), error detection (Luu et al., 2003; Luu et al., 2004), language comprehension (Bastiaansen et al., 2002; Hald et al., 2006) and WM tasks (Gevins et al., 1997; Jensen et al., 2002; Krause et al., 2000; Onton et al., 2005). DMN network activity as measured by PET and fMRI is reported to decrease in a similarly wide variety of cognitive tasks (Mazoyer et al., 2001; Shulman et al., 1997). Moreover, increased DMN activity has been positively related to activities such as self referential processing (Gusnard et al., 2001) and mind-wandering (Mason et al., 2007). These are activities subjects are typically not engaged in during cognitively demanding tasks. This link between frontal theta activity and DMN activity opens avenues to study activity of default network activity with EEG at sub second level by computing the time-course of frontal theta power.

General issues

The relation between frontal theta and DMN activity observed here illustrates that EEG power fluctuations measured at scalp level can be related to the activity in larger networks of brain regions and not only to the region that is the direct source of the

EEG activity. Not all activity in a functional network is readily detectable with EEG. This study illustrates that concurrent registration of EEG and fMRI can be used to reveal an entire network of regions that is related to changes in EEG features like frequency band specific power modulations. In addition, this study illustrates that by correlating single trial EEG measures, in this case power, with the BOLD signal we can separate different networks that show the same task induced BOLD responses. All the regions that were found to be functionally related to WM related increases in either right posterior alpha or frontal theta power show a decrease in BOLD with WM load. By correlating BOLD with single trial alpha and theta power we are able to separate these regions in two separate networks.

We observed here an inverse relationship between the BOLD signal and both right posterior alpha and frontal theta activity. These results are in line with the ideas put forward by Kilner et al. (2005), who concluded on theoretical grounds that increased neural activity should lead to decrease in low frequency power (e.g. delta and theta) and an increase in high frequency power (e.g. beta and gamma). According to their heuristic, the BOLD signal is inversely related to the degree of low versus high frequency components in the EEG. The studies investigating the correlation between electrophysiological measures and hemodynamic measures are largely in line with this hypothesis. Simultaneous recordings of EEG and fMRI have predominantly reported negative correlations with theta (Mizuhara et al., 2004; Scheeringa et al., 2008; present study, but see also: Sammer et al., 2007) and alpha power (Feige et al., 2005; Goldman et al., 2002; Goncalves et al., 2006; Laufs et al., 2006; Laufs et al., 2003a; Moosmann et al., 2003) and positive correlations of the default mode network with beta power in (Laufs et al., 2003b). In anaesthetized cats Niessing et al. (2005) recorded local field potentials while blood oxygenation was simultaneously measured with optical imaging. They reported negative correlations between the two measures in the delta and theta bands and positive correlations in beta and gamma bands during visual stimulation. Especially for the higher gamma frequencies they observed a strong positive correlation with BOLD. This positive BOLD-gamma relation was also observed by Logothetis et al. (2001) who found that the BOLD signal showed a strong positive correlation with gamma band activity observed in local fields potentials (LFP) in monkeys, and Shmuel et al. (2006), who reported that negative BOLD responses go together with a decrease in gamma band activity in the LFP. The majority of studies relating electrophysiological brain signals to hemodynamics thus support the notion of a systematic relation between frequency and direction of the BOLD response, in the sense that low-frequencies are

associated with BOLD decreases, while high frequencies are associated with BOLD increases.

Initially, we set out to determine whether the observed increases in alpha and theta power during WM maintenance are related to the regions that are thought to be involved in WM maintenance (mainly dorsolateral prefrontal cortex, DLPFC). We found that alpha power correlated negatively with BOLD in visual cortex and the posterior part of the right temporal gryus, which we link to the inhibition of activity that may disturb the WM maintenance process. Frontal theta power correlated negatively with BOLD in the DMN, suggesting that the presence of theta reflects 'task-orientedness'. Strikingly, both these processes (inhibiting irrelevant information and being engaged in the task) are necessary for the adequate performance of a WM task, but are not central to WM maintenance per se. In other words, what we are missing in our present results is EEG-BOLD correlations in the WM network itself. This begs the question of why we did not observe any correlations between oscillatory EEG activity (recall that we studied a full 1-100 Hz range) and BOLD signal changes in the usual WM regions (e.g.., DLPFC). We see at least three possible answers to this question. First, it may be that DLPFC synchronizes at relatively high (e.g. gamma) frequencies, and that the relatively low amplitudes of gamma oscillations were not reliably detected within the noisy environment of the MR scanner. Second, it may be that WM-related neuronal activity in DLPFC does not show massive synchronization changes, and as a result we did not find any systematic EEG power changes that stem from DLPFC. The third possibility is that the effects were present in other independent components that were not used to construct regressors. Our selection of the components was based on the effects observed in channel level data. An effect that is obscured at channel level by noise or confounds, might be recovered by ICA. Identifying these possible components however is problematic, since we do not have the channel level information in terms of frequency and topography of the effect.

Despite these unresolved issues, the present results illustrate that correlating BOLD signal changes with EEG power fluctuations measured at the scalp while a subject is engaged in a cognitive task yields interpretable and meaningful patterns of activity, which reveal the existence of neuronal activity in functionally coherent, yet spatially distributed networks in the brain. Not all activity in a functional network is readily detectable with scalp EEG. However, our results show that the current approach of a concurrent registration of EEG and fMRI, combined with the appropriate analytic

techniques, can uncover both the full spatial extent of functional networks, even if more than one network is simultaneously active during the execution of a given task.

Chapter 5

ELECTROPHYSIOLOGICAL CORRELATES OF THE HUMAN BOLD SIGNAL

ABSTRACT

The exact relation between hemodynamic responses (such as BOLD-based fMRI) and underlying neuronal activity is as yet not fully understood. Previous work on anesthetized and awake animals indicates that BOLD is preferentially sensitive to local field potentials, and that it correlates with gamma-band neuronal synchronization (Logothetis et al., 2001; Niessing et al., 2005). In this work, we aim to investigate whether the BOLD-gamma coupling also holds in human subjects engaging in cognitive tasks, and whether neuronal synchronization in other frequency bands contributes independently to the BOLD signal.

We simultaneously recorded EEG and BOLD in humans while they engaged in a cognitive task (a visual attention task) known to induce sustained changes in neuronal synchronization across a wide range of frequencies. Trial-by-trial BOLD fluctuations correlated positively with trial-by-trial fluctuations in EEG gamma power, and negatively with alpha and beta power. Gamma power on the one hand, and alpha and beta power on the other hand, independently contributed to explaining BOLD variance. The data demonstrate that the BOLD-gamma coupling previously evidenced in (anesthetized) animals can be extrapolated to studies of human cognition. In addition, the results suggest that low-frequency neuronal dynamics constitute another, independent mechanism underlying the BOLD signal.

INTRODUCTION

Functional magnetic resonance imaging (fMRI) is now the most widely used research tool in human cognitive neuroscience. In this branch of science, the hemodynamic responses obtained with fMRI measurements are commonly used to infer relationships between brain activity and cognitive functions. However, the exact relation between hemodynamic responses as measured with fMRI Blood Oxygenation-Level Dependent (BOLD) responses on the one hand, and underlying neuronal activity on the other, is not yet fully understood (Logothetis, 2008). Recordings in the anesthetized and awake monkey have shown that hemodynamic responses are preferentially sensitive to local field potentials (LFP) as opposed to action potentials (Goense and Logothetis, 2008; Logothetis et al., 2001). In addition, recordings from anesthetized cat visual cortex have revealed a strong positive correlation between BOLD and neuronal synchronization in the gamma frequency range (> 30 Hz) together with a negative correlation of BOLD

with lower frequency bands (up to 7 Hz; (Niessing et al., 2005)). However, in order for these results to have validity for fMRI studies in human cognitive neuroscience, an important question that needs to be answered is whether the coupling between BOLD and gamma extends to the case of human subjects engaging in cognitive tasks.

Encouraging first findings in this context are that the reactivity patterns of human and monkey gamma-band oscillations appear to show strong similarity, at least in the visual cortex (Hall et al., 2005). Furthermore, single-unit recordings of spike trains and high-frequency LFPs in the auditory cortex of patients watching a movie correlated significantly with fMRI BOLD responses measured in another set of healthy volunteers watching the same movie (Mukamel et al., 2005).

To further answer the question of BOLD-gamma coupling in human cognition, we asked twenty subjects to engage in a visual attention task known to elicit strong, long-lasting (up to several seconds) rhythmic activity in a relatively narrow gamma-frequency band in the MEG (Hoogenboom et al., 2006). This narrow band gamma synchronisation has been found in both human MEG/EEG recordings as well as monkey local field potentials (Fries et al., 2008). This task is therefore well suited to study the electrophysiological correlates of the BOLD signal in humans. We studied the relationship between frequency-specific power changes in the scalp electro-encephalogram (EEG) on the one hand, and simultaneously measured fMRI BOLD changes on the other hand. We hypothesized a positive correlation between BOLD and EEG gamma power, in parallel to what has been observed in animal experiments. In addition, we also explored the relationship between BOLD and other - lower - EEG frequency bands, in order to establish whether the negative correlation between BOLD and lower-frequency neuronal synchronization observed previously (Goldman et al., 2002; Laufs et al., 2003a; Niessing et al., 2005) independently contributes to explaining BOLD variance.

MATERIALS AND METHODS

Subjects

Twenty right handed subjects (13 female, 7 male, mean age 24, range 19-31), without a history of known psychiatric or neurological disorders participated in the simultaneous EEG/fMRI session. All had normal or corrected-to-normal vision. Before the start of the experiment, written informed consent was obtained from each subject. The

experiment was approved by a local ethical committee (CMO region Arnhem/ Nijmegen).

Experimental paradigm and stimuli

It has been established that neuronal synchronization in the gamma frequency range is associated, amongst others, with attentional processes, most notably in the visual system (Bichot et al., 2005; Fries et al., 2001; Lakatos et al., 2008). Therefore, subjects engaged in a visual attention task that is known to elicit strong, long-lasting (up to several seconds), and narrow-band gamma activity in the MEG (Hoogenboom et al., 2006). In this task, subjects attend to circular, inward moving gratings, and are asked to detect a change in inward speed. The experimental paradigm is illustrated in figure 5.1. Each trial started with a reduction in contrast of a fixation point that was present between trials (Gaussian of 0.4°) by 40%. This contrast reduction served as a warning for the upcoming visual stimulation, and instructed the subjects to stop blinking until the end of the trial. After 1100 ms, the fixation point was replaced by a sine wave grating (diameter: 7°; spatial frequency: 2.5 cycles/degree; contrast: 100%). The sine wave grating contracted to the fixation point (1.6 degrees/sec) for one of four stimulus durations: 700, 1050, 1400 or 1750 ms. This was followed by an increase of the contraction speed to 2.2 degrees/sec for maximally 500 ms. Each stimulation length occurred in 20% of the trials. The remaining 20% percent of trials were catch trials without a speed change. Here the stimulus duration was 2100 ms.

Subjects were instructed to press a button with their right index finger as soon as they detected the speed change. The stimulus disappeared after a response was given, after 2100 ms of stimulation (for catch trials), or if no response was given within 500 ms after the speed change. Feedback about the performance was given for 500 ms. In the case of a correct response or if a response was correctly withheld, 'ok!' appeared in green above the fixation point. In case of premature or slow/no responses, 'early' or 'late' respectively appeared in red. Trials were triggered by the onset of an fMRI volume, and occurred every two volumes. FMRI images were recorded in 330 ms, followed by a 3300 ms scan free period. This scan-free period allowed us to collect EEG data that were free of gradient artifacts during the visual stimulation interval.

In total, four blocks of 100 trials (20 of each trial length) were administered. One block had a length of approximately 12 minutes and 30 seconds. All trials were projected on a screen at the back of the MRI scanner, which was made visible for subjects via a mirror

mounted on the head coil. All stimuli were presented using the 'Presentation' software package (Neurobehavioral Systems, Inc.).

MRI data

MRI data were acquired using a 3.0-T whole body MRI scanner (Siemens Magnetom Trio Tim, Siemens, Erlangen, Germany). A custom built eight channel array (Stark Contrast, MRI Coils, Erlangen, Germany; see (Barth and Norris, 2007) for details), covering the occipital cortex was used to record the functional images. Eight slices positioned parallel to the calcarine sulcus were recorded using a gradient echo EPI sequence (TE=30 ms, 90 ° flip angle, 4.0 mm slice thickness, 0.4 mm gap, voxel size 3.5 by 3.5 by 4.0 mm, bias field correction filter was turned on). In order to speed up image acquisition, no fat suppression was used, and a GRAPPA parallel imaging sequence was used with an acceleration factor of 2. As a result, one volume was registered in 330 ms. Each volume was followed by a 3300 ms gap (for gradient-free EEG recording). This resulted in a TR of 3630 ms. As a result of these parameters, the (theoretical) peak of the BOLD signal resulting from a given trial was reached approximately two TRs after the onset of that trial (see figure 5.1).

An anatomical MR was acquired with the same head coil and slice position as the EPI data. A 3D MPRAGE sequence was used (TE=3.49 ms, TR= 2300 ms,10 ° flip angle, 80 slices per slab, 1mm slice thickness, 0.5 mm gap, GRAPPA acceleration factor=2, FOV=224 mm, voxel size 0.9 by 0.9 by 1.0 mm, bias field correction filter was turned on).

EEG data

EEG data were recorded with a custom made MRI compatible cap equipped with carbon wired Ag/AgCL electrodes (Easycap, Herrsching-Breitbrunn, Germany). Data were recorded from 29 scalp sites selected from the 128 channel international 10-10 system (Fp1, Fp2, F3, F4, C3, C4, P3, P4, O1, O2, F7, F8, T7, T8, P7, P8, Fz, Pz, TP9, TP10, PO3, PO4, O9, O10, PO7, PO8, POz, Oz, Iz). The placement of the electrodes was focused over posterior regions, so that signals coming from visual regions could be recorded with greater accuracy. Two dedicated electrodes were placed on the sternum and clavicle to record the ECG. One additional electrode was placed under the right eye to record eye movements. The reference electrode was placed at Cz. A 250 Hz low-pass

analogue hardware filter was placed between the electrode cap and the MRI compatible EEG amplifier (BrainAmp MR plus, Brainproducts, Munich, Germany). The EEG was recorded with a 10-second time constant and continuously sampled at 5 kHz. EEG recordings were performed with Brain Vision Recorder software (Brainproducts GmbH, Germany).

FMRI data analysis

FMRI data of each subject was corrected for movements, coregistered to the individual anatomical scan and smoothed with a 6mm FWHM isotropic Gaussian kernel in SPM5 (Wellcome Department of Imaging Neuroscience, London, UK; see http://www.fil.ion.ucl.ac.uk/spm). In SPM5 a GLM was constructed to isolate the voxels that showed activation related to the visual stimulation. For each block, the visual stimulation was modelled by a regressor that was formed by convolving mini-blocks of the length of the visual stimulation period up until the speed change with the canonical HRF as implemented in SPM5. In addition to this regressor, the design matrix contained a regressor that modelled the behaviourally erroneous trials and a regressor for each of the six movement parameters. Significance was assessed by testing whether the beta values of the regressor modelling the visual simulation period was larger than zero in a t-contrast. For each single subject, all voxels with a t-value greater than 10 formed a region of interest for the integrated EEG-fMRI analysis.

EEG data – preprocessing and time-frequency analysis of power

Preprocessing of the EEG data was carried out in Vision Analyzer (Brainproducts GmbH, Germany). The recorded EEG was first downsampled to 1000 Hz, and rereferenced to common average. The original reference electrode was recomputed as electrode Cz. Subsequently the data was segmented in epochs that started 750 ms before onset of visual stimulation, and ended either 400 ms after the speed change, or 400 ms after the end of stimulation in the catch trials. These segments were manually checked for artifacts, and trials with anomalies such as eye blinks and large muscle artifacts were removed. Behaviourally erroneous trials were excluded from further analysis. Further analysis of the EEG data was carried out in Fieldtrip (Donders Institute for Brain, Cognition and Behaviour, Nijmegen, The Netherlands; see http://www.ru.nl/neuroimaging/fieldtrip/). Time-frequency analysis was carried out

using a multitaper approach (Mitra and Pesaran, 1999). In order to optimize the trade-off between time and frequency resolution, separate analyses were carried out for a lower frequency window (2.5-45 Hz) and a higher frequency window (10-120 Hz). For the lower frequencies, the power was estimated every 50 ms in steps of 1.25 Hz, using 800 ms time smoothing, and ±2.5 Hz frequency smoothing windows. For the higher frequency window, power was estimated every 50 ms in steps of 2.5 Hz, with 400 ms time smoothing and ±10 Hz frequency smoothing windows. An initial analysis was carried out at channel level, revealing a similar sustained gamma band response as described by Hoogenboom et al. (2006) for some of the subjects. However, due to the many artifacts caused by the MR recording environment, data of most subjects was too noisy to observe this effect.

EEG data – ICA-based denoising

To denoise the data we used a two-step independent component analysis (ICA) approach. Each ICA step was performed with the extended infomax algorithm as implemented in EEGLab 5.03, (Delorme and Makeig, 2004), using a weight change of 10^{-7} as a stop criterion. The maximum number of iterations was 1000. In a first step, ICA was performed on the 45-100 Hz band-pass filtered EEG data. The unmixing matrix thus obtained was applied on the unfiltered data. The resulting component time courses therefore have a broadband spectral content, and were subsequently subjected to a time-frequency analysis as described in the previous section. For all subjects we were now able to observe a sustained gamma band response, with some individual variation in the peak frequency of this response. In a second step we again applied ICA, but this time on EEG data that was band-pass filtered with a narrow band of 10-20 Hz (depending on the spectral extent of each subject's gamma response) around the individually adjusted peak of the sustained gamma response). The unmixing weights of this analysis were again applied on the unfiltered data, and a time-frequency analysis of power was run on the component time courses. Components that showed a sustained gamma band response were selected (1-5 components for each subject) and projected back to channel level. Finally, these channel level data were again subjected to a time-frequency analysis, separately for the lower and the higher frequency windows, as described in the previous section. The results of this analysis constitute the basis for the construction of regressors that were used in the integrated EEG-fMRI analysis. The rationale behind the choices is explained in more detail in chapter 2.

Integrated EEG / fMRI analysis – regressor construction

For each subject, the EEG channel with the maximum gamma power increase (defined as the average increase, across time points and trials, during visual stimulation in the 55-85 Hz band, relative to a 200 ms pre-stimulation baseline) was selected. In addition, all the channels were selected that showed a gamma power increase of at least 25% of the maximum gamma power increase. Next, for each frequency bin, separately for the analysis of the lower frequency window and the analysis of the higher frequency window, EEG-based regressors were constructed as follows. For each single trial the power time course during the stimulation interval was averaged across the selected channels. These power time courses were concatenated into one time series (for behaviourally correct trials that were discarded at the artifact rejection stage, the average power time course across all trials of the same length was inserted at the appropriate positions in this time series). This time series was subsequently convolved with the canonical hemodynamic response function as implemented in SPM5, and downsampled to one value for each scan. This resulted in one EEG-based regressor for each frequency bin, both in the analysis of the lower frequency window and in the analysis of the higher frequency window.

Integrated EEG / fMRI analysis – statistical models

The region of interest data obtained from the single subject stimulation versus baseline contrast were analyzed in the context of the general linear model, using frequency-specific design matrices. For each frequency bin, the regressor modelling the single trial power estimates of that frequency bin was included. In addition, five HRF-convolved box-car regressors (one for each trial length) accounted for the main effect of the task on the BOLD signal. For the four regressors showing a speed change separate regressors modelling the reaction time were added. A regressor that modelled the behaviourally incorrect trials was included, and the six realignment parameters were used to control for possible movement artifacts. Finally, one regressor accounting for a linear trend was also included. The four runs from each subject were modelled with separate regressors. In the context of the five regressors modelling the task, the frequency specific EEG power regressor accounts for the relation between single trial variations the EEG power of that particular frequency and the BOLD signal. At the single-subject level, for each frequency the relation between the EEG power regressors

and the BOLD signal is assessed by a single sample t-contrast of these regressors against zero. At group level we averaged these t-values over subjects, and tested whether they significantly differed from zero. We chose t-values since the beta weights critically depend on the scale of the power fluctuations, which can differ by orders of magnitude between frequencies and subjects. Since all sessions for all subjects had the same number of regressors, the t-value is a monotonic transformation of the partial correlation between the EEG-based power regressor and the BOLD signal.

Inferential statistics

Significance, at the group level, of the EEG and MEG power changes relative to baseline (Figure 3A-B), and of the BOLD-EEG power relation (Figure 3C-D), was evaluated by a cluster-based randomization procedure (Maris and Oostenveld, 2007). This effectively controls the Type-1 error rate in a situation involving multiple comparisons (here: all the individual frequency bins). This procedure allows for user-defined test statistics tailored to the effect of interest within the framework of a cluster based randomization test. For the BOLD-EEG power relation, our test statistic was a single sample t-test against zero of the averaged t-value over subjects (giving uncorrected p-values). All data points that do not exceed a pre-set significance level (here 5%) are zeroed. Clusters of adjacent non-zero frequency points were computed, and for each cluster a cluster-level test statistic is calculated by taking the sum of all the individual t-statistics within that cluster. This statistic was entered in the cluster-based randomization procedure. This same procedure was also used to test the difference of the EEG power from baseline where the test statistic was a single-sample t-test of the log-transformed relative power compared to baseline (the 200 ms pre-stimulation interval). The above procedures were applied separately to the analyses of the lower and the higher frequency windows. The results of the analysis detailed above yielded significant negative correlations between alpha and beta power fluctuations and BOLD and a positive correlations between gamma power fluctuations and BOLD. This raised the question of whether this was due to one ore more underlying processes that correlate with the BOLD signal. To investigate this we first ran another GLM in which we included three regressors modelling the trial-by-trial variability in these three frequency bands. For each frequency band the regressor was based on the average of the power across the frequency bins that were part of the significant cluster in the EEG-BOLD correlation. This analysis evaluates whether the regressors can account for

unique variance in the BOLD signal. As a second step, the partial correlation between these three regressors were computed, partialling out the regressors modelling the main effect of visual stimulation.

MEG data

Subjects
Twenty four right-handed, healthy volunteers (13 female, 11 male, age range 18-49 years) participated in the study, after giving their written informed consent. All subjects had normal or corrected-to-normal visual acuity. Subjects were paid a small fee for their participation.

Experimental paradigm
Subjects performed a modified version of the task described earlier. Each trial started with the presentation of a fixation point (Gaussian of diameter 0.5°). After 500 ms, the fixation point contrast was reduced by 40%, which served as a warning. The fixation point was visible for another 1000 ms, which in later analyses served as the baseline period. Subsequently, the fixation point was replaced by a concentrically inward moving circular sine wave grating (diameter: 5°; spatial frequency: 2 cycles/deg; contrast: 100%). The sine wave grating contracted toward the centre, which served as a fixation point (velocity: 1.6 deg/s). These parameters are the same as for the EEG data. Subjects were instructed to maintain fixation on the centre and report a luminance change of the grating at an unpredictable moment in time, between 750 and 1500 ms after stimulus onset, by pressing a button with their right index finger. The luminance changed from 100 percent to 80 percent and this decrement lasted for one refresh period (~17 ms). The stimulus was turned off 500 ms after the response was given, or lasted until a maximum of 1000 ms in case no response was given, after which feedback was presented for 1000 ms. Feedback could either be "Early" (reaction time < 150 ms), "Ok" (150 ms < rt < 650 ms), or "Late" (> 650 ms). Subjects were instructed to blink during feedback presentation. Each subject completed 10 blocks of 100 trials. After each block there was a self-paced break in which feedback about the mean percentage correct, mean reaction times and amount of blocks was presented. All stimuli were presented using the 'Presentation' software package.

Data acquisition

The subjects were lying comfortably on a bed, with their head placed in the MEG-helmet. Ongoing brain activity was measured using a whole head 151-sensor MEG system (CTF systems Inc., Port Coquitlam, Canada). The MEG signals were low-pass filtered at 300 Hz and digitized at 1200 Hz and stored for off-line analysis. The simultaneously recorded horizontal and vertical electro-oculograms (EOGs) were used for off-line artifact rejection. To measure the head position with respect to the sensors, three coils were placed on anatomical landmarks of the head (the subject's nasion, left and right ear channel). The position of the coils was determined by measuring the magnetic signals produced by currents passed through the coils, right before and after the MEG session; hereby it was possible to get an estimate of the subject's head movement.

Data-analysis

All the analyses started with the same preprocessing steps: data epochs of interest were defined as such from the continuously recorded MEG. Data epochs that were contaminated by eye movements, muscle activity or jump artifacts in the SQUIDs were discarded using semi-automatic artifact rejection routines. Power line fluctuations were removed by estimating and subtracting the 50- and 100- Hz components in the MEG data, using a discrete Fourier transform (DFT) on 10-s data segments surrounding the data epochs of interest. The data epochs of interest were then cut out of these cleaned 10s segments and the linear trend was removed from each epoch. After preprocessing a minimum of 700 trials was present for subsequent analyses.

Time-frequency analysis was performed only on the visual stimulation period before the luminance change. Settings for low and high frequencies were the same as for the EEG data. The same cluster based randomization technique as used for the EEG power and EEG-BOLD relation was applied on the EEG data.

Source reconstruction

A frequency domain beam-forming approach was used for source reconstruction (Dynamic Imaging of Coherent Sources, DICS). This technique uses adaptive spatial filters to localize power in the brain (Gross et al., 2001; Liljestrom et al., 2005). For each
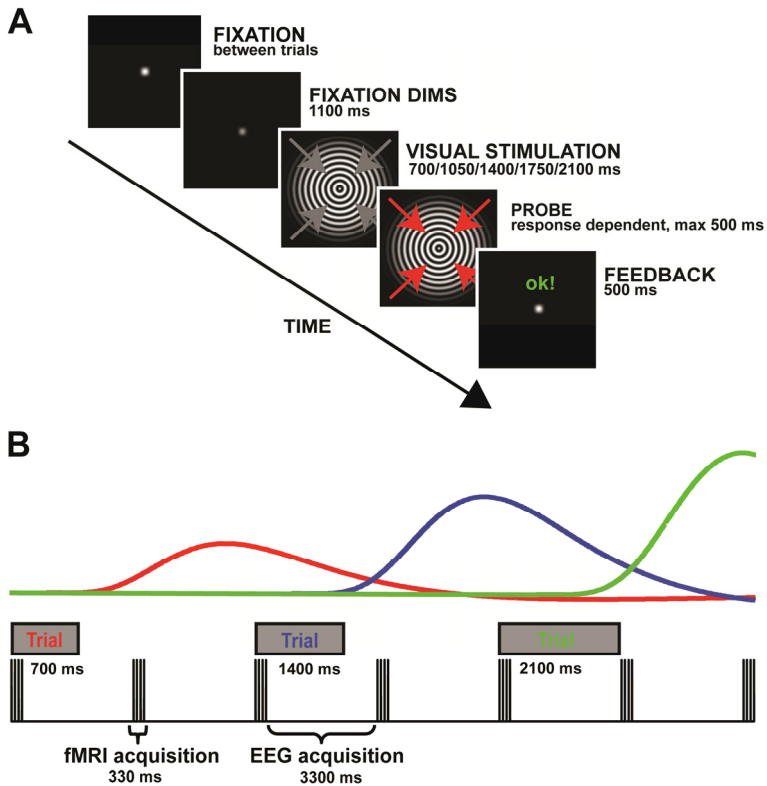
Figure 5.1. Schematic representation of the task. The full captions can be found on page 91.
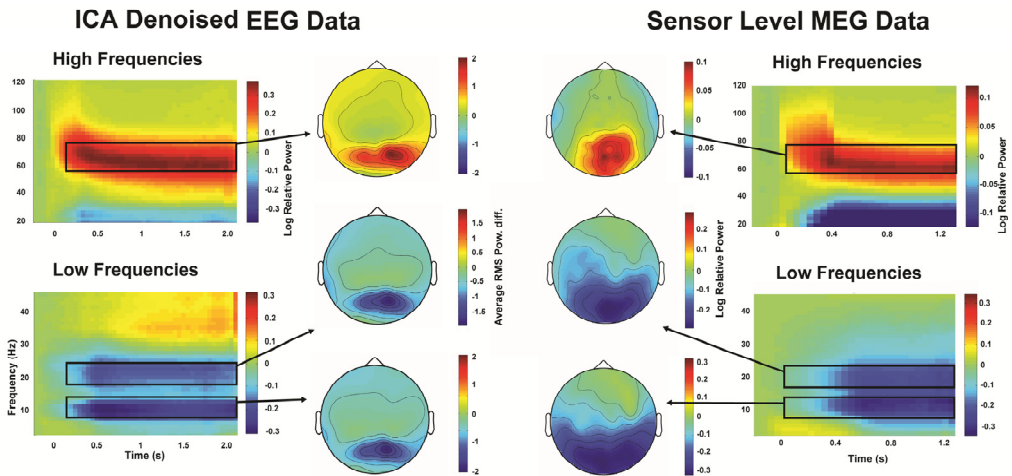

Figure 5.2. Results for EEG and MEG data. The full captions can be found on page 91.

Figure 5.1 (page 90, top). Schematic representation of the task. A: Sequence of events of a single trial. A trial started on the start of the acquisition of an fMRI volume with the reduction of the contrast of the fixation dot (the warning signal). After 1100 ms the fixation point is replaced by a foveal contracting grating, with a duration of either 700, 1050, 1400, 1750 or 2100 ms. Except for the 2100 ms condition (catch trials), visual stimulation was followed by an increase in the speed of the foveal contraction. Subjects were instructed to push a button as soon as they detected the speed change. Subsequently, feedback was presented for 500 ms. B: Illustration of the timing of the trials relative to fMRI data acquisition. Trials were presented every two volumes. Scanning parameters were chosen such that the visual stimulation part of the trial would always be outside the fMRI acquisition, allowing for good quality EEG acquisition. As illustrated by the modelled HRFs to the visual stimulation of different lengths, the second fMRI volume after stimulation onset is close to the expected peak of the BOLD response.

Figure 5.2 (page 90, bottom). Results for EEG and MEG data. The most left side of this figure shows the grand average time-frequency representations of log-transformed EEG power for low and high frequencies after back reconstruction of the selected components to channel level. This grand average is based on individual averages of the channels that formed the regressors in the integrated EEG fMRI analysis. The second column from the left shows the grand average topographies of the alpha, beta and gamma effects, and is computed as the average over the root mean square normalized power differences in the indicated frequency bands. The most right side of this figure shows the grand average time-frequency representations of log-transformed MEG power for low and high frequencies of a selection of occipital-parietal sensors. The second column from the right shows the accompanying topographies that are based on the individual average of the log transformed relative power of the indicated frequency bands.

subject a realistic single-shell description of the brain-scull boundary was constructed based on the anatomical MRI. For each subject an MNI aligned grid with a 1 cm resolution was constructed based on the individuals anatomical MRI (Gross et al., 2001). Subsequently, a lead field was constructed for each grid point (Nolte, 2003). We used the same filter for both baseline and the visual stimulation periods.

A 500 ms pres-stimulus period was used for estimating baseline power. Also for the visual stimulation period 500 ms time windows were extracted. Multiple windows were extracted form one trial if the trial length allowed this. Alpha source power was estimated based on a Fast Fourier Transform of Hanning tapered time windows at the 10 Hz bin. For beta and gamma power a multitaper approach was used. Beta power was estimated for the 22 Hz bin using 4 orthogonal Slepian tapers resulting in a frequency smoothing of $\pm$ 5 Hz. For the gamma band the peak individual gamma increase was determined. Gamma power was estimated for this peak gamma frequency with 9 Slepian tapers resulting in a frequency smoothing of $\pm$ 10 Hz. The relative power compared to baseline was calculated.

RESULTS

Conventional Analyses

The analysis of visually induced power changes in the EEG recorded in the MR revealed a decrease in alpha (around 10 Hz) and beta (around 20 Hz) power, together with an increase in gamma (60-80 Hz) power. Time-frequency representations and scalp topographies of the different time-frequency components are presented in figure 5.2.

A standard analysis of the fMRI data shows BOLD activations in the calcarine sulcus, and lateral visual cortex (figure 5.3D). The locations of the BOLD activations correspond well with the scalp topographies of the EEG and MEG responses (figure 5.2) and MEG source localisation (figure 5.3 A-C; Hoogenboom et al., 2006). The sources of alpha and beta power decreases appear however to be more widespread. The regions obtained by this source analysis largely overlap with the regions found active in the fMRI data. The reported EEG and fMRI effects were highly consistent across subjects.

Joint EEG-fMRI analysis

In order to test for a more direct link between hemodynamic responses and human gamma-band activity, we set up a statistical model that evaluates whether trial-by-trial fluctuations in BOLD co-vary with trial-by-trial fluctuations in frequency-specific EEG power.

We constructed separate design matrices for each individual frequency bin in the EEG signal, from 2.5 to 120 Hz. Each of these design matrices included a frequency-specific regressor based on the single trial EEG power estimates, as well as a set of regressors (one for each trial length) modelling the task.

Investigating all frequencies up to 120 Hz produces a spectrum of beta values that expresses the strength of the relation between EEG power and the BOLD signal. Separate spectra for the low (<45 Hz) and high (20-120 Hz) frequencies were constructed with different spectral concentrations (see Materials and Methods for details and rationale). The results of this analysis are shown in figure 5.4. This analysis shows that there is a significant positive relation between BOLD and EEG gamma power in the 60-80 Hz frequency range (p=0.0038, corrected for multiple comparisons), and a

negative relation between BOLD and low-frequency EEG power in the alpha-frequency range (around 10 Hz; p=0.0276) and in the beta-frequency range (around 20 Hz; p=0.0014). In addition, there is a marked correspondence between the BOLD-EEG correlation spectrum on the one hand, and the spectral changes observed in the EEG compared to the pre-stimulation baseline (compare figure 5.4A-B with figure 5.4 C-D).

In order to test whether the three observed frequency effects in the EEG are independent of each other, we tested a general linear model (GLM) that included regressors modelling the EEG alpha, beta and gamma power fluctuations. These regressors therefore account for a unique part of the variance of the BOLD signal, whereas variance that can be explained by more than one band is excluded for each regressor. The analysis (figure 5.4E) shows that the alpha band only marginally contributes to explaining BOLD variance. The beta band contribution is small but significant, whereas trial-by-trial fluctuations in gamma most strongly and significantly contribute to explaining BOLD variance. A pair-wise correlation of these regressors, (figure 5.4F) shows why this pattern emerges. While alpha and beta regressors show a significant positive correlation, they do not correlate with gamma power. Thus, while the alpha and beta regressors are highly correlated with each other, the gamma regressor is independent from these low-frequency fluctuations.

DISCUSSION

We aimed to investigate (1) whether the positive correlation, previously observed in (anesthetized) animals, between rhythmic neuronal activity in the gamma frequency range on the one hand, and fMRI BOLD on the other, also holds in human subjects engaging in cognitive tasks, and (2) whether rhythmic neuronal activity in other frequency bands contributes independently to the BOLD signal. We found that in human visual cortex during an attentional monitoring task, trial-by-trial BOLD fluctuations correlated positively with simultaneously recorded trial-by-trial fluctuations in EEG gamma power. In addition, BOLD fluctuations correlated negatively with EEG alpha and beta power. Gamma power on the one hand, and alpha and beta power on the other hand, independently contributed to explaining BOLD variance.
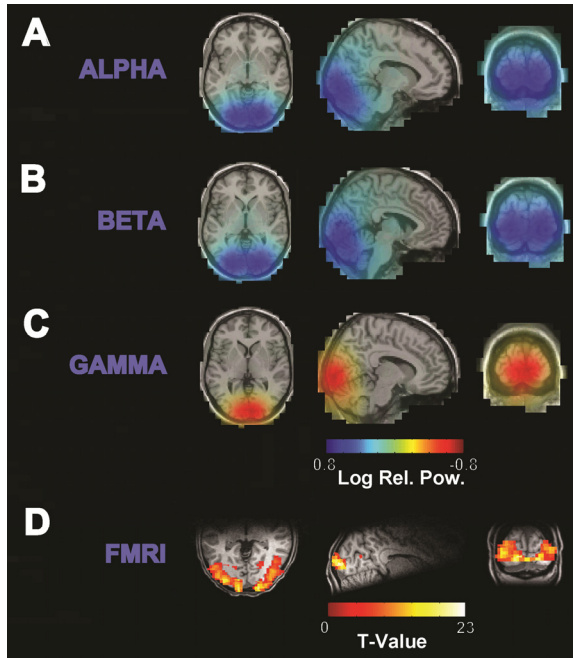
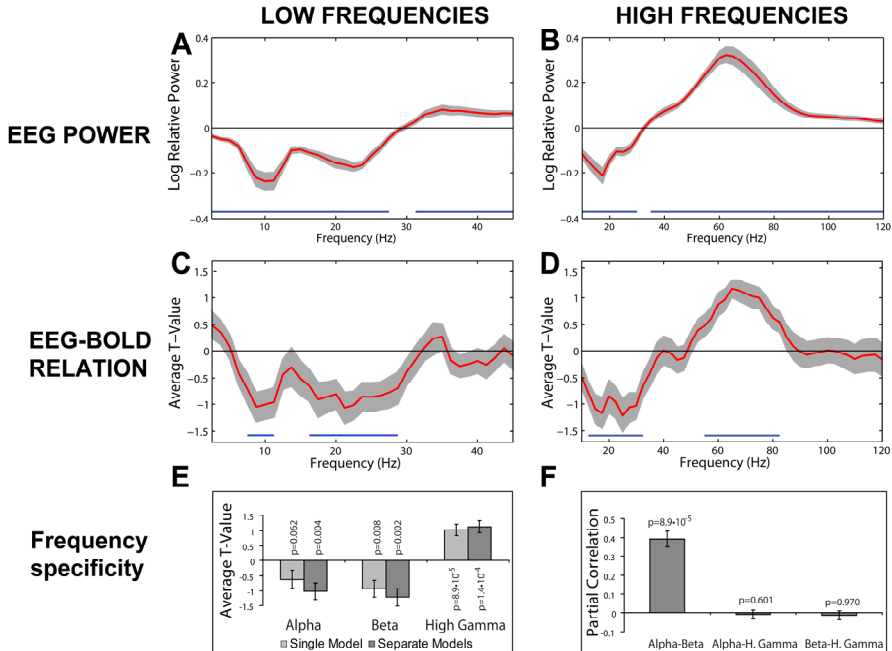Figure 5.3 MEG source localization and fMRI results. The full captions can be found on page 95

Figure 5.4 BOLD-EEG correlations. The full captions can be found on page 95

Figure 5.3 (page94, top). MEG source localization and fMRI results. Figures A-C show the grand average source estimates for the alpha, beta and gamma increase observed in the MEG using the beamformer technique described in the supplementary materials. Figure D shows for a representative subject the fMRI activation in response relate to the visual stimulation.

Figure 5.4 (page 94, top). BOLD-EEG correlations. Panels A and B: Spectra of the group average of the log transformed relative power effects compared to a pre-stimulation baseline for low and high frequencies. Panels C and D: relation between BOLD and EEG power for low and high frequencies expressed in averaged t-values. The shaded area indicates the standard error of the mean; a blue line indicates a significant deviation form zero using a cluster based randomization technique (Maris and Oostenveld, 2007). Panel E shows the average t-values of one general linear model that included regressors modelling alpha, beta and gamma power fluctuations. Panel F shows the partial correlation between the alpha, beta and gamma regressors in this model, controlling for the task effect. The error bars in panels E and F indicate the standard error of the mean. The p-values in panels E and F are based on the Wilcoxon ranked sign test (Wilcoxon, 1945)

Our results indicate that, apart from gamma-band neuronal synchronization, another, independent mechanism underlying hemodynamic responses is inversely related to neuronal dynamics in the lower (alpha and beta) frequency ranges. This is consistent with previous work that established a negative correlation between fMRI BOLD activations and low-frequency (4-30 Hz) neuronal synchronization (Goldman et al., 2002; Laufs et al., 2006; Laufs et al., 2003a; Mukamel et al., 2005; Niessing et al., 2005; Scheeringa et al., 2008; Scheeringa et al., 2009; Yuan et al., 2010). The interdependence of alpha-band and beta-band power fluctuations suggests that neuronal dynamics in these two frequency ranges are strongly related. Although this would fit the observation that event-related changes in alpha and beta rhythms often co-occur, e.g. during self-paced movements (Pfurtscheller et al., 1996a, b), these rhythms are often considered to subserve different (though not very consistently specified) functions (Jokisch and Jensen, 2007; Klimesch et al., 1998; Klimesch et al., 2007; Palva and Palva, 2007; Posthuma et al., 2001). An important implication of our observations is that alpha and beta rhythms contribute to explaining BOLD variance independently of gamma-band dynamics.

The independence of low and high frequency oscillations has also been established recently in mouse cortex. Using cell type specific optogenetic activation Cardin and colleagues (2009) were able to show a cell type specific double dissociation. Where activation of fast spiking interneurons selectively increased gamma band LFP power, direct activation of the pyramidal neurons only increased low frequency power. Some

evidence in humans also suggests alpha and gamma can be dissociated. In a task closely related to our task, larger visual gamma power increases were observed with larger contrast, while alpha and beta power remain largely unaltered (Koch et al., 2009).

In our view, or findings of an independent contribution of low- and high-frequency dynamics, together with the converging evidence discussed above, may have substantial implications for our understanding of the BOLD signal.

First, our findings indicate that the relationship between BOLD and neurophysiology does not hinge primarily on neuronal dynamics in the gamma frequency range, as recent animal work has suggested (Goense and Logothetis, 2008; Logothetis et al., 2001; Niessing et al., 2005). Our results support the notion that more frequency bands should be taken into account as correlates of the BOLD signal (Kilner et al., 2005; Laufs et al., 2006; Rosa et al., 2010).

Second, our findings contradict the hypothesis that BOLD activation is closely related to a shift in the EEG spectral profile to higher frequencies as a consequence of larger energy dissipation (Kilner et al., 2005). This theory would predict an inverse trial-by-trial coupling between low and high frequency power, which is clearly not observed here. We do find the expected pattern of negative correlations between BOLD and low frequency power and a positive correlation between BOLD and high frequency power. At trial-by-trial level the high and low power effects are however not correlated, as would be expected based on this theory. In a recent article Rosa and colleagues reported evidence for a spectral profile shift in a simultaneous EEG-fMRI experiment (Rosa et al., 2010). However, here only frequencies up to 40 Hz were considered. The gamma band effect we observed is of a substantially higher frequency (roughly 60-80 Hz). It is therefore possible that a shift in spectral profile contributes to the BOLD signal, but the high gamma band effect observed in our study is clearly independent of the effects observed in lower frequency bands, and therefore also likely independent of the proposed shift in spectral profile. Although average power around 40 Hz is elevated compared to baseline, no reliable 40 Hz peak was observed. The BOLD-power correlation did also not deviate significantly from zero around this frequency range. Although a relation between ~ 40Hz gamma power and BOLD has been reported (Mulert et al., 2010), Muthukumaraswamy and Singh (Muthukumaraswamy and Singh, 2009) also showed evidence for a decoupling between gamma power and the BOLD signal in this frequency range.

Third, the independent contributions of low- and high-frequency neuronal dynamics to the BOLD signal imply that simultaneous recording of electrophysiology and

hemodynamic activity can potentially dissociate whether an observed BOLD activation or deactivation is related to either low or high frequency effects, or a combination of both. In conventional hemodynamic studies it is impossible to make these distinctions. The ability to relate hemodynamic (de)activations to frequency-specific power changes can substantially benefit the interpretation of results obtained by hemodynamic studies, since neuronal activity in different frequency bands has been hypothesized to subserve different functions. For instance, the band limited gamma effects observed here have been linked to enhanced neural communication (Fries, 2005) while alpha oscillations have been related to functional inhibition (Klimesch et al., 2007).

Concerning the relationship between BOLD and gamma, the combined results of the different analyses presented in this work confirm previous findings from animal work (Goense and Logothetis, 2008; Logothetis et al., 2001; Niessing et al., 2005), of a strong coupling between hemodynamic responses on the one hand, and high gamma-band (60-80 Hz) neuronal synchronization on the other hand. Our results are in line with a recent study that combined NIRS and EEG, and that also suggested a BOLD-gamma coupling in humans (Koch et al., 2009). The inference in this study was primarily based on a parametric modulation of both BOLD and gamma, and no trial-by-trial coupling was reported. Our results are also supported by findings from a study using separate intracranial recordings of EEG and fMRI (Lachaux et al., 2007). Studies using simultaneous EEG-fMRI until now only investigated the lower gamma range up to 40 Hz in both task (Mulert et al., 2010) as well as in a resting state conditions (Giraud et al., 2007; Mantini et al., 2007). In line with our results, these studies also yielded positive BOLD-gamma correlations. Others using separate MEG and fMRI recordings however have reported a decoupling with BOLD in this low gamma frequency range (Muthukumaraswamy and Singh, 2009). In our study we however are able to show BOLD-gamma coupling in a frequency range up to twice the frequency (80 Hz) reported in these studies for a region that has been identified as the source region by MEG (Hoogenboom et al., 2006). Although gamma power was elevated compared to baseline in the lower gamma band, no significant correlation with BOLD was observed in our data either.

In conclusion, our data provides the most direct evidence yet that the coupling between BOLD and high gamma band oscillations in animal work also holds in humans performing a cognitive task. More importantly, our data suggest that at least two independent neurophysiological mechanisms contribute to the generation of the BOLD signal that can observed during cognitive neuroscientific experiments in humans: (1) A

mechanism related to high-frequency (gamma-band) neuronal synchronization, which correlates positively with BOLD signal changes, and (2) a mechanism reflected in low-frequency (alpha- and beta-band) neuronal synchronization, which correlates negatively with BOLD signal changes. As such, the present work provides a step forward in understanding the electrophysiological underpinnings of cognition-related hemodynamic responses in humans.

Chapter 6

FMRI CONNECTIVITY WITHIN AND BETWEEN RESTING STATE NETWORKS VARIES AS A FUNCTION OF EEG ALPHA BAND SYNCHRONIZATION

In the past decade, the fast and transient coupling and uncoupling of functionally related brain regions into networks has received much attention in cognitive neuroscience. Empirical tools to study network coupling include fMRI-based functional and/or effective connectivity, and EEG/MEG-based measures of neuronal synchronization changes. In this article we use simultaneous EEG-fMRI to assess whether fMRI-based BOLD connectivity and frequency-specific EEG power are related phenomena. Using a psychophysiological interaction approach on resting state EEG-fMRI data, we studied whether connectivity within the visual network and between visual network and the rest of the brain is modulated as a function of posterior alpha EEG power. The results show that when alpha power increases (1) BOLD connectivity within a network of visual regions decreases and (2) the inverse coupling between the visual cortex and regions of the default mode network weakens, especially with the posterior cingulate. The decreased connectivity within the visual system is in line with the notion that alpha represents functional inhibition, which subsequently results in decreased connectivity between closely connected regions. The decreased negative coupling between visual cortex and default mode network regions might be related to increased positive coupling when activity in the visual system is low and activity in the default mode network is high. A tentative interpretation of this observation is that the function of the default mode network might be to couple to inactive regions in order to prevent them from interfering with processes in other regions. In general, this study illustrates that the current methodology makes it possible to study how the temporal dynamics within and between resting state networks is related to changes in synchronisation measured with electrophysiological recording techniques.

INTRODUCTION

In the past few years most studies using simultaneously recorded EEG and fMRI addressed the relation between EEG power and the BOLD signal. These EEG-fMRI studies have predominantly investigated where in the brain EEG power fluctuations correlate with the BOLD signal. While some of these studies have investigated the relation between task-evoked changes in frequency band specific power and the BOLD signal (Sammer et al., 2007; Scheeringa et al., 2009; Yuan et al., 2010), many studies have focussed on the relation between 'spontaneous' fluctuations in both the fMRI BOLD

signal and EEG power during resting state (Feige et al., 2005; Goldman et al., 2002; Goncalves et al., 2006; Laufs et al., 2006; Laufs et al., 2003a; Laufs et al., 2003b; Mantini et al., 2007; Moosmann et al., 2003; Scheeringa et al., 2008). Within these studies most interest has been in the BOLD correlates of (posterior) alpha power. These studies have reported mostly negative correlations with the BOLD signal, although exactly which anatomical regions are correlated seems to be related to more subtle differences across frequency bands (Goncalves et al., 2006; Laufs et al., 2006). Besides conventional analysis investigating which regions show task related changes in the strength of the BOLD signal, fMRI also offers the possibility to investigate the connectivity in the BOLD signal from different brain regions. In a task context the psycho-physiological interaction (Friston et al., 1997) and dynamic causal modelling (Friston et al., 2003) are often the methods of choice for studying task related changes in connectivity. In resting state fMRI studies more straightforward correlational methods (e.g. Biswal et al., 1995; Fox et al., 2005) and independent component analysis are often used (e.g. Damoiseaux et al., 2006). How changes in fMRI connectivity depend on EEG power however is largely uncharted territory.

In this study we explore how fMRI connectivity in a well known resting state network, the visual system, changes as a function of posterior alpha power. This system was chosen since the visual system is a reliably observed network in resting state fMRI studies (Damoiseaux et al., 2006; Mantini et al., 2007), and comprises of both early and late/extra-striate visual regions. More importantly, the strongest alpha oscillations are recorded from the posterior region of the scalp and have been linked to visual processing. In addition, source analyses of both MEG and EEG data have located task related changes in this posterior alpha rhythm in early visual regions (Hoogenboom et al., 2006; Makeig et al., 2004a; Makeig et al., 2004b). The visual system and the posterior alpha rhythm therefore seem to be the best suited candidates to start to explore how changes in fMRI connectivity relate to changes in EEG power.

While alpha oscillations oscillation were originally seen as an 'idling rhythm' indicating inactivity of (mostly visual) brain regions (Pfurtscheller et al., 1996a), recent findings suggest alpha oscillations as recorded with EEG and MEG are closely tied to cognitive functions. Experiments have shown that alpha power actually increases in task irrelevant regions (Jensen et al., 2002; Klimesch et al., 1999; Scheeringa et al., 2009), and that this increase is related positively to behavioural performance (Haegens et al., 2010; Scheeringa et al., 2009). This has led to the notion that alpha oscillations are a reflection

of functional inhibition of neural activity in task irrelevant regions (Klimesch et al., 2007). Such spurious activity could otherwise influence activity in task relevant regions. Based on this inhibition theory we hypothesize that a region that exhibits increased alpha power should not only show a decrease in the BOLD signal, but also a decrease in connectivity of this region with closely connected regions. To test this hypothesis we used simultaneously recorded EEG and fMRI data during an eyes-open resting state session. By using the psycho-physiological interaction (PPI) approach we test whether connectivity of the primary visual cortex with other visual regions differs for high versus low posterior alpha power. Our posterior alpha power estimate is based on the central-posterior alpha component obtained by independent component analysis. This is a component that is reliably observed when ICA is applied on EEG data, and source analysis revealed that its most likely source localisation lies in the primary visual cortex (Makeig et al., 2004a; Makeig et al., 2004b).

METHODS

Subjects

Twenty right handed volunteers (17 female, 3 male, age range: 18–28) participated in the study after giving written informed consent. None had a neurological impairment, experienced neurological trauma or had used neuroleptics. The subjects were paid a small fee for their participation. The experiment was approved by a local ethical committee (CMO region Arnhem / Nijmegen).

Design and procedure

First the electrode cap was applied and instructions were given. While in the scanner, the subjects first participated in a working memory experiment for approximately one hour, divided in three blocks (see Scheeringa et al., 2009, for further details). Then a resting-state measurement was carried out in which subjects were asked to watch a black fixation cross presented on a grey background for 10 min. At the end of the scanning sessions a T1-weighted anatomical MRI was acquired. Between measurements there were small breaks of a few minutes. Subjects were also allowed to go outside the scanner during these breaks. Only the data from the resting-state measurement is used in the analysis presented here.

Electrophysiological recordings

EEG was recorded at 29 scalp sites (Fp1, Fp2, F3, F4, C3,C4, P3, P4, O1, O2, F7, F8, T7, T8, P7, P8, Fz, Cz, Pz, FC1,FC2, CP1, CP2, FC5, FC6, CP5, CP6, TP9, TP10) with a MR-compatible BrainAmp MR amplifier (Brainproducts, Munich, Germany) and an MR-compatible electrode cap equipped with carbon wired sintered Ag/AgCl electrodes (Easycap, Herrsching-Breitbrunn, Germany). The reference electrode was located at FCz. To record the vertical EOG one electrode was placed under the right eye. The ECG was measured by two dedicated electrodes attached to the electrode cap. One electrode was placed on the sternum, the other electrode was placed on the clavicle, near the shoulder. A 250-Hz hardware filter was placed between the electrode cap and the amplifier. The EEG was recorded with a 0.16 s time constant and a 100 Hz low-pass software filter, and continuously sampled at 5 kHz. Impedances were kept under 5 kΩ. All recordings were done with Brain Vision Recorder software (Brainproducts).

Image acquisition

MRI measurements were performed using a 1.5 T Sonata whole body scanner (Siemens, Erlangen, Germany). Functional images were acquired using a gradient echo EPI sequence (TR 2.34 s including 50 ms dead time; FOV=224 mm, TE=30 ms, 33 slices, 3.0 mm slice-thickness with 0.5 mm slice-gap; resulting in an isotropic voxel size of 3.5×3.5×3.5 mm).

MR artifact removal EEG

The EEG data were corrected for gradient and pulse artifacts along the lines described by Allen et al. (2000; 1998) using Vision Analyzer (Brainproducts). A 20-volume, baseline corrected sliding average was used for the correction of the gradient artifacts. In order to achieve this, 10 extra volumes were recorded before and after the 10 min of data used for analysis. After gradient correction the data were low-pass filtered at 100 Hz and downsampled to 500 Hz. The average pulse artifact was calculated based on a sliding average, time locked to the R-peak present in the bipolar derivation of the two ECG electrodes. This sliding average was scaled to an optimum least squares fit for each heart beat using the scaling option in Vision Analyzer before it was subtracted from the

data. The data were subsequently re-referenced to a common average reference. The original reference channel was recomputed as FCz.

FMRI preprocessing

Processing of the fMRI data was carried out in SPM5. The fMRI data was corrected for movements and slice acquisition time differences, anatomically normalized to the canonical EPI template provided by SPM5 and smoothed with an isotropic Gaussian kernel (FWHM=8 mm).

Alpha power extraction

Alpha power was estimated based on the central posterior alpha component that is reliably observed if independent component analysis is applied on EEG data (Makeig et al., 2004a; Makeig et al., 2004b; Makeig et al., 2002). Source analysis of this component has indicated that the primary visual cortex is the most likely source of this component (Makeig et al., 2004a; Makeig et al., 2004b). Here we applied extended infomax ICA as implemented in EEGLab 5.02 (Delorme and Makeig, 2004) on 7-13 Hz band pass filtered EEG data. Since many brain and artefact processes occur at specific frequencies (e.g. the medial frontal theta component and residual MR gradient artifacts), band-pass filtering before applying ICA increases the reliability of observing the central posterior alpha component. For each subject one posterior alpha component was selected by hand based on the following criteria: it should have (i) a peak in the alpha range (8-12 Hz) and (ii) a central-posterior topography of the mixing weights. The average power spectrum of the selected components was based on power spectra computed from FFTs applied on Hanning tapered 2s windows of the component time courses. These settings result in a resolution of the spectra of 0.5Hz. These 2s windows were shifted in 0.1 s steps. To be able to show the spectrum outside the alpha range the unmixing weights were applied on the unfiltered EEG data before the spectrum was calculated. The average topography and power spectrum of the selected components are depicted in figure 6.1.

Strategy for the connectivity analysis

The best estimate is that the posterior alpha power component is generated in the primary visual cortex (Makeig et al., 2004a; Makeig et al., 2004b; Makeig et al., 2002). Previous work has also shown that alpha power is inversely related to the BOLD signal at source level (see also chapter 5). We therefore chose to base the selection of the seed region on a correlational analysis between power fluctuations in the posterior component and early visual cortex. A region located for the major part in primary visual cortex was observed to correlate negatively with alpha power, and was selected as seed for the PPI analysis. A problem with the PPI results is that it does not indicate whether the baseline connectivity between regions is positive or negative. A positive PPI effect can therefore be related to a decrease in negative coupling strength or an increase in positive coupling strength. Therefore, we performed also a functional connectivity analysis using the same seed region, since this will indicate whether average connectivity with the seed region is negative or positive.

Alpha-BOLD correlational analysis

The construction of the alpha power regressor was based on a 4 Hz band centred around the individual alpha peak (mean 9.73 Hz, standard deviation 1.15 Hz) observed in the average spectrum of the selected independent component. Power was averaged over the four frequency bins (of 0.5 Hz each) below the peak frequency, the peak frequency bin and the 3 bins above, resulting in a power time course of 10 minutes with resolution of 0.1 s. An EEG based power regressor was formed from this time course by subsequently z-transforming the values for normalisation, convolution with the hemodynamic response implemented in SPM5 (Wellcome Department of Imaging Neuroscience, London, UK; see http://www.fil.ion.ucl.ac.uk/spm) and downsampling to one value for each scan. Together with nuisance variables consisting of the six realignment parameters and four compartment signals (modelling the average signal in the gray matter, white matter, cerebrospinal fluid and outside the brain), this formed a design matrix for the analysis using the general linear model as implemented in SPM5. The compartment signal averages were based on the segmented individual anatomical images provided by SPM5. Significance was assessed using the Gaussian random field correction on cluster level. Clusters were defined as adjacent voxels passing a p=0.005 uncorrected threshold.

Functional connectivity analysis

The correlation analysis of alpha and BOLD yielded a negative correlation between alpha and BOLD with the strongest effect observed in primary visual cortex. The exact region for this negative correlation formed the basis for the seed signal for the functional connectivity analysis. The significant cluster observed at a voxel level threshold level of 0.001 was largely inside Brodmann Area 17 (69.0 % of the volume of the cluster, anatomy toolbox; Eickhoff et al., 2005). The realignment parameters and the four compartment signals were included as nuisance variables. Multiple comparison correction was carried out at cluster level using Gaussian random field theory after applying a uncorrected voxel level threshold of $p = 0.005$.

EEG modulation of BOLD connectivity: PPI analysis

The modulatory effect of EEG power on BOLD functional connectivity between the alpha correlation based seed region in visual cortex (the same seed as for the connectivity analysis) and the rest of the brain was assessed using a standard psycho-physiological interaction (PPI) approach (Friston et al., 1997). The EEG power time-course used to construct the alpha regressor (see above) formed the basis for the 'psychological factor' (physio-physiological interaction is a more suiting label in this study). The 'psychological factor' regressor was based on a median split on the power values. This resulted in a time-course that contrasted high versus low power, which was subsequently convolved with the HRF. The PPI-regressor was formed by multiplying this regressor with the BOLD time course from the seed region. The design matrix for the PPI analysis consisted of this PPI regressor, two regressors modelling high and low power based on the median split, the time course of the seed region and the motion parameters. The beta values of the PPI regressor were tested at group level using a one-sample t-test. Multiple comparison correction was carried out at cluster level using Gaussian random field theory after applying a uncorrected voxel level threshold of $p = 0.005$.

RESULTS

Alpha-BOLD correlation

The maps for the correlation between alpha power and BOLD are shown in figure 6.2. Negative correlations between alpha and BOLD were observed in the occipital lobe. The largest cluster is located in early visual cortex with its local maxima located in primary visual cortex (MNI coordinates: 2 -86 10, k=1182, z =3.73). Two other clusters were observed in extrastriate regions in the left (MNI: -40 -80 -4; k=280, z= 3.58) and right (MNI: 30 -92 22; k=280, z= 3.58) occipital cortex.

The strongest positive correlations are observed in the posterior cingulate/precuneus (MNI: 6 -62 28; k=997, z= 5.27). Other positive correlations were observed in the medial prefrontal cortex (MNI: 0 56 -10; k=4372, z= 5.02), left lateral inferior parietal cortex (MNI: -38 -82 38; k=357, z= 3.91) and the left (MNI: -56 -14 -12; k=466, z= 4.96) and the right (MNI: 64 -12 -16; k=371, z= 4.64) middle temporal gyrus. These regions have all been found to be part of the default mode network (DMN) (Raichle et al., 2001; Raichle and Snyder, 2007; Shulman et al., 1997).

Functional Connectivity

The maps for the functional connectivity with the (alpha-based) seed in primary visual cortex are depicted in figure 6.3. Positive correlation with the seed regions are observed across a large part of the occipital lobe, encompassing both striate and extra-striate visual regions. In addition, positive clusters are observed in the dorsal anterior cingulate cortex and the right temporal-parietal junction. In contrast, negative correlations are observed in posterior cingulate/precuneus, medial frontal cortex, lateral inferior parietal cortices, left and right middle temporal gyrus, bilateral inferior frontal cortices, bilateral hippocampus, and bilateral supplementary motor areas. Thus, these regions comprise the full extent of the DMN, and additional areas.

PPI analysis

The results for the PPI analysis are depicted in figure 6.4. Clusters of significant negative contrast estimates for the PPI regressor were observed in three clusters in the occipital lobe (left inferior occipital cluster: MNI: -12 -62 2; k=450, z= 3.60; right inferior
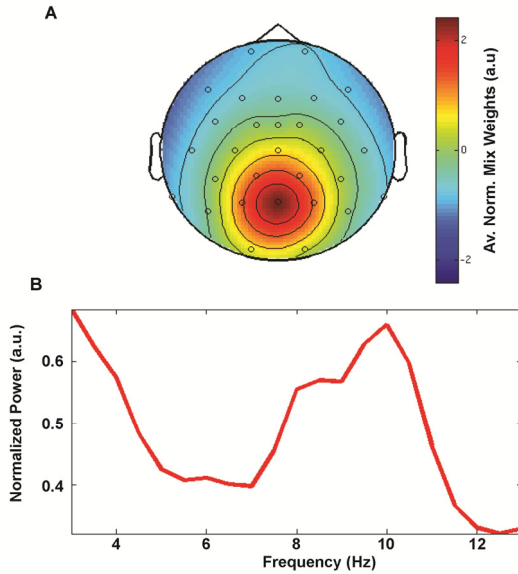
Figure 6.1. Average topography (A) and power spectrum (B) of the independent components selected for further analyses. The topography is based on root mean square normalized single subject topographies of the mixing weights. The single subject power spectra that constitute the average spectrum were calculated after the unmixing weights were applied on the unfiltered EEG data. The power spectrum was averaged after normalizing the single subject spectra to the maximum in the alpha frequency range (8-12 Hz).
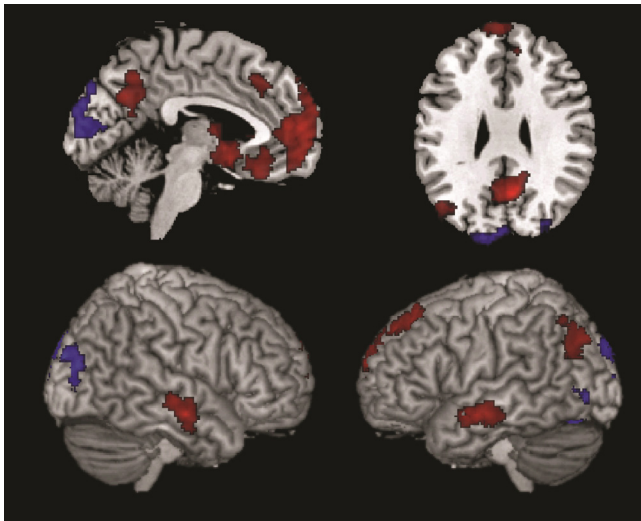

Figure 6.2. Maps of the anatomical locations of the significant positive (red) and negative (blue) correlations with posterior alpha power. All the regions shown here are significant after cluster level correction for multiple comparisons (p<0.05), after passing an uncorrected threshold of p=0.005.

occipital cluster: MNI: 14 -72 6; k=715, z= 4.07; right superior occipital cluster: MNI: 20 -90 24; k=1400, z= 4.83). In addition one negative cluster was observed in the left insula (MNI: -32 2 -10; k=293, z= 3.75). The three clusters in the occipital lobe are largely located outside V1. Only 14.9% of the voxels fall within BA17, as assessed with the anatomy toolbox (Eickhoff et al., 2005). A significant positive effect was observed in the posterior cingulate/precuneus (MNI: -10 -56 24; k=296, z= 4.37), additionally a trend (p=0.07, corrected) was observed in the lateral inferior parietal cortex (MNI: -36 -64 22; k=202, z= 3.75). These two regions are part of the DMN. Interestingly, the next region that appears when the extend threshold is lowered (k>100 voxels) is the medial prefrontal cortex (MNI: -4 60 14; k=107, z= 3.97), which is also part of this network.

To be able to interpret the clusters we also need to know whether the positive effects are related to either an increase in positive connectivity strength of a region with the seed region, or a decrease in negative connectivity strength. Similarly for negative clusters we need to know whether baseline connectivity is negative or positive. Direct comparison between the connectivity maps for high and low power is however not possible for the method applied here, since the separate connectivity maps for high and low alpha power are not computed. We therefore compared the locations obtained in the PPI analysis with the functional connectivity maps, which is a close approximation for the average of these two maps. This gives a tentative idea whether we for instance a positive effect is related to a stronger positive connection or a less strong negative connection.

This comparison shows that the clusters in the occipital cortex fall within the large occipital cluster that is positively related to the seed region. This indicates that connectivity within the visual system decreases as a function of alpha power. For the negative cluster in the left insula there is no significant effect in the functional connectivity analysis for the threshold at which the data is presented here. At a lower uncorrected voxel level threshold the cluster falls within a region spanning a large part of the cortex that shows a negative correlation with the seed in primary visual cortex. This indicates the negative relation is stronger when alpha power is high. The positive effects are only observed in regions that are part of the DMN. Functional connectivity shows a negative correlation between the DMN and the seed in primary visual cortex. The connectivity results therefore suggest that the positive PPI effect is related to a less strong negative connectivity. Another possibility is that also the sign of the correlation changes between low and high power, but the current analysis does not allow verifying this.
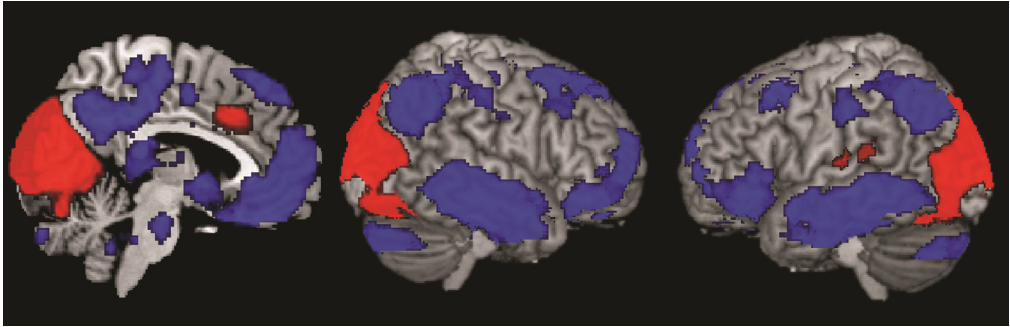
Figure 6.3. Functional connectivity maps for a seed region in the primary visual cortex. Positive connections are depicted in red, negative in blue. The same seed region as used for the PPI analysis was used here and is shown in figure 4. All the regions shown here are significant after cluster level correction for multiple comparisons (p<0.05), after passing an uncorrected threshold of p=0.005.
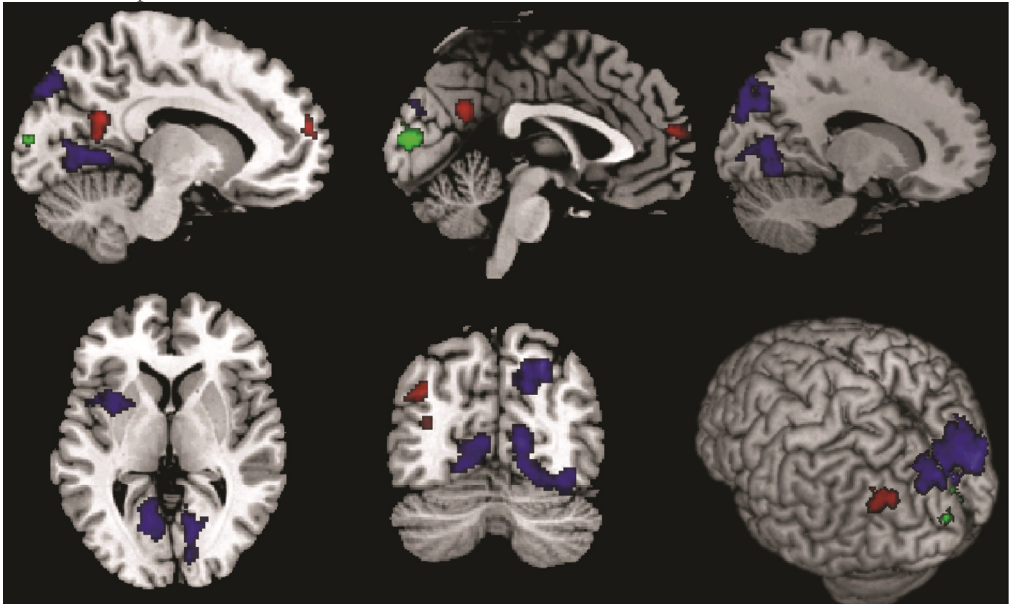

Figure 6.4. Anatomical maps of the contrast estimates for the alpha-based PPI analysis. Red indicates a positive contrast estimate, blue a negative. The seed region is depicted in green. All the negative effects and the positive effect in the posterior cingulate are significant after cluster level correction for multiple comparisons (p<0.05), after passing an uncorrected threshold of p=0.005. The lateral inferior parietal cluster shows a trend at corrected level (p=0.07 corrected). The effect in the medial prefrontal cortex also passes the voxel level threshold, but is not significant at corrected cluster level and is shown for illustration purposes since it is well known part of the default mode network, as are the other positive effects.

DISCUSSION

In this experiment we studied how resting state connectivity within the visual system and between the visual system and the rest of the brain is modulated as a function of posterior alpha power. We observed that increased alpha power originating from the visual system is associated with decreased connectivity within this system. In addition, during episodes of high alpha power the average negative connectivity between the primary visual cortex and regions forming the default mode network (Raichle et al., 2001; Raichle and Snyder, 2007; Shulman et al., 1997) became less strong, and possibly might have been positive.

The fact that alpha-band neuronal synchronization is inversely related to connectivity between regions involved in visual processing suggests that local alpha-band synchronization serves to block, or at least reduce, the communication with closely connected regions. This notion is in line with the general functional role of alpha-band synchronization as inhibiting spurious activity as described in for example the alpha inhibition hypothesis proposed by Klimesch and colleagues (Klimesch et al., 2007), and as hypothesized in neurophysiological models of alpha generation (Lopes da Silva, 1991; Steriade et al., 1990). In addition our data indicate that not only activity within this region is decreased when the level of alpha synchronisation is high (as evidenced through the BOLD-power correlation analysis), but that as a consequence also connectivity and communication with tightly connected brain regions is reduced (shown by the PPI analysis). This implies that an increase in synchrony in the alpha band indicates a decrease in connectivity and in inter-regional communication.

The finding that increased synchrony is related to decreased connectivity seems to contradict the idea of synchronisation subserving functional integration (Varela et al., 2001). It is however important to consider that the most likely source location of the alpha lies within the primary visual cortex (Makeig et al., 2004a; Makeig et al., 2004b), and the reduced connectivity is mainly with surrounding extrastriate regions. This strongly suggests that local increases in synchrony in the alpha band might be related to decreased communication with regions further removed. We do however also find negative correlations between BOLD and alpha power in surrounding regions. If these regions would be partly the source of the alpha power reflected in the central independent alpha component, it would imply that within a region showing increased synchronization in the alpha frequency range, connectivity as measured with fMRI is decreased. This would then also imply that electrophysiological measures for

connectivity (phase-synchronization) and hemodynamic measures for connectivity (e.g. PPI) can yield contradicting results.

The reduced strength of the negative connectivity between visual cortex and brain regions that are part of the default mode network comes as a surprise. We would have expected a stronger negative coupling between visual regions and the default mode network since activity in visual cortex and the default mode network is anti correlated in the functional connectivity analysis, and alpha shows a negative correlation with the visual cortex and a positive with the DMN. These results therefore require an alternative explanation. The results observed here might suggest that when the visual cortex is in low state of activity, which is related to an increase in alpha synchronization, its activity is more susceptible to be influenced positively by activity in regions of the DMN, whose activity is actually stronger at those moments. This would then suggest that the function of the DMN is to dynamically couple to inactive brain regions, which would also explain why activity in the DMN is in general higher during baseline conditions (Shulman et al., 1997), when more brain regions are inactive. In this respect it is also interesting to note that the strongest effect is observed in the posterior cingulate cortex. Especially this region has been identified as a major node in the brain that is connected to many regions across the brain (Buckner et al., 2009; Hagmann et al., 2008). It is therefore ideally suited to dynamically couple to various regions or networks. The functional relevance of this might be that while regions are coupled to the DMN they are less likely to unpredictably influence regions engaged in task execution, and as a consequence influence behaviour in a non-adaptive way. This could also relate to the seemingly contradicting finding that increased activity in this network has both been related to increased (Sadaghiani et al., 2009) and decreased (Eichele et al., 2008) performance. When increased coupling with task irrelevant regions is established, this might have a facilitating effect on performance, while when this occurs with task relevant regions this can have deteriorating effect. The main function of the DMN might therefore be to keep other brain regions or networks in their default state of activity.

This work presents an initial report of changes in functional connectivity that correlate with changes in measures of neuronal synchronization. In our view, this methodology allows the study of connectivity dynamics at a relatively good time scale. As such, it is in line with recent work studying the temporal dynamics of resting state networks in MEG (De Pasquale et al., 2010). Our approach of combining EEG and fMRI based measures for studying dynamic network coupling opens up new avenues for investigating the behaviour of functional networks at detailed temporal and spatial scales. This is a

departure from the static view that prevails in most of the work studying these networks in fMRI.

Chapter 7
SUMMARY AND DISCUSSION

In this thesis the focus has been on the relation between oscillatory EEG activity and the BOLD signal. This relation was investigated in both resting state as well as task contexts. In this chapter first the separate chapters are summarized and the implications that each of them provides are discussed. The second part discusses the general implications that arise from the chapters collectively. The last part discusses how to proceed from what has been learned in this thesis, and explore new avenues where concurrently recorded EEG/fMRI can provide further insight above and beyond recording them separately.

Summary

In **chapter 3** we investigated in which brain regions the BOLD signal correlates with frontal theta power during eyes open resting state. The frontal theta rhythm is the most prominent in the theta range (3-8 Hz). It reliably shows up as a single component when independent component analysis is applied on EEG data (Makeig et al., 2002; Onton et al., 2005). The rhythm was thought to be involved in active processing of information like working memory maintenance. Based on this idea, increases in activity in regions involved in working memory or cognitive control was assumed to be related to the generation of the frontal theta rhythm. The results in this chapter however indicate this rhythm is negatively correlated with the default mode network (Gusnard and Raichle, 2001). This is a network of brain regions that deactivates, as measured by PET and fMRI, during many cognitive tasks. Dipole analysis revealed the medial frontal part of this network is the likely source of the frontal theta rhythm. Activation within this network has been associated with processes like self referential processing (Gusnard et al., 2001) and mind wandering (Mason et al., 2007). These activities people are usually not engaged in during cognitive tasks.

In the next chapter (**chapter 4**) we investigated the same frontal theta rhythm, as well as the alpha rhythm (8-12 Hz) in a task context. Both rhythms have been reported to increase parametrically with load during working memory maintenance. In an EEG session outside the MRI scanner we indeed observed such a parametric increase, in midline frontal theta power and right posterior alpha power. Inside the scanner we obtained single trial estimates of these effects using independent component analysis. These estimates were used to locate the brain regions where the BOLD signal is related to the increases in alpha and theta power. Since trial-by-trial variation in power can also be related to task-independent variations or other sources of variability that were not

fully removed with ICA, we reasoned that regions in which the BOLD response is related to the working memory-induced power increases should correlate with this trial-by-trial variance in EEG power, and additionally these regions should show the same parametric increase with working memory load in the BOLD signal as is observed in the EEG. For frontal theta power we found positive as well as negative correlations of the BOLD signal with trial-by-trial variability of power. However, the regions showing a negative correlation with trial-by-trial variation in power also showed a parametric modulation (decrease) of the BOLD signal with working memory load. As was expected from the negative correlations observed in the resting state condition, the default mode network showed both a negative correlation with trial-by-trial variations in frontal theta power as well as a decrease in BOLD. This corroborates the notion that a decrease in default mode network BOLD activity is directly related to an increase in frontal theta power as measured by EEG. It also suggests it is possible to track default mode activity at a higher temporal resolution as with BOLD by studying the temporal evolution of frontal theta power.

We used the same strategy to investigate the right posterior alpha increase. Here we observed only negative correlations in several regions in predominantly the right hemisphere. Two of these regions showed a strong parametric decrease in the BOLD signal with working memory load. These regions were located in the primary visual cortex and posterior part of the right middle temporal gyrus. These results were interpreted in the context of a theory that states that increased alpha is a reflection of inhibition of task-irrelevant regions (Jokisch and Jensen, 2007; Klimesch et al., 2007). Corroborating this notion was the finding that increased right posterior alpha during working memory maintenance predicted shorter reaction times only in the working memory conditions, and not in the control condition. This chapter demonstrates the added value of using trial-by-trial variation in power in disentangling the different networks that activate and deactivate during task conditions.

In the **chapters 3 and 4** we observed an inverse relation between the BOLD signal and fluctuations in low frequency bands (alpha and theta). In **chapter 5** we attempted to answer the question whether other frequency bands do show a positive relation with the BOLD signal. Work in cats and monkeys indicate that especially power fluctuations in high gamma frequencies show a strong positive relation with the BOLD signal (Niessing et al., 2005). In this chapter we set out to replicate these findings in humans during task execution. We used an adapted version of a task that reliably induces strong increases in

the gamma band as well as strong decreases in the beta and alpha bands (Hoogenboom et al., 2006). Moreover, from previous MEG source localization and fMRI experiments the localization of these sources is well known. Based on this work we were able to study the relation between the BOLD signal and EEG power for each single frequency at a trial-by-trial level. This yields a spectrum reflecting the trial-by-trial correlation between BOLD signal and EEG power. We observed that both alpha and beta power correlated negatively with the BOLD signal, while the high gamma-band increase showed the expected positive correlation with the BOLD signal. In addition we were able to show that the low frequency decreases in alpha and beta power are not correlated with the gamma band increases, suggesting that low and high frequency oscillations are a reflection of different underlying neural processes that both contribute to the BOLD signal.

We used a conventional correlation approach in chapters 3 to 5 to see how fluctuations in EEG power correlate with the BOLD signal. In **chapter 6** we adopted a novel approach and investigated whether EEG power modulates the connectivity between brain regions when subjects are at rest. As a network of interest we chose the visual system, which is a network that is regularly observed in resting state fMRI studies. Moreover, the posterior alpha rhythm observed at parieto-occipital electrodes, is most likely generated within this network. This network is therefore well suited to investigate whether connectivity within the visual system and of the visual system with other brain regions is modulated as a function of alpha power.

As a first step we performed a straightforward correlational analysis between posterior alpha power and the BOLD signal across the entire brain. Posterior alpha power was separated from other artifacts and brain related EEG activity by means of ICA, in a similar way as done in chapter 3. Negative correlations between posterior alpha power and BOLD were observed in the visual cortex, with the main cluster located in the primary visual cortex. A positive correlation was observed with regions part of the default mode network. The cluster in the primary visual cortex that correlated negatively with alpha power formed the seed for a functionally connectivity analysis and psycho-physiological interaction analysis with the rest of the brain.

The functional connectivity analysis revealed that the selected seed region correlated positively with most of the visual system. A negative correlation was observed with regions that together form the default mode network. The PPI analysis revealed the connectivity of the cluster in the primary visual cortex with extra-striate regions in the

visual system decreases as a function of alpha power. The negative relation observed in the functional connectivity analysis with regions in the default mode network however also decreased in strength. The decreased connectivity within the visual system is in line with the notion that alpha represents functional inhibition (Jokisch and Jensen, 2007; Klimesch et al., 2007), which subsequently results in decreased connectivity with closely connected regions. This hypothesis states that increased alpha power is related to the inhibition of spurious activity in task-irrelevant regions that can otherwise disturb processing going on in other parts of the network. The decreased negative coupling between visual cortex and default mode network regions might be related to an increase in positive coupling when activity in the visual system is low and activity in the default mode network is high. A tentative interpretation of this observation is that the function of the default mode network might be to couple to inactive regions in order to prevent them from randomly interfering with processes in other regions.

General Discussion

The general theme in the four previous chapters is the relation of oscillatory EEG activity with the BOLD signal. A common finding in the previous four chapters is the negative correlation found between BOLD and EEG power in the lower frequency bands, while we for the first time demonstrated a positive correlation between BOLD and high gamma band EEG power in humans. This pattern of negative correlations with low frequencies and positive correlations with high frequencies fits well with intracranial recordings of LFPs and hemodynamic measures in animals. The question arises whether these decreases in low frequencies and the increase in high frequencies are coupled, and therefore represent the same underlying neurophysiological process as suggested by some (Kilner et al., 2005), or different processes. In chapter 6 we were able to show that correlations between BOLD on the one hand, and EEG oscillations in the lower frequencies (alpha and beta) on the other hand are coupled, and might therefore reflect (partly) the same underlying process. The trial-by-trial variation in the observed gamma band response power was however not correlated with power variations in the alpha and beta bands. This strongly suggests low frequency modulations of power are a reflection of underlying neurophysiologic processes that are independent from those related to the high-frequency power changes, and that these two processes contribute independently to the BOLD signal. This would also imply that fMRI activations might be related to low frequency decreases, high frequency increases

or both. Since low and high frequencies have been linked to different neural processes, this distinction might be very important for the interpretation of neuroimaging data. Without relating fMRI activations to electrophysiology it is not possible to make this differentiation.

For the low frequency bands (<30 Hz) we only found negative correlations between BOLD and EEG power. This was a surprise, since computational models and animal work suggest an important involvement of theta oscillations in spatial navigation and working memory maintenance (Jensen, 2006). Several explanations for these surprising negative correlations with frontal theta power can be envisaged.

The first possibility is that the negative correlation between theta and BOLD is indirect: the source location is actually located outside the regions that show a negative correlation with theta. This implicates the negative correlation is indicative of a change in different neural process than the one directly generating frontal theta power. In chapter 3 we showed however that the medial frontal cluster that correlated negatively with frontal theta oscillations is also the likely source location for frontal theta, a notion that is also supported by other studies investigating the source location of frontal theta oscillation (Ishii et al., 1999; Martinez-Montes et al., 2004; Miwakeichi et al., 2004). This therefore is not a likely scenario.

If we accept that frontal theta is generated in this medial frontal cluster of the default mode network, this leaves two explanations that are in line with the negative correlation with the BOLD signal in this region and the rest of the default mode network. The first explanation is that the increased frontal theta power still indicates increased processing in the (medial prefrontal part of the) default mode network. This would have serious implications for cognitive neuroscience using the fMRI-BOLD signal as dependent measure. The fundamental assumption in fMRI research is that increases in the BOLD signal are related to increases in neural activity that is a consequence of increased information processing. If both increases and decreases in BOLD could indicate increased involvement of a region in a task, any contrast between two conditions would be uninterpretable. The data presented in this thesis however do not favour such a far reaching conclusion. On the contrary, the network where BOLD was found to correlate with frontal theta power is the so called default mode network. This is a network that shows decreased BOLD activity in wide variety of cognitive tasks (Shulman et al., 1997). This lack of specificity of tasks in which this network shows a decrease in the BOLD signal indicates that this decrease is not related to a specific cognitive process. In

agreement with this is that frontal theta power is known to increase in a similar wide variety of tasks.

The most likely interpretation of the data is therefore that this increase in frontal theta reflects a decrease in neural activity and processing. This however requires reinterpretation of the role frontal theta plays in information processing. Instead of an active role in processes like working memory maintenance, the role of frontal theta oscillations might be similar to that of alpha oscillations in other (e.g. visual) regions. This would imply that frontal theta increases signal a disengagement or inhibition of the (medial prefrontal part of the) default mode network during task execution, since activity in these regions would otherwise interfere with the ongoing processing in other regions.

The fact that we only find negative power-BOLD correlations for low frequencies certainly does not implicate that all low frequencies show negative correlations with the BOLD response. Most ERPs are in the theta-alpha frequency range, and several papers have reported regions positively related to the BOLD response. Moreover, Debener et al. (Debener et al., 2005) showed that the region found to correlate positively with the Error Related Negativity is also a likely source for this ERP component. But also non-phase-locked low frequency activity can still be positively related to the BOLD signal. Intracranial EEG recordings in humans and hippocampal recordings in mainly in rodents have shown that theta oscillations are involved in cognitive processes like navigation and working memory. A recent study that recorded intracranial EEG from the hippocampal region and fMRI in the same subjects in separate sessions suggests that these rhythms are positively related to the BOLD signal (Ekstrom et al., 2009). The crucial question for simultaneously recorded EEG-fMRI research to be able to take advantage of these rhythms (or any other electrophysiological brain response) is whether or not we can detect these signals at scalp level. A first prerequisite for this is that this low frequency activity is synchronous over a larger patch of cortex than is typically recorded from with intracranial EEG in humans or LFPs in animals. If this synchrony is not strong, picking up these activities with EEG is unlikely, certainly in the context of other processes and artifacts present in the same frequency bands. Another problem might be that the structures most strongly related to theta are in the medial temporal lobe, which is relatively far from the channels at scalp level, and might therefore be hard to pick up. A recent MEG study however suggests that MEG is able to pick up hippocampal theta activity in a task context (Cornwell et al., 2008). This suggests it might be detectable in the EEG signal too. A disadvantage here is that spatial blurring in

EEG is much larger than in MEG, and hippocampal theta might therefore be more easily obscured by other more superficial processes in the theta range like the dominant frontal theta rhythm, which activity is present at all channels, due to reference effects and volume conduction. Possibly the approach we applied recently to investigate the EEG correlates of the salience network (Sadaghiani, 2010) can help here. In this study the BOLD signal from a predefined brain network was correlated with all channels frequency over a wide frequency range. This approach might shed more light whether, on which channels, and for which specific frequencies (or other regions) these oscillations might be detectable.

In three chapters we describe the relation between variations of oscillatory EEG activity in the alpha range and the BOLD signal (**chapters 4, 5 and 6**). In these chapters the results support the notion that alpha is indicative of functional inhibition of regions whose activity might otherwise disturb task relevant processes (Jokisch and Jensen, 2007; Klimesch et al., 2007). This is a deviation from the long-standing idea that alpha oscillations are an idling rhythm (Pfurtscheller et al., 1996a) emerging when regions are not engaged in a task. Recent experiments however have reported increases in the alpha frequency range in a variety of tasks. It has also been shown that the strength and phase of alpha power can influence visual perception (Mathewson et al., 2009; Romei et al., 2008; van Dijk et al., 2008). The idea that activity in task-irrelevant regions can influence task-relevant activity has recently also been investigated using fMRI. Fox et al. (2007) report that during a finger tapping task, spontaneous BOLD fluctuations in the ipsilateral motor cortex (e.g. the one not related to the finger tapping) not only correlates with the contralateral motor cortex, but also predicts the strength of the motor output. These data suggest that during task execution it is especially important to silence task-irrelevant regions that are strongly connected to task relevant regions. The study in chapter 6 suggests just this is what is reflected in increases in alpha power, since we showed that increased alpha power predicts decreased connectivity between regions in the visual system that are strongly connected anatomically and in resting state BOLD.

This notion that decreased activation can also be task-relevant suggests an alternate view on brain function compared to the one that has been most prevalent in cognitive neuroimaging. The major part of the literature in which either PET or fMRI has been used to obtain the neural correlates of specific brain functions focused on increases in the BOLD response to a particular experimental manipulation using the subtraction

paradigm (Fox et al., 1986). Although this approach has been immensely successful in segregating and identifying regions based on their task dependent BOLD increases, the data presented here and recent advances in network oriented analysis of neuroimaging data indicate that the subtraction paradigm is ultimately flawed in giving a full account of all the task relevant processes in the brain. The flaw in the subtraction approach lies in the fact that it depends on the subtraction of tightly matched conditions in which one or more critical variables are under experimental control. This means that only differences between conditions can be detected, but ultimately this is not what is important for behaviour. Behaviour might be more guided by the difference in activity across brain regions within a certain task context, then solely by the activity in regions where differences in activation across conditions are detected. This does not mean the subtraction paradigm is useless in this respect, but it does mean that its results should be interpreted within a different, more network-oriented framework. Differences in activity in one task context compared to another can give important clues about which regions are involved in processing specific aspects of the task, within the context of the presence or absence of activity in the rest of the relevant network(s). The importance of more network oriented research is reflected in the recent development of network oriented methods in both fMRI and electrophysiology. Examples can be found in the development of dynamic causal modelling for both fMRI (Friston et al., 2003) as well as electrophysiological data (Kiebel et al., 2009), and the increase in interest in existing functionally connected regions in both resting state and task contexts in fMRI in recent years.

Compared to the fMRI BOLD signal that basically can only go up or down, electrophysiological signals are potentially richer in content, since such signals detect phase locked events like ERPs as well as differential effects across multiple frequency bands. Since simultaneous fMRI and intracranial or MEG recordings are not possible, the most promising technique at the moment in humans for relating changes in BOLD to electrophysiological phenomena is simultaneously recorded fMRI and EEG. Interpretation of the effects found in fMRI can be greatly improved by being able to relate regions of increased or decreased BOLD activity to specific EEG phenomena, since these different EEG phenomena have often been linked to different processes. In the ERP domain, it for instance has been argued that early components are rather related to bottom up processes while late ERP component are more related to feedback processes (Garrido et al., 2007). Also in the frequency domain responses in different

frequency bands have been linked to different processes. For example, alpha oscillations have been related to functional inhibition, while gamma oscillations have been argued to be fundamental to binding processes (Gray et al., 1989) and neuronal communication (Fries, 2005). Previous research using simultaneously recorded EEG and fMRI has shown entire networks of regions that can be related to different ERP components (Eichele et al., 2005). We have demonstrated in this thesis that this is also the case for different frequency components. Conversely, this research also contributes considerably to our understanding of specific oscillatory EEG phenomena. By integrating EEG with fMRI we are able to link whole networks to certain EEG characteristics, as is demonstrated by the relation of frontal theta to the entire default mode network. In this case this finding also suggests we should reinterpret an EEG measure, midline frontal theta oscillations in this case, differently than has been done in the past.

Combined EEG and fMRI in the future

Combined registration of EEG and fMRI is a relatively new technique, and both recording techniques, preprocessing of data as well as applications will therefore likely continue to develop rapidly in currently unpredictable ways. Several interesting lines of research that already have gained some ground will probably be continued. A good example is the study of epileptiform activity, which will most likely continue to be a fruitful enterprise in the future. What is foreseeable in the future is that other clinical conditions that have well known EEG correlates will also be investigated in more detail with simultaneous EEG / fMRI. One such example can be found in children with Attention Deficit Hyperactivity Disorder (ADHD). A large proportion of theses children show enhanced theta band and reduced beta band activity (Barry et al., 2003). Obtaining the neural correlates of these rhythms might inform us also on the neural underpinnings of the clinical manifestation of ADHD.

Besides clinical applications, the interest in the BOLD correlates of ERPs and oscillatory activity (both in resting state and in a task context) will probably remain, and the recording and analysis procedures will become more refined. Where the first studies mainly focused on well known components in well known paradigms, it is likely that more novel and more elaborate paradigms will also be used to investigate which regions are related to more subtle experimentally manipulated EEG features.

The advancement of EEG-fMRI is until now also tightly bound to methodological developments. The first correlations reported between alpha oscillations and BOLD

(Goldman et al., 2002; Laufs et al., 2003a; Moosmann et al., 2003) very much depended on the development of the first adequate correction algorithms for the MR gradient and ballisto-cardiac artifact (Allen et al., 2000; Allen et al., 1998). Likewise, single trial coupling between EEG and fMRI critically depended on the ability to isolate specific EEG features from artifacts and other nuisances in order to harness variation over trials. It is therefore very likely that future applications will also go hand in hand with both technical as well as methodological advances. This development is not only restricted to the EEG side. Also developments on the fMRI side could very well influence future research lines. An example can be found in the recent advances in high-resolution scanning protocols, which allows one to asses the BOLD response in different cortical layers (Goense and Logothetis, 2008; Goense et al., 2007; Koopmans et al., 2010). Low and high frequency oscillations for instance have been related to activity in different cell types. Where gamma band oscillations have been closely linked to activity of fast spiking inhibitor interneurons, while low frequency oscillations have been related to regular spiking excitatory pyramidal neurons (Cardin et al., 2009). Since these different cell types are differentially distributed over the cortical layers, and both rhythms show an independent relation with the BOLD signal, the profile of their correlation with the BOLD over the cortical layers might very well differ. The development of faster high-resolution fMRI sequences opens the way to study whether EEG features actually have layer-specific BOLD correlates.

A question that emerged in this thesis is whether electrophysiological signals recorded intracranial result from the same neural processes as the signal recorded with EEG and MEG, which integrate electrophysiological activity over a much larger brain region. Where we found frontal theta to be negatively related to the BOLD signal, others using separate intracranial and fMRI recordings in humans suggest a positive relation between theta and BOLD in the hippocampus (Ekstrom et al., 2009). This begs the question of whether intracranial recorded theta reflects fundamentally different processes than that recorded at the scalp. This question can potentially be addressed by taking the BOLD signal from regions that we know from intracranial recordings to show strong task relevant theta oscillations and correlate this theta activity in the EEG recorded at the scalp.

Until now EEG-fMRI has mainly relied on correlational methods either in resting state or in a task context. By sorting on an aspect of prestimulus activity in one modality this technique however makes it possible to make more causal claims. In recent years there has been a growing interest in the influence of spontaneous fluctuations in brain activity

on behaviour and the processing of incoming stimuli. This theme has been explored in fMRI (Herrmann and Debener, 2008; Herrmann et al., 2000; Sadaghiani et al., 2009) as well as in EEG and MEG (Mazaheri et al., 2009; van Dijk et al., 2008). The combination of EEG and fMRI might turn out to be a very powerful tool to investigate this, giving us the opportunity to really harness the advantage of the superior temporal resolution of the EEG and the superior spatial resolution of fMRI. With EEG we are able to asses the brain state up to several milliseconds before a stimulus is presented. A good example for an EEG feature that indexes the brain state would be ongoing fluctuations in posterior alpha power or alpha phase, but also more complicated measures like coherence measures or cross frequency coupling can be envisaged. With fMRI we can subsequently asses the effect this brain state has on the processing of this stimulus in various brain regions. Since the EEG activity precedes the stimulus, under some not too unreasonable assumptions we are able to make causal inferences. These assumptions are that (i) fluctuations of the EEG feature of interest are indeed reflecting some kind of underlying neural process (and not an artifact) and (ii) we can properly adjust for the effect the EEG feature has on the BOLD signal. If these two assumptions hold, we can assume the differences in the BOLD response to that stimulus can be causally related to fluctuations in underlying neural activity that is reflected in the pre-stimulus EEG.

REFERENCES

Allen, P.J., Josephs, O., and Turner, R. (2000). A method for removing imaging artifact from continuous EEG recorded during functional MRI. NeuroImage *12*, 230-239.

Allen, P.J., Polizzi, G., Krakow, K., Fish, D.R., and Lemieux, L. (1998). Identification of EEG events in the MR scanner: the problem of pulse artifact and a method for its subtraction. NeuroImage *8*, 229-239.

Barry, R.J., Clarke, A.R., and Johnstone, S.J. (2003). A review of electrophysiology in attention-deficit/hyperactivity disorder: I. Qualitative and quantitative electroencephalography. Clin Neurophysiol *114*, 171-183.

Barth, M., and Norris, D.G. (2007). Very high-resolution three-dimensional functional MRI of the human visual cortex with elimination of large venous vessels. NMR in biomedicine *20*, 477-484.

Bell, A., and Sejnowski, T. (1995). An information-maximization approach to blind separation and blind deconvolution. Neural. Comput. *7*, 1129-1159.

Benjamini, Y., and Hochberg, Y. (1995). Controlling the False Discovery Rate - a Practical and Powerful Approach to Multiple Testing. J. R. Stat. Soc. Ser. B. Meth. *57*, 289-300.

Bichot, N.P., Rossi, A.F., and Desimone, R. (2005). Parallel and serial neural mechanisms for visual search in macaque area V4. Science *308*, 529-534.

Biswal, B., Yetkin, F.Z., Haughton, V.M., and Hyde, J.S. (1995). Functional connectivity in the motor cortex of resting human brain using echo-planar MRI. Magn Reson Med *34*, 537-541.

Buckner, R.L., Sepulcre, J., Talukdar, T., Krienen, F.M., Liu, H., Hedden, T., Andrews-Hanna, J.R., Sperling, R.A., and Johnson, K.A. (2009). Cortical hubs revealed by intrinsic functional connectivity: mapping, assessment of stability, and relation to Alzheimer's disease. J Neurosci *29*, 1860-1873.

Cabeza, R., Dolcos, F., Graham, R., and Nyberg, L. (2002). Similarities and differences in the neural correlates of episodic memory retrieval and working memory. NeuroImage *16*, 317-330.

Cardin, J.A., Carlen, M., Meletis, K., Knoblich, U., Zhang, F., Deisseroth, K., Tsai, L.H., and Moore, C.I. (2009). Driving fast-spiking cells induces gamma rhythm and controls sensory responses. Nature *459*, 663-667.

Cornwell, B.R., Johnson, L.L., Holroyd, T., Carver, F.W., and Grillon, C. (2008). Human hippocampal and parahippocampal theta during goal-directed spatial navigation predicts performance on a virtual Morris water maze. J Neurosci *28*, 5983-5990.

Dale, A.M., and Halgren, E. (2001). Spatiotemporal mapping of brain activity by integration of multiple imaging modalities. Current opinion in neurobiology *11*, 202-208.

Dale, A.M., Liu, A.K., Fischl, B.R., Buckner, R.L., Belliveau, J.W., Lewine, J.D., and Halgren, E. (2000). Dynamic statistical parametric mapping: combining fMRI and MEG for high-resolution imaging of cortical activity. Neuron *26*, 55-67.

Damoiseaux, J.S., Rombouts, S.A.R.B., Barkhof, F., Scheltens, P., Stam, C.J., Smith, S.M., and Beckmann, C.F. (2006). Consistent resting-state networks across healthy subjects. Proc. Natl. Acad. Sci. U. S. A. *103*, 13848-13853.

De Munck, J.C., Van Dijk, B.W., and Spekreijse, H. (1988). Mathematical dipoles are adequate to describe realistic generators of human brain activity. IEEE transactions on bio-medical engineering *35*, 960-966.

De Pasquale, F., Della Penna, S., Snyder, A.Z., Lewis, C., Mantini, D., Marzetti, L., Belardinelli, P., Ciancetta, L., Pizzella, V., Romani, G.L., and Corbetta, M. (2010). Temporal dynamics of spontaneous MEG activity in brain networks. Proc Natl Acad Sci U S A *107*, 6040-6045.

Debener, S., Ullsperger, M., Siegel, M., Fiehler, K., von Cramon, D.Y., and Engel, A.K. (2005). Trial-by-trial coupling of concurrent electroencephalogram and functional magnetic resonance imaging identifies the dynamics of performance monitoring. J. Neurosci. *25*, 11730-11737.

Delorme, A., and Makeig, S. (2004). EEGLAB: an open source toolbox for analysis of single-trial EEG dynamics including independent component analysis. Journal of neuroscience methods *134*, 9-21.

Eichele, T., Debener, S., Calhoun, V.D., Specht, K., Engel, A.K., Hugdahl, K., von Cramon, D.Y., and Ullsperger, M. (2008). Prediction of human errors by maladaptive changes in event-related brain networks. Proc Natl Acad Sci U S A *105*, 6173-6178.

Eichele, T., Specht, K., Moosmann, M., Jongsma, M.L.A., Quiroga, R.Q., Nordby, H., and Hugdahl, K. (2005). Assessing the spatiotemporal evolution of neuronal activation with single-trial event-related potentials and functional MRI. Proc. Natl. Acad. Sci. U. S. A. *102*, 17798-17803.

Eickhoff, S.B., Stephan, K.E., Mohlberg, H., Grefkes, C., Fink, G.R., Amunts, K., and Zilles, K. (2005). A new SPM toolbox for combining probabilistic cytoarchitectonic maps and functional imaging data. NeuroImage *25*, 1325-1335.

Ekstrom, A., Suthana, N., Millett, D., Fried, I., and Bookheimer, S. (2009). Correlation between BOLD fMRI and theta-band local field potentials in the human hippocampal area. J Neurophysiol *101*, 2668-2678.

Feige, B., Scheffler, K., Esposito, F., Di Salle, F., Hennig, J., and Seifritz, E. (2005). Cortical and subcortical correlates of electroencephalographic alpha rhythm modulation. J. Neurophysiol. *93*, 2864-2872.

Fox, M.D., Snyder, A.Z., Vincent, J.L., Corbetta, M., Van Essen, D.C., and Raichle, M.E. (2005). The human brain is intrinsically organized into dynamic, anticorrelated functional networks. Proc. Natl. Acad. Sci. U. S. A. *102*, 9673-9678.

Fox, M.D., Snyder, A.Z., Vincent, J.L., and Raichle, M.E. (2007). Intrinsic fluctuations within cortical systems account for intertrial variability in human behavior. Neuron *56*, 171-184.

Fox, M.D., Snyder, A.Z., Zacks, J.M., and Raichle, M.E. (2006). Coherent spontaneous activity accounts for trial-to-trial variability in human evoked brain responses. Nature neuroscience *9*, 23-25.

Fox, P.T., Mintun, M.A., Raichle, M.E., Miezin, F.M., Allman, J.M., and Van Essen, D.C. (1986). Mapping human visual cortex with positron emission tomography. Nature *323*, 806-809.

Fries, P. (2005). A mechanism for cognitive dynamics: neuronal communication through neuronal coherence. Trends Cogn Sci *9*, 474-480.

Fries, P., Reynolds, J.H., Rorie, A.E., and Desimone, R. (2001). Modulation of oscillatory neuronal synchronization by selective visual attention. Science *291*, 1560-1563.

Fries, P., Scheeringa, R., and Oostenveld, R. (2008). Finding gamma. Neuron *58*, 303-305.

Friston, K.J., Buechel, C., Fink, G.R., Morris, J., Rolls, E., and Dolan, R.J. (1997). Psychophysiological and modulatory interactions in neuroimaging. NeuroImage *6*, 218-229.

Friston, K.J., Harrison, L., and Penny, W. (2003). Dynamic causal modelling. NeuroImage *19*, 1273-1302.

Fujimaki, N., Hayakawa, T., Nielsen, M., Knosche, T.R., and Miyauchi, S. (2002). An fMRI-constrained MEG source analysis with procedures for dividing and grouping activation. NeuroImage *17*, 324-343.

Garrido, M.I., Kilner, J.M., Kiebel, S.J., and Friston, K.J. (2007). Evoked brain responses are generated by feedback loops. Proc Natl Acad Sci U S A *104*, 20961-20966.

George, J.S., Aine, C.J., Mosher, J.C., Schmidt, D.M., Ranken, D.M., Schlitt, H.A., Wood, C.C., Lewine, J.D., Sanders, J.A., and Belliveau, J.W. (1995). Mapping function in the human brain with magnetoencephalography, anatomical magnetic resonance imaging, and functional magnetic resonance imaging. J Clin Neurophysiol *12*, 406-431.

Giraud, A.L., Kleinschmidt, A., Poeppel, D., Lund, T.E., Frackowiak, R.S., and Laufs, H. (2007). Endogenous cortical rhythms determine cerebral specialization for speech perception and production. Neuron *56*, 1127-1134.

Goense, J.B., and Logothetis, N.K. (2008). Neurophysiology of the BOLD fMRI signal in awake monkeys. Curr Biol *18*, 631-640.

Goense, J.B., Zappe, A.C., and Logothetis, N.K. (2007). High-resolution fMRI of macaque V1. Magn Reson Imaging *25*, 740-747.

Goldman, R.I., Stern, J.M., Engel, J., and Cohen, M.S. (2002). Simultaneous EEG and fMRI of the alpha rhythm. Neuroreport *13*, 2487-2492.

Goncalves, S.I., de Munck, J.C., Pouwels, P.J.W., Schoonhoven, R., Kuijer, J.P.A., Maurits, N.M., Hoogduin, J.M., Van Someren, E.J.W., Heethaar, R.M., and da Silva, F.H.L. (2006). Correlating the alpha rhythm to BOLD using simultaneous EEG/fMRI: Inter-subject variability. NeuroImage *30*, 203-213.

Gratton, G., Coles, M.G.H., and Donchin, E. (1983). A New Method for Off-Line Removal of Ocular Artifact. Electroencephalography and clinical neurophysiology *55*, 468-484.

Gray, C.M., Konig, P., Engel, A.K., and Singer, W. (1989). Oscillatory responses in cat visual cortex exhibit inter-columnar synchronization which reflects global stimulus properties. Nature *338*, 334-337.

Gross, J., Kujala, J., Hamalainen, M., Timmermann, L., Schnitzler, A., and Salmelin, R. (2001). Dynamic imaging of coherent sources: Studying neural interactions in the human brain. Proc Natl Acad Sci U S A *98*, 694-699.

Gusnard, D.A., Akbudak, E., Shulman, G.L., and Raichle, M.E. (2001). Medial prefrontal cortex and self-referential mental activity: Relation to a default mode of brain function. Proc. Natl. Acad. Sci. U. S. A. *98*, 4259-4264.

Gusnard, D.A., and Raichle, M.E. (2001). Searching for a baseline: Functional imaging and the resting human brain. Nat. Rev. Neurosci. *2*, 685-694.

Haegens, S., Osipova, D., Oostenveld, R., and Jensen, O. (2010). Somatosensory working memory performance in humans depends on both engagement and disengagement of regions in a distributed network. Hum Brain Mapp *31*, 26-35.

Hagmann, P., Cammoun, L., Gigandet, X., Meuli, R., Honey, C.J., Wedeen, V.J., and Sporns, O. (2008). Mapping the structural core of human cerebral cortex. PLoS biology *6*, e159.

Hall, S.D., Holliday, I.E., Hillebrand, A., Singh, K.D., Furlong, P.L., Hadjipapas, A., and Barnes, G.R. (2005). The missing link: analogous human and primate cortical gamma oscillations. NeuroImage *26*, 13-17.

Herrmann, C.S., and Debener, S. (2008). Simultaneous recording of EEG and BOLD responses: a historical perspective. Int J Psychophysiol *67*, 161-168.

Herrmann, C.S., Oertel, U., Wang, Y., Maess, B., and Friederici, A.D. (2000). Noise affects auditory and linguistic processing differently: an MEG study. Neuroreport *11*, 227-229.

Hoogenboom, N., Schoffelen, J.M., Oostenveld, R., Parkes, L.M., and Fries, P. (2006). Localizing human visual gamma-band activity in frequency, time and space. NeuroImage *29*, 764-773.

Im, C.H., Jung, H.K., and Fujimaki, N. (2005). fMRI-constrained MEG source imaging and consideration of fMRI invisible sources. Hum Brain Mapp *26*, 110-118.

Ishii, R., Shinosaki, K., Ukai, S., Inouye, T., Ishihara, T., Yoshimine, T., Hirabuki, N., Asada, H., Kihara, T., Robinson, S.E., and Takeda, M. (1999). Medial prefrontal cortex generates frontal midline theta rhythm. Neuroreport *10*, 675-679.

Ives, J.R., Warach, S., Schmitt, F., Edelman, R.R., and Schomer, D.L. (1993). Monitoring the patient's EEG during echo planar MRI. Electroencephalography and clinical neurophysiology *87*, 417-420.

Jensen, O. (2006). Maintenance of multiple working memory items by temporal segmentation. Neuroscience *139*, 237-249.

Jensen, O., Gelfand, J., Kounios, J., and Lisman, J.E. (2002). Oscillations in the alpha band (9-12 Hz) increase with memory load during retention in a short-term memory task. Cereb Cortex *12*, 877-882.

Jokisch, D., and Jensen, O. (2007). Modulation of gamma and alpha activity during a working memory task engaging the dorsal or ventral stream. J Neurosci *27*, 3244-3251.

Kahana, M.J., Seelig, D., and Madsen, J.R. (2001). Theta returns. Curr. Opin. Neurobiol. *11*, 739-744.

Kiebel, S.J., Garrido, M.I., Moran, R., Chen, C.C., and Friston, K.J. (2009). Dynamic causal modeling for EEG and MEG. Hum Brain Mapp.

Kilner, J.M., Mattout, J., Henson, R., and Friston, K.J. (2005). Hemodynamic correlates of EEG: a heuristic. NeuroImage *28*, 280-286.

Klimesch, W. (1999). EEG alpha and theta oscillations reflect cognitive and memory performance: a review and analysis. Brain Res Brain Res Rev *29*, 169-195.

Klimesch, W., Doppelmayr, M., Russegger, H., Pachinger, T., and Schwaiger, J. (1998). Induced alpha band power changes in the human EEG and attention. Neurosci Lett *244*, 73-76.

Klimesch, W., Doppelmayr, M., Schwaiger, J., Auinger, P., and Winkler, T. (1999). 'Paradoxical' alpha synchronization in a memory task. Brain research *7*, 493-501.

Klimesch, W., Sauseng, P., and Hanslmayr, S. (2007). EEG alpha oscillations: the inhibition-timing hypothesis. Brain research reviews *53*, 63-88.

Koch, S.P., Werner, P., Steinbrink, J., Fries, P., and Obrig, H. (2009). Stimulus-induced and state-dependent sustained gamma activity is tightly coupled to the hemodynamic response in humans. J Neurosci *29*, 13962-13970.

Koopmans, P.J., Barth, M., and Norris, D.G. (2010). Layer-specific BOLD activation in human V1. Hum Brain Mapp. doi:10.1002/hbm.20936.

Lachaux, J.P., Fonlupt, P., Kahane, P., Minotti, L., Hoffmann, D., Bertrand, O., and Baciu, M. (2007). Relationship between task-related gamma oscillations and BOLD signal: new insights from combined fMRI and intracranial EEG. Hum Brain Mapp *28*, 1368-1375.

Lakatos, P., Karmos, G., Mehta, A.D., Ulbert, I., and Schroeder, C.E. (2008). Entrainment of neuronal oscillations as a mechanism of attentional selection. Science *320*, 110-113.

Laufs, H., Daunizeau, J., Carmichael, D.W., and Kleinschmidt, A. (2008). Recent advances in recording electrophysiological data simultaneously with magnetic resonance imaging. NeuroImage *40*, 515-528.

Laufs, H., and Duncan, J.S. (2007). Electroencephalography/functional MRI in human epilepsy: what it currently can and cannot do. Current opinion in neurology *20*, 417-423.

Laufs, H., Holt, J.L., Elfont, R., Krams, M., Paul, J.S., Krakow, K., and Kleinschmidt, A. (2006). Where the BOLD signal goes when alpha EEG leaves. NeuroImage *31*, 1408-1418.

Laufs, H., Kleinschmidt, A., Beyerle, A., Eger, E., Salek-Haddadi, A., Preibisch, C., and Krakow, K. (2003a). EEG-correlated fMRI of human alpha activity. NeuroImage *19*, 1463-1476.

Laufs, H., Krakow, K., Sterzer, P., Eger, E., Beyerle, A., Salek-Haddadi, A., and Kleinschmidt, A. (2003b). Electroencephalographic signatures of attentional and cognitive default modes in spontaneous brain activity fluctuations at rest. Proc. Natl. Acad. Sci. U. S. A. *100*, 11053-11058.

Lemieux, L., Allen, P.J., Franconi, F., Symms, M.R., and Fish, D.R. (1997). Recording of EEG during fMRI experiments: patient safety. Magn Reson Med *38*, 943-952.

Liljestrom, M., Kujala, J., Jensen, O., and Salmelin, R. (2005). Neuromagnetic localization of rhythmic activity in the human brain: a comparison of three methods. NeuroImage *25*, 734-745.

Linden, D.E., Prvulovic, D., Formisano, E., Vollinger, M., Zanella, F.E., Goebel, R., and Dierks, T. (1999). The functional neuroanatomy of target detection: an fMRI study of visual and auditory oddball tasks. Cereb Cortex *9*, 815-823.

Liu, A.K., Belliveau, J.W., and Dale, A.M. (1998). Spatiotemporal imaging of human brain activity using functional MRI constrained magnetoencephalography data: Monte Carlo simulations. Proc Natl Acad Sci U S A *95*, 8945-8950.

Logothetis, N.K. (2008). What we can do and what we cannot do with fMRI. Nature *453*, 869-878.

Logothetis, N.K., Pauls, J., Augath, M., Trinath, T., and Oeltermann, A. (2001). Neurophysiological investigation of the basis of the fMRI signal. Nature *412*, 150-157.

Lopes da Silva, F. (1991). Neural mechanisms underlying brain waves: from neural membranes to networks. Electroencephalography and clinical neurophysiology *79*, 81-93.

Makeig, S., Debener, S., Onton, J., and Delorme, A. (2004a). Mining event-related brain dynamics. Trends Cogn. Sci. *8*, 204-210.

Makeig, S., Delorme, A., Westerfield, M., Jung, T.P., Townsend, J., Courchesne, E., and Sejnowski, T.J. (2004b). Electroencephalographic brain dynamics following manually responded visual targets. PLoS biology *2*, e176.

Makeig, S., Jung, T.P., Bell, A.J., Ghahremani, D., and Sejnowski, T.J. (1997). Blind separation of auditory event-related brain responses into independent components. Proc Natl Acad Sci U S A *94*, 10979-10984.

Makeig, S., Westerfield, M., Jung, T.P., Enghoff, S., Townsend, J., Courchesne, E., and Sejnowski, T.J. (2002). Dynamic brain sources of visual evoked responses. Science *295*, 690-694.

Mantini, D., Perrucci, M.G., Del Gratta, C., Romani, G.L., and Corbetta, M. (2007). Electrophysiological signatures of resting state networks in the human brain. Proc Natl Acad Sci U S A *104*, 13170-13175.

Maris, E., and Oostenveld, R. (2007). Nonparametric statistical testing of EEG- and MEG-data. Journal of neuroscience methods *164*, 177-190.

Martinez-Montes, E., Valdes-Sosa, P.A., Miwakeichi, F., Goldman, R.I., and Cohen, M.S. (2004). Concurrent EEG/fMRI analysis by multiway Partial Least Squares. NeuroImage *22*, 1023-1034.

Mason, M.F., Norton, M.I., Van Horn, J.D., Wegner, D.M., Grafton, S.T., and Macrae, C.N. (2007). Wandering minds: the default network and stimulus-independent thought. Science *315*, 393-395.

Mathewson, K.E., Gratton, G., Fabiani, M., Beck, D.M., and Ro, T. (2009). To see or not to see: prestimulus alpha phase predicts visual awareness. J Neurosci *29*, 2725-2732.

Mazaheri, A., Nieuwenhuis, I.L., van Dijk, H., and Jensen, O. (2009). Prestimulus alpha and mu activity predicts failure to inhibit motor responses. Hum Brain Mapp.

Meltzer, J.A., Negishi, M., Mayes, L.C., and Constable, R.T. (2007). Individual differences in EEG theta and alpha dynamics during working memory correlate with fMRI responses across subjects. Clin Neurophysiol *118*, 2419-2436.

Mitra, P.P., and Pesaran, B. (1999). Analysis of dynamic brain imaging data. Biophysical journal *76*, 691-708.

Miwakeichi, F., Martinez-Montes, E., Valdes-Sosa, P.A., Nishiyama, N., Mizuhara, H., and Yamaguchi, Y. (2004). Decomposing EEG data into space-time-frequency components using Parallel Factor Analysis. NeuroImage *22*, 1035-1045.

Mizuhara, H., Wang, L.Q., Kobayashi, K., and Yamaguchi, Y. (2004). A long-range cortical network emerging with theta oscillation in a mental task. Neuroreport *15*, 1233-1238.

Moosmann, M., Eichele, T., Nordby, H., Hugdahl, K., and Calhoun, V.D. (2008). Joint independent component analysis for simultaneous EEG-fMRI: principle and simulation. Int J Psychophysiol *67*, 212-221.

Moosmann, M., Ritter, P., Krastel, I., Brink, A., Thees, S., Blankenburg, F., Taskin, B., Obrig, H., and Villringer, A. (2003). Correlates of alpha rhythm in functional magnetic resonance imaging and near infrared spectroscopy. NeuroImage *20*, 145-158.

Moradi, F., Liu, L.C., Cheng, K., Waggoner, R.A., Tanaka, K., and Ioannides, A.A. (2003). Consistent and precise localization of brain activity in human primary visual cortex by MEG and fMRI. NeuroImage *18*, 595-609.

Mukamel, R., Gelbard, H., Arieli, A., Hasson, U., Fried, I., and Malach, R. (2005). Coupling between neuronal firing, field potentials, and FMRI in human auditory cortex. Science *309*, 951-954.

Mulert, C., Leicht, G., Hepp, P., Kirsch, V., Karch, S., Pogarell, O., Reiser, M., Hegerl, U., Jager, L., Moller, H.J., and McCarley, R.W. (2010). Single-trial coupling of the gamma-band response and the corresponding BOLD signal. NeuroImage *49*, 2238-2247.

Muthukumaraswamy, S.D., and Singh, K.D. (2009). Functional decoupling of BOLD and gamma-band amplitudes in human primary visual cortex. Hum Brain Mapp *30*, 2000-2007.

Niessing, J., Ebisch, B., Schmidt, K.E., Niessing, M., Singer, W., and Galuske, R.A. (2005). Hemodynamic signals correlate tightly with synchronized gamma oscillations. Science *309*, 948-951.

Nolte, G. (2003). The magnetic lead field theorem in the quasi-static approximation and its use for magnetoencephalography forward calculation in realistic volume conductors. Phys Med Biol *48*, 3637-3652.

Onton, J., Delorme, A., and Makeig, S. (2005). Frontal midline EEG dynamics during working memory. NeuroImage *27*, 341-356.

Oostenveld, R., Praamstra, P., Stegeman, D.F., and van Oosterom, A. (2001). Overlap of attention and movement-related activity in lateralized event-related brain potentials. Clin. Neurophysiol. *112*, 477-484.

Opitz, B., Mecklinger, A., Friederici, A.D., and von Cramon, D.Y. (1999). The functional neuroanatomy of novelty processing: integrating ERP and fMRI results. Cereb Cortex *9*, 379-391.

Palva, S., and Palva, J.M. (2007). New vistas for alpha-frequency band oscillations. Trends Neurosci *30*, 150-158.

Pfurtscheller, G., Stancak, A., Jr., and Neuper, C. (1996a). Event-related synchronization (ERS) in the alpha band--an electrophysiological correlate of cortical idling: a review. Int J Psychophysiol *24*, 39-46.

Pfurtscheller, G., Stancak, A., Jr., and Neuper, C. (1996b). Post-movement beta synchronization. A correlate of an idling motor area? Electroencephalography and clinical neurophysiology *98*, 281-293.

Phillips, C., Rugg, M.D., and Friston, K.J. (2002). Anatomically informed basis functions for EEG source localization: combining functional and anatomical constraints. NeuroImage *16*, 678-695.

Posthuma, D., Neale, M.C., Boomsma, D.I., and de Geus, E.J. (2001). Are smarter brains running faster? Heritability of alpha peak frequency, IQ, and their interrelation. Behav Genet *31*, 567-579.

Raichle, M.E., MacLeod, A.M., Snyder, A.Z., Powers, W.J., Gusnard, D.A., and Shulman, G.L. (2001). A default mode of brain function. Proc. Natl. Acad. Sci. U. S. A. *98*, 676-682.

Raichle, M.E., and Snyder, A.Z. (2007). A default mode of brain function: A brief history of an evolving idea. NeuroImage.

Ritter, P., and Villringer, A. (2006). Simultaneous EEG-fMRI. Neurosci Biobehav Rev *30*, 823-838.

Romei, V., Brodbeck, V., Michel, C., Amedi, A., Pascual-Leone, A., and Thut, G. (2008). Spontaneous fluctuations in posterior alpha-band EEG activity reflect variability in excitability of human visual areas. Cereb Cortex *18*, 2010-2018.

Rosa, M.J., Kilner, J., Blankenburg, F., Josephs, O., and Penny, W. (2010). Estimating the transfer function from neuronal activity to BOLD using simultaneous EEG-fMRI. NeuroImage *49*, 1496-1509.

Sadaghiani, S., Hesselmann, G., and Kleinschmidt, A. (2009). Distributed and antagonistic contributions of ongoing activity fluctuations to auditory stimulus detection. J Neurosci *29*, 13410-13417.

Sadaghiani, S., Scheeringa, R., Lehonbgre, K., Morillon, B., Giraud, A., Kleinschmidt, A (2010). Intrinsic Connectivity Networks, Alpha Oscillations and Tonic Alertness: A simultaneous EEG/fMRI Study. Journal of Neuroscience *In Press*.

Sammer, G., Blecker, C., Gebhardt, H., Bischoff, M., Stark, R., Morgen, K., and Vaitl, D. (2007). Relationship between regional hemodynamic activity and simultaneously recorded EEG-theta associated with mental arithmetic-induced workload. Hum Brain Mapp *28*, 793-803.

Sammer, G., Blecker, C., Gebhardt, H., Kirsch, P., Stark, R., and Vaitl, D. (2005). Acquisition of typical EEG waveforms during fMRI: SSVEP, LRP, and frontal theta. NeuroImage *24*, 1012-1024.

Scheeringa, R., Bastiaansen, M.C., Petersson, K.M., Oostenveld, R., Norris, D.G., and Hagoort, P. (2008). Frontal theta EEG activity correlates negatively with the default mode network in resting state. Int J Psychophysiol *67*, 242-251.

Scheeringa, R., Petersson, K.M., Oostenveld, R., Norris, D.G., Hagoort, P., and Bastiaansen, M.C. (2009). Trial-by-trial coupling between EEG and BOLD identifies networks related to alpha and theta EEG power increases during working memory maintenance. NeuroImage *44*, 1224-1238.

Schulz, M., Chau, W., Graham, S.J., McIntosh, A.R., Ross, B., Ishii, R., and Pantev, C. (2004). An integrative MEG-fMRI study of the primary somatosensory cortex using cross-modal correspondence analysis. NeuroImage *22*, 120-133.

Shmuel, A., Augath, M., Oeltermann, A., and Logothetis, N.K. (2006). Negative functional MRI response correlates with decreases in neuronal activity in monkey visual area V1. Nat. Neurosci. *9*, 569-577.

Shulman, G.L., Fiez, J.A., Corbetta, M., Buckner, R.L., Miezin, F.M., Raichle, M.E., and Petersen, S.E. (1997). Common blood flow changes across visual tasks .2. Decreases in cerebral cortex. J. Cogn. Neurosci. *9*, 648-663.

Smith, S.M., Fox, P.T., Miller, K.L., Glahn, D.C., Fox, P.M., Mackay, C.E., Filippini, N., Watkins, K.E., Toro, R., Laird, A.R., and Beckmann, C.F. (2009). Correspondence of the brain's functional architecture during activation and rest. Proc Natl Acad Sci U S A *106*, 13040-13045.

Steriade, M., Gloor, P., Llinas, R.R., Lopes de Silva, F.H., and Mesulam, M.M. (1990). Report of IFCN Committee on Basic Mechanisms. Basic mechanisms of cerebral rhythmic activities. Electroencephalography and clinical neurophysiology *76*, 481-508.

Stone, J.V. (2004). Independent component analysis : a tutorial introduction (Cambridge, Mass.: MIT Press).

Tuladhar, A.M., Huurne, N.T., Schoffelen, J.M., Maris, E., Oostenveld, R., and Jensen, O. (2007). Parieto-occipital sources account for the increase in alpha activity with working memory load. Hum Brain Mapp.

van Dijk, H., Schoffelen, J.M., Oostenveld, R., and Jensen, O. (2008). Prestimulus oscillatory activity in the alpha band predicts visual discrimination ability. J Neurosci *28*, 1816-1823.

van Dijk, H., van der Werf, J., Mazaheri, A., Medendorp, W.P., and Jensen, O. (2010). Modulations in oscillatory activity with amplitude asymmetry can produce cognitively relevant event-related responses. Proc Natl Acad Sci U S A *107*, 900-905.

Varela, F., Lachaux, J.P., Rodriguez, E., and Martinerie, J. (2001). The brainweb: phase synchronization and large-scale integration. Nature reviews *2*, 229-239.

Wibral, M., Turi, G., Linden, D.E., Kaiser, J., and Bledowski, C. (2008). Decomposition of working memory-related scalp ERPs: crossvalidation of fMRI-constrained source analysis and ICA. Int J Psychophysiol *67*, 200-211.

Wilcoxon, F. (1945). Individual comparisons by ranking methods. Biometrics Bulletin *1*, 80-83.

Woldorff, M.G., Tempelmann, C., Fell, J., Tegeler, C., Gaschler-Markefski, B., Hinrichs, H., Heinz, H.J., and Scheich, H. (1999). Lateralized auditory spatial perception and the contralaterality of cortical processing as studied with functional magnetic resonance imaging and magnetoencephalography. Hum Brain Mapp *7*, 49-66.

Yuan, H., Liu, T., Szarkowski, R., Rios, C., Ashe, J., and He, B. (2010). Negative covariation between task-related responses in alpha/beta-band activity and BOLD in human sensorimotor cortex: an EEG and fMRI study of motor imagery and movements. NeuroImage *49*, 2596-2606.

SAMENVATTING IN HET NEDERLANDS

INLEIDING

Elektro-encefalografie (EEG) en *functional Magnetic Resonance Imaging* (fMRI) zijn op het moment de twee meest gebruikte methoden voor het registreren van menselijke hersenactiviteit tijdens het uitvoeren van cognitieve taken. Met fMRI meten we de toe- en afname van zuurstofrijk bloed in de hersenen. Het signaal dat we meten is het zogenaamd *Blood Oxygenation Level Dependent* (BOLD) signaal. Hiermee kunnen we een goed beeld krijgen waar in de hersenen de toevoer van zuurstofrijk bloed toe of afneemt wanneer een bepaalde taak wordt uitgevoerd. De impliciete assumptie hierbij is dat gebieden die betrokken zijn bij een bepaalde taak door de verhoogde neurale activiteit een verhoogde toevoer van zuurstofrijk bloed krijgen. Deze verhoogde toevoer treedt echter op met een vertraging van enkele seconden en is uitgesmeerd over een langere tijdsperiode. FMRI geeft dus geen goede informatie over wanneer activiteit precies plaatsvindt.

Het EEG is een reflectie van de elektrofysiologische activiteit van het brein. Door middel van het plaatsen van elektroden op het hoofd, kan een deel van de elektrofysiologische activiteit van de onderliggende hersengebieden worden geregistreerd met milliseconde precisie. Hiermee krijgen we een idee van de elektrofysiologische reactie van het brein op bijvoorbeeld een visuele stimulus. Er zijn verschillende manieren waarop dit EEG signaal kan worden geanalyseerd. Als proefpersonen vele malen dezelfde taak uitvoeren, kan het EEG-signaal gemiddeld over alle presentaties. De verschillende pieken die in dit gemiddelde signaal te onderscheiden zijn worden ook wel *Event Related Potentials* (ERP) genoemd. Een andere manier van analyseren is door te kijken hoe de frequentie-inhoud van het EEG signaal varieert over tijd, en hoe deze gemanipuleerd kan worden door het doen van een taak. Het EEG kan namelijk ook beschouwd worden als een signaal dat is opgebouwd uit elektrische golven van verschillende frequenties. Veranderingen in de sterkte van verschillende frequenties kunnen over een tijdsbestek worden gevolgd, en worden ook beïnvloed door het uitvoeren van een taak. Het grote nadeel van EEG is dat we de signalen alleen op het hoofd kunnen meten. Hierdoor is het moeilijk om erachter te komen waar deze signalen in het brein vandaan komen.

De motivatie voor het ontwikkelen van het gelijktijdig registreren van EEG en fMRI is dat de voordelen van de ene techniek de nadelen van de andere techniek kunnen compenseren. FMRI levert informatie op over waar in het brein de activiteit plaatsvindt, terwijl het EEG aangeeft wanneer dat precies gebeurt. Het gelijktijdig meten van de

signalen op zich levert echter geen voordeel op wanneer we alsnog naar de EEG data en fMRI data afzonderlijk zouden kijken. Men zou zich dan de technologische problemen die gelijktijdige metingen met zich meebrengen kunnen besparen. Gelijktijdige metingen hebben alleen zin wanneer we de analyse van de EEG en fMRI data op een manier kunnen integreren die ons informatie oplevert die we niet kunnen halen uit afzonderlijke metingen. In dit proefschrift wordt gedemonstreerd hoe we extra informatie kunnen halen uit het feit dat we gelijktijdig EEG en fMRI gemeten hebben. Hierbij maken we expliciet gebruik van het feit dat we voor elk tijdspunt informatie hebben over zowel het EEG signaal als het fMRI signaal. Dit is informatie die alleen te verkrijgen is door gelijktijdig EEG en fMRI te meten.

De meest voorkomende toepassing van simultane metingen is in epilepsie onderzoek, waarbij wordt onderzocht in welke gebieden het BOLD signaal dat wordt gemeten met fMRI, samenhangt met het voorkomen van epileptische activiteit in het EEG. Gelijktijdig meten van EEG en fMRI is hier noodzakelijk omdat het optreden van deze epileptische activiteit onvoorspelbaar is. Buiten deze klinische context is de techniek in het begin voornamelijk gebruikt om te onderzoeken in welke hersengebieden activiteit gemeten met fMRI samenhangt met spontane veranderingen in specifieke frequentiebanden in het EEG zonder dat er een taak uitgevoerd wordt. Verscheidene van deze studies hebben onderzoek gedaan naar de alfa frequentieband, die van 8 tot 12 Hertz loopt. Het alfa ritme is het sterkste ritme in het EEG van de wakkere mens. Het is vaak met het blote oog waar te nemen in het ruwe EEG-signaal, en is vooral sterk als de ogen van de proefpersoon gesloten zijn. Het is daarom een voor de hand liggend ritme om als eerste met gelijktijdig EEG en fMRI te onderzoeken. Interessanter is echter om te weten welke gebieden betrokken zijn bij taakgerelateerde effecten in het EEG. Inmiddels zijn er onderzoeken verschenen die er met behulp van gelijktijdige EEG en fMRI metingen in zijn geslaagd om hersengebieden te identificeren die gerelateerd zijn aan ERP's in verschillende taaksituaties. Een essentiële stap hierbij was dat zij in staat zijn gebleken om de taak-oninteressante activiteit dusdanig te reduceren, dat ook voor elke aanbieding afzonderlijk een goede schatting van de ERP waarin men geïnteresseerd is kon maken. In conventioneel onderzoek wordt deze taakoninteressante activiteit als ruis beschouwd verwijderd door te middelen over herhaalde aanbiedingen van dezelfde taak, maar dit is voor indivuduele aanbiedingen van een taak niet mogelijk. Door taakoninteressante activiteit door middel van andere manieren te reduceren waren de onderzoekers in staat voor elke taakaanbieding een schatting van de sterkte van de

ERP te maken. Variaties hierin vertoonden hersengebied specifieke correlaties met het BOLD signaal.

De experimenten die gepresenteerd worden in dit proefschrift bouwen voort op dit werk. In dit proefschrift draait het specifiek om de vraag hoe we met een geïntegreerde analyse van simultaan gemeten EEG en fMRI data kunnen onderzoeken hoe variaties in de sterkte van de verschillende frequenties waaruit het EEG is opgebouwd samenhangen met veranderingen in het BOLD signaal. De methodologische overwegingen die hierbij een rol spelen worden in Hoofdstuk 2 besproken. Hierin wordt onder andere uitengezet hoe oninteresante acitiviet in het EEG kan worden verwijderd en hoe de geintegreerde analyse is uitgevoerd. In de vier hoofdstukken die hierop volgen worden de uitkomsten en interpretaties van verschillende experimenten die zijn uitgevoerd besproken. Twee van de vier hoofdstukken (Hoofdstuk 3 en Hoofdstuk 6) behandelen de relatie tussen spontane fluctuaties in het EEG en hersengebiedspecifieke veranderingen in het BOLD signaal tijdens rust. In de andere twee hoofdstukken (Hoofdstuk 4 en Hoofdstuk 5) is juist onderzocht hoe taakgerelateerde veranderingen in de sterkte van verschillende frequenties in het EEG samenhangen met veranderingen in het BOLD signaal. Hieronder wordt voor elk van de vier hoofdstukken kort de inhoud beschreven.

DE EXPERIMENTEN

Hoofdstuk 3

In Hoofdstuk 3 onderzoeken we in welke hersengebieden het BOLD signaal correleert met fluctuaties in de sterkte, ook wel power genoemd, van het mediaal frontale theta ritme in het EEG terwijl de proefpersonen met de ogen open rusten. Dit ritme is het sterkste ritme in de theta band (3-8 Hertz), en wordt onder andere geassocieerd met werkgeheugen en cognitieve controle. De resultaten in dit hoofdstuk wijzen er echter op dat veranderingen in de sterkte van dit ritme niet samengaan met veranderingen in het BOLD signaal in gebieden die betrokken zijn bij werkgeheugen of cognitieve controle. Er bleek wel een negatieve correlatie tussen frontale theta power en het BOLD signaal in het zogenaamde *default mode network* te bestaan. Dit is een netwerk van gebieden dat bestaat uit de mediale frontale cortex, de posterieure cingulate gyrus en de linker en rechter angulaire gyrus. Van dit netwerk is bekend dat de gebieden onderling een sterke correlatie vertonen in zowel taak als rust condities. Uit fMRI en PET onderzoek is ook

gebleken dat de activiteit van dit netwerk verlaagd wordt tijdens het uivoeren van de meeste cognitieve taken. Activiteit in dit netwerk is onder andere gerelateerd aan dagdromen. De negatieve correlatie tussen frontale theta power in het EEG in dit default mode network, impliceert dus dat een verhoging van frontale theta EEG power direct gerelateerd is aan de-activatie van dit default mode network. Een verhoging van frontale theta activiteit lijkt dus te maken te hebben met het onderbreken van bijvoorbeeld dagdromen en is niet gerelateerd aan activiteit in gebieden die direct bij werkgeheugen of cognitieve controle betrokken zijn

Hoofdstuk 4

In Hoofdstuk 4 onderzoeken we met behulp van gelijktijdig gemeten EEG en fMRI welke gebieden gerelateerd zijn aan door werkgeheugen geïnduceerde verhoging van frontale theta en posterieure alfa (8-12 Hz) power. Van beide ritmes is bekend dat de amplitude toeneemt bij een grotere belasting van het werkgeheugen. In een EEG sessie buiten de MRI scanner werd inderdaad een toename van mediale frontale theta power en rechts posterieure alfa power gevonden naarmate de werkgeheugenbelasting hoger werd. Tijdens de meting in de scanner observeerden we hetzelfde effect van werkgeheugenbelasting op alfa en theta power.

Voor het frontale theta ritme vonden we zowel gebieden waar het BOLD signaal positief, als gebieden waar het negatief met theta correleerd. Hieruit volgt echter niet meteen dat deze gebieden ook direct betrokken zijn bij de werkgeheugen gerelateerde toename in theta power. Het is mogelijk dat ze alleen correleren met niet aan werkgeheugen gerelateerde fluctuaties power. Gebieden die betrokken zijn bij de met werkgeheugen gerelateerde toename in theta power zouden naast een correlatie met theta power ook een effect van werkgeheugenbelasting op het BOLD signaal moeten laten zien die overeenkomt met diezelfde toename in theta power. Wanneer we dit criterium toepassen, blijven gebieden over die een negatieve correlatie met theta fluctuaties over trials en een afname in het BOLD signaal naarmate de werkgeheugenbelasting groter wordt vertonen.

Deze gebieden bleken allen in het default mode netwerk te liggen, in overeenstemming met de resultaten in Hoofdstuk 3. Hieruit kan dus worden geconcludeerd dat de toename in frontale theta oscillaties met werkgeheugenbelasting direct gerelateerd is aan een afname in activiteit van het default mode netwerk.

Voor het effect van werkgeheugenbelasting op rechts posterieure alfa power volgden we dezelfde strategie. Hierbij werden meerdere gebieden gevonden waar frontale theta negatief correleerd met het BOLD signaal. Maar twee van deze gebieden vertoonden echter een afname in het BOLD signaal met werkgeheugenbelasting die overeenkomt met de toename in alfa power. Deze twee gebieden bevinden zich in de primaire visuele cortex en het achterste gedeelte van de rechter middelste temporale gyrus. Deze resultaten zijn te interpreteren in de context van de functionele inhibitie theorie voor alfa oscillaties. Hierbij word gesteld dan verhoogde alfa amplitude een gevolg is van inhibitie van hersengebieden die niet direct bij een taak betrokken zijn, maar de activiteit van gebieden die dat wel zijn zouden kunnen verstoren.

De analyse en resultaten in dit hoofdstuk demonstreren hoe met gelijktijdig gemeten EEG en fMRI de hersengebieden kunnen worden gevonden die gerelateerd zijn aan taakgeïnduceerde veranderingen in EEG power. In dit geval vertonen de gebieden die gerelateerd zijn aan alfa en de gebieden die gerelateerd zijn aan theta beiden een afname van het BOLD signaal met werkgeheugenbelasting. We zijn dus ook in staat een differentiatie te maken tussen deze gebieden op basis van de relatie die ze hebben met frontale theta dan wel rechts posterieure alfa EEG power.

Hoofdstuk 5

In zowel Hoofdstuk 3 als Hoofdstuk 4 observeerden we een inverse relatie tussen het BOLD signaal en power fluctuaties in de lage frequentiebanden (alfa en theta). In Hoofdstuk 5 onderzochten we of andere frequentiebanden een positieve correlatie met het BOLD signaal vertonen. Studies in katten en apen suggereren dat voornamelijk power fluctuaties in de gamma band (ca 30 - 100 Hz) een positieve correlatie met het BOLD signaal vertonen. In dit hoofdstuk probeerden we deze bevindingen te repliceren in mensen tijdens het uitvoeren van een cognitieve taak. Hiervoor gebruikten we een taak waarvan bekend is dat het een sterke toename in gamma power en een sterke afname in alfa en bèta power (12-30 Hz) induceert. Daarbij is vanuit MEG onderzoek ook bekend dat de waarschijnlijke bronlocatie van deze power effecten te vinden is in de visuele cortex. Door het BOLD signaal in gebieden in de visuele cortex die taakgerelateerde activiteit vertonen te correleren met EEG power voor alle frequenties tot en met 120 Hz waren we in staat de relatie tussen het BOLD signaal en frequentie specifieke veranderingen in EEG power te onderzoeken.

De correlatie tussen het BOLD signaal en EEG power voor elke frequentie tot 120 Hz leverde een correlatiespectrum op. Dit spectrum vertoonde een significante negatieve correlatie van het BOLD signaal met alfa en bèta power en een significante positieve correlatie met gamma power tussen 60 en 80 Hz. Deze resultaten repliceren de eerdere bevindingen van de studies in katten en apen. Daarnaast bleek ook dat de gamma band fluctuaties ongecorreleerd waren aan de alfa en bèta fluctuaties. Dit suggereert dat er ten minste twee onafhankelijke neurale processen zijn die een effect hebben op het BOLD signaal. Eén van deze processen hangt samen met amplitude fluctuaties in de lagere frequenties van de alfa en bèta band en één met de hogere frequenties in de gamma band.

Hoofdstuk 6

In de vorige hoofdstukken maakten we gebruik van een conventionele correlationele benadering om te onderzoeken hoe EEG power samenhangt met het BOLD signaal in verschillende hersengebieden. In dit hoofdstuk kozen we voor een nieuwe benadering waarbij we onderzochten of de interactie tussen hersengebieden samenhangt met power veranderingen in het EEG. Het netwerk waarin we dit onderzochten is het visuele netwerk. Van dit netwerk is bekend dat het een sterk alfa ritme genereerd dat goed te meten is met electroden achter op het hoofd. Hierdoor is het een geschikt newerk om te onderzoeken of de connectiviteit binnen en tussen dit netwerk en andere hersengebieden afhangt van de sterkte van het alfa ritme.
Uit een conventionele analyse van data gemeten tijdens rust bleek dat het BOLD signaal uit de primaire visuele cortex negatief samenhangt met de sterkte van het alfa ritme. Dit komt overeen met eerder studies die alfa en BOLD gecorreleerd hebben, en ook met de waarschijnlijke locatie van de posterieure alfabron zoals gerapporteerd in de literatuur. Voor dit gebied is onderzocht of de sterkte van de samenhang met andere gebieden in het visuele systeem en met gebieden buiten het visuele systeem afhangt van de sterkte van het alfa ritme. Hier blijkt dat dat de sterkete van de koppeling met gebieden binnen het visuele systeem afneemt wanneer de sterkte van het alfa-ritme toeneemt. De verminderde interactie met dit gebied past goed in de functionele inhibitie theorie voor alfa oscillaties. Deze suggereert dat alfa oscillaties te maken hebben met de inhibitie van gebieden binnen een netwerk van gebieden waartussen sterke connectiviteit bestaat.
Naast een minder sterke positieve koppeling binnen het visuele systeem is een toename in de sterkte van het alfa ritme ook gerelateerd aan een mider sterke negatieve koppeling

met gebieden in het default mode network. Dit is mogelijk gerelateerd aan een sterkere positieve invloed van het default mode network wanneer alfa power hoog is en de activitiet dus laag is. Het default mode network vertoont over het algemeen juist verhoogde activiteit wanneer andere gebieden minder actief worden, wat ook tot uitdrukking komt in een positieve correlatie met het alfa ritme en een over het algemeen negatieve correlatie met de primaire visuele cortex. Dit suggereerd dat de functie van het default mode network mogelijk te maken heeft met het verbinden met en het onder controle houden van inactieve hersengebieden.

DISCUSSIE

In dit proefschrift wordt de relatie onderzocht tussen het EEG en het BOLD signaal. Een van de patronen die consistent uit de verschillende experimenten en analyses in de verschillende hoofdstukken naar voren komt is de negatieve relatie tussen BOLD en laag frequente (theta, alfa en bèta) oscillaties. Alleen gamma band activiteit vertoonde een positieve relatie met het BOLD signaal. Dit patroon komt goed overeen met wat bekend is uit onderzoek op dieren. De onderliggende neurale processen voor de hoge en lage frequenties lijken ook onafhankelijk van elkaar bij te dragen aan het BOLD signaal. Een implicatie hiervan is dat een fMRI activatie samen kan hangen met zowel afname in power in de lagere frequentiebanden als een toename in power in hogere frequentiebanden. Alleen door fMRI activatie te relateren aan elektrofysiologische activiteit is een differentiatie hiertussen mogelijk.

Het was verassend dat laag frequente EEG activiteit alleen negatief correleerde met het BOLD signaal. Vooral van theta EEG activiteit werd gedacht dat dit samenhing met actieve verwerking van informatie in het werkgeheugen. Dit zou in het BOLD signaal als een toename, en niet een afname, naar voren moeten komen. In het discussiehoofdstuk van dit proefschrift worden verscheidene redenen aangevoerd voor deze discrepantie. Een belangrijke reden zou kunnen zijn dat de meeste evidentie voor de rol van theta oscillaties in bijvoorbeeld werkgeheugen komt van intracraniële metingen in dieren en mensen. In dit type metingen wordt voornamelijk locale neurale synchroniciteit gemeten, terwijl EEG de synchroniciteit over een veel groter deel van de cortex registreert. Een bijkomend probleem is dat de mediale temporale cortex waar theta effecten in dieren voornamelijk worden gevonden relatief ver van de EEG kanalen ligt en daardoor in menselijk EEG mogelijk niet wordt opgepikt. Van bepaalde ERP's is echter bekend dat deze wel een positieve correlatie hebben met het BOLD signaal en

ERP's zijn doorgaans golven van een lage frequentie. De negatieve relatie tussen BOLD en power fluctuaties in lage frequenties hoeft dus niet noodzakelijk voor alle electrophysiologische activiteit in de lagere frequenties te gelden.

In drie van de vier analyses observeerden wij een negatieve correlatie tussen alfa en het BOLD signaal. Dit werd geïnterpreteerd in het licht van de functionele inhibitie theorie voor alfa. Deze stelt dat alfa oscillaties gerelateerd zijn aan de inhibitie van taak irrelevante gebieden. De observatie dat verhoogde alfa power samenhangt met verlaagde interactie tussen hersengebieden past ook in deze interpretatie. Voor de interpretatie van fMRI experimenten heeft dit als gevolg dat zowel gebieden met deactivaties als activaties van belang kunnen zijn voor een goede taakuitvoering. Tot nu toe lag de nadruk in fMRI onderzoek voornamelijk op taak gerelateerde activaties en niet op deactivaties.

De belangrijkste conclusie van dit proefschrift is dat het gelijktijdig meten en analyseren van EEG en fMRI het begrip van de effecten in beide modaliteiten afzonderlijk kan vergroten. Uit dit onderzoek, blijkt bijvoorbeeld dat frontale theta EEG activiteit niet zoals werd aangenomen te maken heeft met activiteit in werkgeheugen gerelateerde gebieden, maar met verminderde activiteit in het default mode netwerk. Dit geeft ook meteen aan dat variaties in EEG activiteit kunnen samenhangen met veranderingen in een netwerk van gebieden. De bevinding dat alfa en gamma afzonderlijk van elkaar bijdragen aan het BOLD signaal is een goed voorbeeld van hoe het EEG de interpretatie van fMRI resultaten kan bevorderen.

LIST OF PUBLICATIONS

Scheeringa R, Mazaheri A, Bojak I, Norris DG and Kleinschmidt A.
Modulation of visually evoked cortical fMRI responses by phase of ongoing occipital alpha oscillations.
Accepted for publication in Journal of Neuroscience.

Scheeringa R, Fries P, Petersson KM, Oostenveld R, Grothe I, Norris DG, Hagoort P and Bastiaansen MCM.
Neuronal dynamics underlying high and low frequency EEG oscillations contribute independently to the human BOLD signal.
Accepted for publication in Neuron.

Sadaghiani S, Scheeringa R, Lehongre K, Morillon B, Giraud AL, Kleinschmidt A.
Intrinsic connectivity networks, alpha oscillations, and tonic alertness: a simultaneous electroencephalography/functional magnetic resonance imaging study.
Journal of Neuroscience 30: 10243-50 (2010).

Helmich RC, Derikx LC, Bakker M, Scheeringa R, Bloem BR, Toni I.
Spatial Remapping of Cortico-striatal Connectivity in Parkinson's Disease.
Cerebral Cortex, 20:1175-86 (2010).

Menenti L, Petersson KM, Scheeringa R, Hagoort P.
When elephants fly: differential sensitivity of right and left inferior frontal gyri to discourse and world knowledge.
Journal of Cognitive Neuroscience, 21: 2358-2368 (2009).

Moosmann M, Schönfelder VH, Specht K, Scheeringa R, Nordby H, Hugdahl K.
Realignment parameter-informed artefact correction for simultaneous EEG–fMRI recordings.
Neuroimage, 45:1140 (2009).

Scheeringa R, Petersson KM, Oostenveld R, Norris DG, Hagoort P, Bastiaansen M.
Trial-by-trial coupling between EEG and BOLD identifies networks related to alpha and theta EEG power increases during working memory maintenance.
Neuroimage, 44:1224-1238 (2009).

Fries P, Scheeringa R, Oostenveld R.
Finding gamma.
Neuron 58: 303-305 (2008).

Bakker M, De Lange FP, Helmich RC, Scheeringa R, Bloem BR, Toni I.
Cerebral correlates of motor imagery of normal and precision gait.
Neuroimage 41: 998-1010 (2008).

Scheeringa R, Bastiaansen MCM, Petersson KM, Oostenveld R, Norris DG, Hagoort P.
Frontal theta EEG activity correlates negatively with the default mode network in restingstate.
International Journal of Psychophysiology 67:242-551 (2008).

Maurits NM, Scheeringa R, Van der Hoeven J, De Jong, R.
EEG coherence obtained from an auditory oddball task increases with age.
Journal of Clinical Neurophysiology 23:395-403 (2006).

whom I would like to thank here. Some persons however deserve a special word of gratitude.

First of all I would like to thank my paranimfen Laura Menenti and Ali Mazaheri. Laura, thank you for letting me stay over when I was escaping Paris, for somehow adding my name to the author list of a language article and most of all for your friendship throughout the years.

Ali, I would like to thank you for being the best housemate and friend throughout my PhD I could have wished for. There are a lot of cherished memories I will never forget. I would also like to thank you for introducing me to the two ladies in your life, Lucy and Katrien.

Katrien, thank you for being a wonderful housemate during the last year of my PhD. I don't know anybody else that would have been able to move into a new apartment together with the two most unpractical persons on earth. Thank you also for simultaneously being the most efficient shopper and interior designer ever.

Michael Plöchl, I will always remember you for the totally random moments you would drop by for beers or hamburgers. With your ear ring, bold shaven head and hard rock appearance it might not be obvious to most people, but I will bet a t******e on this: Michael, jij bent de liefste van de hele wereld!

Gijs van Elswijk I really got to know well during conferences in San Diego and Melbourne. I really enjoyed the time we spent there in these cities and Sydney, and the times there after in Nijmegen. Gijs, I still feel honoured to have been you paranimf.

Throughout my time as a PhD student and also during my time after there is a seamlessly endless list of people that at one point or another have enriched my life. This list is far too long to be listed here; its shear length would devaluate my gratitude to anyone that is on it, let alone the people I would shamefully forget to mention. I however would very much like to make an exception for

……………………………………………… (write or let me write down your name here if applicable)

who I would like to thank for the great time we had (strikethrough if not applicable, multiple choices possible) during Friday Afternoon Drinks or other alcohol related gatherings/ during poker nights/ at parties/ at conferences/ during de Vierdaagse Feesten/ at Dagje Uit afterparties / sharing an office/ constructing my new IKEA furniture/ during games nights/ at any other occasion (s) being:

……………………………………………

Furthermore I would like to thank the Superboer at nr. 49 for losing his focus on the nr. 50 spot.

Mijn familie wil ik bedanken voor hun steun gedurende mij gehele van mijn school- en studie- en promotietijd. Ik ben vooral mijn vader en moeder erg dankbaar voor alles wat ze hebben moeten doen en laten om me de kansen te kunnen bieden die uiteindelijk tot dit proefschrift hebben geleid.

CURRICULUM VITTEA

René Scheeringa was born in Leeuwarden on January 13th 1980. He graduated from high school at the CSG Lauwers College in Buitenpost in 1999. In 2004 he acquired his MSc degree at in psychology, specializing in Experimental Psychology and Methodology. In December 2004 he started his research as a PhD at the F.C. Donders Centre for Cognitive Neuroimaging of the Radboud University Nijmegen, which later became part of the larger Donders Institute for Brain, Cognition and Behaviour at the same university. Here he studied the relation between oscillatory EEG activity and the fMRI BOLD signal by simultaneously recording both imaging simultaneously. The work carried out in this period is presented in this thesis. Between January 2009 and August René Scheeringa worked as a post-doc at the INSERM-CEA Cognitive Neurospin unit at Neurospin located in Gif sur Yvette (south of Paris), France, where he investigated where he continued the line of work started in Nijmegen. Currently he is back in Nijmegen where he works as a post-doc at the Donders Institute for Brain, Cognition and Behaviour.

CURRICULUM VITEA

René Scheeringa was born in Leeuwarden on January 13th 1980. He graduated from high school at the CSG Lauwers College in Buitenpost in 1999. In 2004 he acquired his MSc degree in psychology, specializing in Experimental Pscychology and Methodology at the University of Groningen. In December 2004 he started his research as a PhD at the F.C. Donders Centre for Cognitive Neuroimaging of the Radboud Univiersity Nijmegen, which after a later became part of the larger Donders Insitute for Brain, Cognition and Behaviour at the same university. Here he studied the relation between oscillatory EEG activity and the fMRI BOLD signal by simultaneously recording both imaging simultaneously. The work carried out in this period is presented in this thesis. Between January 2009 and August René Scheeringa worked as a post-doc at the INSERM-CEA Ccognitive Neurospin unit at Neurospin located in Gif sur Yvette (south of Paris), France, where he investigated where he coninued the line of work started in Nijmegen. Currently he is back in Nijmegen where he works as a post-doc at the Donders Insitute for Brain, Cognition and Behaviour.

DONDERS GRADUATE SCHOOL FOR COGNITIVE NEUROSCIENCE SERIES

1. van Aalderen-Smeets, S.I. (2007). *Neural dynamics of visual selection.* Maastricht University, Maastricht, The Netherlands.
2. Schoffelen, J.M. (2007). *Neuronal communication through coherence in the human motor system.* Radboud University Nijmegen, Nijmegen, The Netherlands.
3. de Lange, F.P. (2008). *Neural mechanisms of motor imagery.* Radboud University Nijmegen, Nijmegen, The Netherlands.
4. Grol, M.J. (2008). *Parieto-frontal circuitry in visuomotor control.* University Utrecht, Utrecht, The Netherlands.
5. Bauer, M. (2008). *Functional roles of rhythmic neuronal activity in the human visual and somatosensory system.* Radboud University Nijmegen, Nijmegen, The Netherlands.
6. Mazaheri, A. (2008). *The Influence of Ongoing Oscillatory Brain Activity on Evoked Responses and Behaviour.* Radboud University Nijmegen, Nijmegen, The Netherlands.
7. Hooijmans, C.R. (2008). *Impact of nutritional lipids and vascular factors in Alzheimer's Disease.* Radboud University Nijmegen, Nijmegen, The Netherlands.
8. Gaszner, B. (2008). *Plastic responses to stress by the rodent urocortinergic Edinger-Westphal nucleus.* Radboud University Nijmegen, Nijmegen, The Netherlands.
9. Willems, R.M. (2009). *Neural reflections of meaning in gesture, language and action.* Radboud University Nijmegen, Nijmegen, The Netherlands.
10. Van Pelt, S. (2009). *Dynamic neural representations of human visuomotor space.* Radboud University Nijmegen, Nijmegen, The Netherlands.
11. Lommertzen, J. (2009). *Visuomotor coupling at different levels of complexity.* Radboud University Nijmegen, Nijmegen, The Netherlands.
12. Poljac, E. (2009). *Dynamics of cognitive control in task switching: Looking beyond the switch cost.* Radboud University Nijmegen, Nijmegen, The Netherlands.
13. Poser, B.A. (2009) *Techniques for BOLD and blood volume weighted fMRI.* Radboud University Nijmegen, Nijmegen, The Netherlands.
14. Baggio, G. (2009). *Semantics and the electrophysiology of meaning. Tense, aspect, event structure.* Radboud University Nijmegen, Nijmegen, The Netherlands.
15. van Wingen, G.A. (2009). *Biological determinants of amygdala functioning.* Radboud University Nijmegen Medical Centre, Nijmegen, The Netherlands.
16. Bakker, M. (2009). *Supraspinal control of walking: lessons from motor imagery.* Radboud University Nijmegen Medical Centre, Nijmegen, The Netherlands.
17. Aarts, E. (2009). *Resisting temptation: the role of the anterior cingulate cortex in adjusting cognitive control.* Radboud University Nijmegen, Nijmegen, The Netherlands.
18. Prinz, S. (2009). *Waterbath stunning of chickens – Effects of electrical parameters on the electroencephalogram and physical reflexes of broilers.* Radboud University Nijmegen, Nijmegen, The Netherlands.

19. Knippenberg, J.M.J. (2009). *The N150 of the Auditory Evoked Potential from the rat amygdala: In search for its functional significance.* Radboud University Nijmegen, Nijmegen, The Netherlands.
20. Dumont, G.J.H. (2009). *Cognitive and physiological effects of 3,4-methylenedioxymethamphetamine (MDMA or 'ecstasy') in combination with alcohol or cannabis in humans* Radboud University Nijmegen, Nijmegen, The Netherlands.
21. Pijnacker, J. (2010). *Defeasible inference in autism: a behavioral and electrophysiogical approach.* Radboud Universiteit Nijmegen, The Netherlands.
22. de Vrijer, M. (2010). *Multisensory integration in spatial orientation.* Radboud University Nijmegen, Nijmegen, The Netherlands.
23. Vergeer, M. (2010). *Perceptual visibility and appearance: Effects of color and form.* Radboud University Nijmegen, Nijmegen, The Netherlands.
24. Levy, J. (2010). *In Cerebro Unveiling Unconscious Mechanisms during Reading.* Radboud University Nijmegen, Nijmegen, The Netherlands.
25. Treder, M. S. (2010). *Symmetry in (inter)action.* Radboud University Nijmegen, Nijmegen, The Netherlands.
26. Horlings C.G.C. (2010). *A Weak balance; balance and falls in patients with neuromuscular disorders.* Radboud University Nijmegen, Nijmegen, The Netherlands
27. Snaphaan, L.J.A.E. (2010). *Epidemiology of post-stroke behavioural consequences.* Radboud University Nijmegen Medical Centre, Nijmegen, The Netherlands.
28. Dado – Van Beek, H.E.A. (2010). *The regulation of cerebral perfusion in patients with Alzheimer's disease.* Radboud University Nijmegen Medical Centre, Nijmegen, The Netherlands.
29. Derks, N.M. (2010). *The role of the non-preganglionic Edinger-Westphal nucleus in sex-dependent stress adaptation in rodents.* Radboud University Nijmegen, Nijmegen, The Netherlands.
30. Wyczesany, M. (2010). *Covariation of mood and brain activity. Integration of subjective self-report data with quantitative EEG measures.* Radboud University Nijmegen, Nijmegen, The Netherlands.
31. Beurze S.M. (2010). *Cortical mechanisms for reach planning.* Radboud University Nijmegen, Nijmegen, The Netherlands.
32. van Dijk, J.P. (2010). *On the Number of Motor Units.* Radboud University Nijmegen, The Netherlands .
33. Lapatki, B.G. (2010). *The Facial Musculature – Characterization at a Motor Unit Level.* Radboud University Nijmegen, Nijmegen, The Netherlands.
34. Kok, P. (2010). *Word Order and Verb Inflection in Agrammatic Sentence Production.* Radboud University Nijmegen, Nijmegen, The Netherlands.
35. van Elk, M. (2010). *Action semantics: Functional and neural dynamics.* Radboud University Nijmegen, Nijmegen, The Netherlands.
36. Majdandzic, J. (2010). *Cerebral mechanisms of processing action goals in self and others.* Radboud University Nijmegen, Nijmegen, The Netherlands.

37. Snijders, T.M. (2010). *More than words – neural and genetic dynamics of syntactic unification.* Radboud University Nijmegen, Nijmegen, The Netherlands.
38. Grootens, K.P. (2010). *Cognitive dysfunction and effects of antipsychotics in schizophrenia and borderline personality disorder.* Radboud University Nijmegen Medical Centre, Nijmegen, The Netherlands.
39. Nieuwenhuis, I.L.C. (2010). *Memory consolidation: A process of integration – Converging evidence from MEG, fMRI and behavior.* Radboud University Nijmegen Medical Centre, Nijmegen, The Netherlands.
40. Menenti, L.M.E. (2010). *The right language: differential hemispheric contributions to language production and comprehension in context.* Radboud University Nijmegen, Nijmegen, The Netherlands.
41. van Dijk, H.P. (2010). *The state of the brain, how alpha oscillations shape behaviour and event related responses.* Radboud University Nijmegen, Nijmegen, The Netherlands.
42. Meulenbroek, O.V. (2010). *Neural correlates of episodic memory in healthy aging and Alzheimer's disease.* Radboud University Nijmegen, Nijmegen, The Netherlands.
43. Oude Nijhuis, L.B. (2010). *Modulation of human balance reactions.* Radboud University Nijmegen, Nijmegen, The Netherlands.
44. Qin, S. (2010) *Adaptive memory: imaging medial temporal and prefrontal memory systems.* Radboud University Nijmegen, The Netherlands.
45. Timmer, N.M. (2011). *The interaction of heparan sulfate proteoglycans with the amyloid β protein.* Radboud University Nijmegen, Nijmegen, The Netherlands.
46. Crajé, C. (2011). *(A)typical motor planning and motor imagery.* Radboud University Nijmegen, Nijmegen, The Netherlands.
47. van Grootel, T.J. (2011). *On the role of eye and head position in spatial localisation behaviour.* Radboud University Nijmegen, Nijmegen, The Netherlands.
48. Lamers, M.J.M. (2011). *Levels of selective attention in action planning.* Radboud University Nijmegen, Nijmegen, The Netherlands.
49. Van der Werf, J. (2011). *Cortical oscillatory activity in human visuomotor integration.* Radboud University Nijmegen, Nijmegen, The Netherlands.
50. Scheeringa, R. (2011). *On the relation between oscillatory EEG activity and the BOLD signal.* Radboud University Nijmegen, Nijmegen, The Netherlands.